Exploring the Scope and Utility of Dynamic Covalent Chemistry within Polymeric Nanoparticles

Alexander William Jackson

A thesis submitted for the degree of

Doctor of Philosophy in Chemistry

School of Chemistry

Newcastle University

April 2012

ABSTRACT OF THE DISSERTATION

Exploring the Scope and Utility of Dynamic Covalent Chemistry within Polymeric
Nanoparticles

by

Alexander William Jackson

Dynamic covalent chemistry encompasses reversible bond forming reactions which proceed under equilibrium control, where the position of the equilibria are sensitive to changes in environment, and which are often able to undergo component exchange. These virtues provide polymeric nanoparticles incorporating dynamic covalent bonds with the ability to reconfigure or change their structural properties in response to stimuli. In Chapter 1 we critically discuss and evaluate the current state of the art whereby polymer chemists have exploited dynamic covalent bonds within responsive and adaptive polymeric nanoparticles. Chapter 2 describes the synthesis and study of a chemoresponsive polymeric micelle. In this work, aldehyde and alkoxyamine end-functionalized polymers are shown to link together through a single oxime bond and then self-assemble into micellar aggregates. The chemoresponsive nature of these micellar aggregates is expressed when their disassembly is triggered through the addition of a small molecule alkoxyamine. Chemoresponsive core cross-linked star and nanogel nanoparticles which contain multiple imine cross-links are presented in Chapter 3. These imine linkages are utilized to facilitate the self-assembly process of the nanoparticles, which display chemoresponsive disassembly upon the addition of a small molecule amine. Chapter 4 describes the preparation of core cross-linked star polymers which are both pH-responsive and thermoresponsive. The pH-responsive nature is imparted through the pH-responsiveness of multiple imine linkages, and their thermoresponsive nature arises on account of the thermoresponsive polymer chains contained within their cores. In Chapter 5 nanoparticles possessing pH-responsive imine and redox-responsive disulfide cross-links have been developed where the simultaneous application of both low pH and a reducing agent is required to trigger their disassembly. It is shown that the application of either low pH or a reducing agent does not trigger disassembly. The research presented throughout this dissertation confirms the great potential of dynamic covalent chemistry in the development of stimuli-responsive polymeric nanoparticles.

ACKNOWLEDGEMENTS

Over the past four years I have been extremely fortunate to conduct my research in an incredibly exciting and pleasurable environment. My PhD supervisor Dr David A Fulton has not simply been concerned only with 'my results', but has also strived to provide me with the tools to become an all-round more conscientious and accomplished scientist. For his inspiration, guidance and encouragement I am infinitely grateful. The fundamental approach within the Fulton group is to perform and present our research with the highest levels of professionalism and scientific integrity, an approach which will serve me well in all my future endeavours, and I am grateful to all the members of the Fulton group for their assistance and support. I have spent most of my PhD studies working alongside Dr Ben Murray and Clare Mahon, both of whom possess a great understanding of chemistry, and are also very creative and insightful, their help has been immeasurable and I thank them both for all the enjoyable hours we have spent together in the laboratory.

I am also indebted to Newcastle University, where I have studied chemistry for nearly eight years. When I started my university life I had no idea how long it would last or how much I would eventually benefit. The School of Chemistry at Newcastle University is a truly stimulating environment and the quality of teaching has been of great value. I have had such a brilliant time at Newcastle University, not least because it is where I met my wonderful girlfriend Natalie, her unwavering support throughout my PhD has been fantastic.

I owe my deepest gratitude to my parents, they have always placed great importance on education, and have continuously ensured that I reach my potential through remarkable support and encouragement.

TABLE OF CONTENTS

Chapter 1: Stimuli-Responsive Dynamic Covalent Polymeric Nanoparticles and Materials

Table of Contents

Chapter 2: Dynamic Covalent Diblock Copolymers

Table of Contents

Chapter 3: Imine Cross-Linked Star Polymer and Nanogel Nanoparticles

Table of Contents

Chapter 4: Dual Stimuli-Responsive Core Cross-Linked Star Polymers

Table of Contents

Chapter 5: Triggering Polymeric Nanoparticle Disassembly through the Application of Two Different Stimuli

Table of Contents

LIST OF FIGURES

Chapter 1: Stimuli-Responsive Dynamic Covalent Polymeric Nanoparticles and Materials

Chapter 2: Dynamic Covalent Diblock Copolymers

Chapter 3: Imine Cross-Linked Star Polymer and Nanogel Nanoparticles

Chapter 4: Dual Stimuli-Responsive Core Cross-Linked Star Polymers

Hydrodynamic radii obtained from batch dynamic light scattering analysis at 20 °C.

Chapter 5: Triggering Polymeric Nanoparticle Disassembly through the Application of Two Different Stimuli

LIST OF TABLES

Chapter 5: Triggering Polymeric Nanoparticle Disassembly through the Application of Two Different Stimuli

LIST OF SCHEMES

Chapter 4: Dual Stimuli-Responsive Core Cross-Linked Star Polymers

Chapter 5: Triggering Polymeric Nanoparticle Disassembly through the Application of Two Different Stimuli

LIST OF SYMBOLS AND ABBREVIATIONS

AIBN	Azobis(isobutyronitrile)
ATRP	Atom transfer radical polymerization
Boc$_2$O	Di-*tert*-butyl dicarbonate
^{t}BP	*tert*-Butyl peroxide
CAN	Covalently adaptable network
CCS	Core cross-linked star
CPADB	4-(4-Cyanopentanoic acid)dithiobenzoate
CTA	Chain transfer agent
Da	Dalton
DBU	1,8-Diazabicyclo[5.4.0]undec-7-ene
DCC	Dynamic covalent chemistry
DDMAT	*S*-1-dodecyl-*S'*-(α,α'-dimethyl-α''-acetic acid)trithiocarbonate
DTT	Dithiothreitol
DLS	Dynamic light scattering
DMA	*N,N'*-Dimethylacrylamide
DMAP	4-(Dimethylamino)pyridine
DMF	*N,N'*-Dimethylformamide
dn/*dc*	Specific refractive index increment
dRI	Differential refractive index
EDC	*N*-Ethyl-*N'*-(3-dimethylaminopropyl)carbodiimide
EtOAc	Ethylacetate
Et$_3$N	Triethylamine
FITC	Fluorescein isothiocyanate
FT-IR	Fourier transform infrared spectroscopy
GPC	Gel permeation chromatography
HRMS	High resolution mass spectrometry
K	Kelvin
K$_a$	Association constant
LCT	Liquid chromatography time of flight
LRP	Living radical polymerization
MALDI-TOF	Matrix-assisted laser desorption/ionization - time of flight
MALLS	Multi-angle laser light scattering
MHz	Megahertz

MMA	Methyl methacrylate
M_n	Number average molecular weight
M_w	Weight average molecular weight
m/z	Mass-to-charge ratio
NMP	Nitroxide-mediated polymerization
NMR	Nuclear magnetic resonance
NIPAm	*N*-Isopropylacrylamide
OEGMA	Oligoethylene glycol methacrylate
PA	Prednisolone 21-acetate
PAPMA	3-Aminopropyl methacrylamide
PDI	Polydispersity index
PDSMA	2-Pyridyldisulfide ethylmethacrylate
PEG	Poly(ethylene glycol)
PI	Poly(isoprene)
PIC	Polyion complex
PS	Poly(styrene)
PSBA	Poly(styreneboronic acid)
PMMA	Poly(methyl methacrylate)
ppm	Parts per million
RAFT	Reversible Addition-Fragmentation Chain Transfer
R_g	Radius of gyration
R_h	Hydrodynamic radius
TCEP	*tris*(carboxyethyl)phosphine
TDA	Terephthaldicarboxaldehyde
TEMPO	2,2,6,6-Tetramethylpiperidine-1-oxyl
THF	Tetrahydrofuran
TFA	Trifluoroacetic acid
UV-vis	Ultraviolet-visible

PUBLICATIONS AND PRESENTATIONS

A. W. Jackson and D. A. Fulton, "Dynamic Covalent Diblock Copolymers Prepared from RAFT Generated Aldehyde and Alkoxyamine End-Functionalized Polymers" *Macromolecules*, 2010, **43**, 1069 – 1075.

A. W. Jackson and D. A. Fulton, "The Formation of Core Cross-Linked Star Polymers Containing Cores Cross-Linked by Dynamic Covalent Imine Bonds" *Chem. Commun.*, 2010, **46**, 6051 – 6053.

B. S. Murray, **A. W. Jackson**, C. S. Mahon and D. A. Fulton, "Reactive Thermoresponsive Copolymer Scaffolds" *Chem. Commun.*, 2010, **46**, 8651 – 8653.

A. W. Jackson and D. A. Fulton, "pH Triggered Self-Assembly of Core Cross-Linked Star Polymer Possessing Thermoresponsive Cores" *Chem. Commun.*, 2011, **47**, 6807 – 6809.

C. S. Mahon, **A. W. Jackson**, B. S. Murray and D. A. Fulton, "Templating a Polymer-Scaffolded Dynamic Combinatorial Library" *Chem. Commun.*, 2011, **47**, 7209 – 7211.

A. W. Jackson, C. Stakes and D. A. Fulton, "The formation of core cross-linked star polymer and nanogel assemblies facilitated by the formation of dynamic covalent imine bonds" *Polym. Chem.*, 2011, **2**, 2500 – 2511.

A. W. Jackson and D. A. Fulton, "Triggering Polymeric Nanoparticle Disassembly through the Simultaneous Application of Two Different Stimuli" *Macromolecules*, 2012, **45**, 2699 – 2708.

A.W. Jackson, "pH Triggered Self-Assembly of Core Cross-Linked Star Polymers Possessing Thermoresponsive Cores" RSC Postgraduate Symposium on Nanotechnology, Birmingham University, UK, *Oral Presentation*, 2011.

A. W. Jackson, "The Incorporation of Dynamic Covalent Bonds into Polymer-Based Assemblies" Northern Sustainable Chemistry Seminar Meeting, York University, UK, *Oral Presentation*, 2011.

Chapter 1

Stimuli-Responsive Dynamic Covalent Polymeric Nanoparticles and Materials

Table of Contents:

1.1   Abstract

The development of responsive and adaptive polymeric nanoparticles and materials is a key goal of contemporary polymer/materials chemistry. By possessing responsive and dynamic attributes, polymeric materials are able to display 'intelligent' behaviours, such as the ability to respond to stimuli or undergo self-repair. The recent progress in the field of responsive and adaptive polymeric nanoparticles which incorporate dynamic covalent bonds is outlined.

1.2   Introduction

There is currently a great drive amongst polymer scientists to develop synthetic polymers and polymeric nanoparticles which possess stimuli-responsive and adaptive properties. Polymers which can reconfigure their structures or incorporate and release other components upon the application of a specific stimulus will lead to new and exciting novel materials[1-3] with great potential in fields such as nanotechnology, materials science and medical devices. A particularly exciting potential application for stimuli-responsive polymeric nanoparticles is as vehicles for the targeted and controlled delivery of pharmaceuticals,[4-6] and many synthetic polymer research groups are developing responsive and adaptive polymeric nanoparticles which can encapsulate and release high value cargo within a specific biological environment.[7] Another interesting development is the emergence of self-healing materials[8, 9] which utilize stimuli-responsive and adaptive polymers.

A key driver of recent progress in polymeric nanoparticles has been the development of living radical polymerization (LRP) techniques,[10] which have provided polymer scientists with experimentally powerful and straightforward methods to prepare polymers with high levels of molecular precision. Techniques such as reversible addition-fragmentation chain transfer (RAFT) polymerization,[11] atom transfer radical polymerization (ATRP)[12] and nitroxide mediated polymerization (NMP)[13] allow the synthesis of polymer chains with desired molecular weights, narrow molecular weight distributions and the incorporation and retention of desired end-group functionality. Their tolerance of a wide variety of chemical functional groups allows their incorporation along the polymer backbone. These techniques are currently being exploited to prepare functional polymer building blocks which can be used for the self-

assembly of novel and exciting polymeric nanostructures which were difficult to prepare of even completely inaccessible before the development of LRP techniques.

The research presented throughout this thesis exploits the potential of LRP techniques to prepare linear polymer building blocks with a high level of molecular precision and the incorporation of different functionalities along the polymer backbone and chain terminus. In particular, the living free-radical RAFT polymerization technique developed by Moad, Rizzardo and Thang has been utilized throughout this work. This method was first presented[14] in 1998, and it has since been widely employed by polymer chemists on account of its experimental simplicity and versatility.

Traditional free radical polymerizations are commonly used for the commercial preparation of high molecular weight polymers, and have been so frequently applied as they are relatively cheap, whilst being tolerant of different monomer varieties (styrenic, (meth)acrylates and (meth)acrylamides) and monomer functionalities (OH, COOH, NR_2 and $CONR_2$). They are also experimentally very simple on account of their tolerance of water and protic solvents, and their only experimental requirement is the removal of oxygen from the reaction mixture prior to polymerization. However, there are notable and significant disadvantages to traditional radical polymerizations, such as the inability to prepare multi-block copolymer chains and poor accessibility to complex macromolecular architectures. Their most significant shortcoming is the lack of control over molecular weight distributions, as traditional radical initiators afford polymer samples with polydispersity indices typically between 2 and 4.

The development of LRP techniques has allowed a high level of control over the polymerization process whilst retaining the versatility of conventional radical polymerizations. For a polymerization to be classed as "living", all chains must be initiated at the beginning of the reaction, grow at the same rate, survive the process in order to remain "living" and possess the ability to re-initiate the polymerization to furnish multi-block copolymers if desired. Living polymerizations are characterized by a linear consumption of monomer units and polymer molecular growth with time. To ensure "living" characteristics and prevent undesirable radical-radical chain termination, all chains cannot be simultaneously active. To achieve this desirable situation, the RAFT technique (Scheme 1.1) employs a chain transfer agent (CTA) which contains a thiocarbonylthio functional group, in the form of ZC(=S)SR (**2**). After conventional radical initiation (Scheme 1.1i) the propagating radical polymer chains (**1**) react with the CTA (Scheme 1.1ii) to afford a dormant polymeric thiocarbonylthio compound (**3**). This step also produces a stable free-radical (R$^•$) which is then able to re-initiate

polymer growth (Scheme 1.1iii), and these newly formed polymer chains (**4**) are then able to react (Scheme 1.1iv) with the dormant polymeric species (**3**) which caps the growing chains and regenerates previously dormant chains which then continue to grow. This process is completely reversible and the rapid equilibration between dormant polymeric thiocarbonylthio compounds (**3** and **5**) and propagating polymer chains (**1** and **4**) ensures all polymer chains grow intermittently and at an equal rate. This chain equilibration between the dormant and active species gives the RAFT technique its "living" nature and affords polymer chains which possess low polydispersities. The reaction mixture always contains a higher proportion of CTA to radical initiator, and therefore the majority of polymer chains are present in the dormant forms (**3** and **5**), reducing the probability of chain-chain termination (Scheme 1.1v).

i) Initiation

$$\text{Radical Initiator} \longrightarrow I^{\bullet} \xrightarrow{M} \xrightarrow{M} P_n^{\bullet}$$
1

ii) Reversible Chain Transfer

iii) Reinitiation

$$R^{\bullet} \xrightarrow[k_i]{M} R\text{-}M^{\bullet} \xrightarrow{M} P_m^{\bullet}$$
4

k_p = Propagation rate constant
k_{add} = Addition rate constant
k_f = Fragmentation rate constant
k_i = Reinitiation rate constant
k_t = Termination rate constant

iv) Chain Equilibrium

v) Termination

$$P_n^{\bullet} + P_m^{\bullet} \xrightarrow{k_t} \text{Dead Polymer}$$

Scheme 1.1 Reversible addition-fragmentation chain transfer (RAFT) polymerization technique mechanism.

The selection of the Z and R groups is crucial and has a huge influence on the process of polymerization. The Z group must activate the C=S bond, making it susceptible to radical attack, and the R group must furnish a stable radical which can then re-initiate

5

polymer growth. The rate of radical addition to the C=S double bond is affected by the substituent Z. When Z = aryl, alkyl (dithioesters) or *S*-alkyl (trithiocarbonates) the rate of addition is relatively high favouring the polymerization of styrenic, (meth)acrylate and (meth)acrylamide monomer units. When Z = *O*-alkyl (xanthates) or *N,N'*-dialkyl (dithiocarbamates) the rate of addition is lower, which favours other vinyl monomers such as vinyl acetate. The R group must be a good homolytic leaving group relative to the propagating radical polymer chain ($P_n{}^\bullet$), otherwise fragmentation will not occur and the growing polymer chains will not exist as the dormant form and subsequent reinitiation and chain equilibrium will not ensue. The leaving group ability of the substituent R must be balanced with its ability to reinitiate polymerization. In this regard, tertiary dialkylcyano and dialkylphenyl R groups possess high fragmentation rates and are largely employed for the polymerization of styrenic, (meth)acrylate and (meth)acrylamide monomers units. Primary alkylcyano and alkylphenyl R groups on the other hand possess lower fragmentation rates, and are appropriate for vinyl monomer units. A wide range of CTAs have been developed[11, 15, 16] which are compatible with different monomer units. When the polymerization is stopped most polymer chains retain the thiocarbonylthio functional group, which after purification, allows the polymerization to be continued, allowing the preparation of complex and functional multi-block copolymers. Another highly advantageous feature of the RAFT technique is the ability to introduce a wide range of functionalities into the CTA within the Z and/ or R groups to prepare[17] novel end-functionalized polymer chains, circumventing the problems of post-polymerization functionalization. These extremely advantageous features of the RAFT process have resulted in its utilization in the development of highly novel and functional polymer building blocks which have been used to prepare numerous complex nano-sized structures (Figure 1.1). A selection of these diverse architectures, prepared utilising the RAFT process, have recently been reviewed by Davis *et al.*[18]

Graft Polymers   Core Cross-Linked Star Polymers   Micelles   Nanogels   Macroscopic Gels
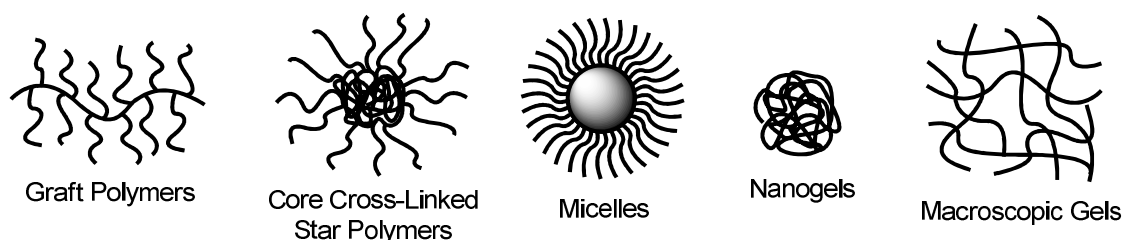
Figure 1.1 Examples of nano-sized polymeric nanoparticles and materials prepared using the RAFT polymerization technique.

One of the most exciting and interesting recent advances in polymer chemistry is the preparation of highly sophisticated functional nanoparticles and materials, which is often a direct result of the diverse functionality incorporated into polymer building blocks made possible through the utilization of LRP techniques. It is well understood that linear diblock copolymers possessing blocks that exhibit different solubilities in a given solvent will self-assemble through non-covalent aggregation into nano-sized micellar assemblies.[19] LRP techniques have been used to introduce diverse functionality into component diblock copolymer building blocks, which can then be used to facilitate cross-linking of the micelle shell or core after self-assembly. This approach[20] can be used to increase structural robustness, and stimuli-responsive characteristics can be imparted through post-formation cross-linking if the incorporated cross-links possess a dynamic nature. Consequently, the potential utility of micellar assemblies has been greatly increased, in particular as possible drug delivery vehicles, as a consequence of dynamic shell/ core cross-linking.

The ability to precisely introduce functionality along the polymer backbone has led to a greater diversity of covalently assembled polymer nanoparticle architectures. Core cross-linked star (CCS) polymers, for instance are defined as cores of cross-linked polymer chains surrounded by a corona of linear polymer chains, and these architectures can be prepared through traditional arm-first[21] or core-first[22] method via LRPs. The development of LRPs also allows the synthesis of diblock copolymer chains possessing complementary functionalities which can then be used to facilitate the formation of CCS polymers through covalent bond formation.[23-25] Covalent aggregation can be used to introduce stimuli-responsiveness if, for example, the incorporated linkages can be cleaved with the application of a specific stimulus.[26] Functional linear polymer building blocks can also be covalently cross-linked to form discrete cross-linked nanogel architectures, and these nanoparticles can also be imparted with stimuli-responsive characteristics.[27]

Polymer chemists have also utilized living radical polymerization techniques to prepare linear polymer chains which are able to cross-link into macroscopic gels. The incorporation of diverse functionalities into these polymer building blocks and resulting macroscopic gels has led to the development[8, 9] of materials which can change their mechanical and physical properties. This chapter highlights the recent developments in the field of stimuli-responsive polymeric nanoparticles. Polymeric architectures which are assembled through non-covalent aggregation are described, followed by examples where covalent aggregation is driven through dynamic covalent bond formation.

1.3   Non-Covalently Aggregated Polymeric Nanoparticles

It has long been known that some classes of polymer possess an inherent stimuli-responsiveness, and these polymers can change their charge, solubility or hydrophobicity in response to changes in their environment, such as pH or temperature. These stimuli-triggered changes in physical properties can be exploited to *e.g.* facilitate self-assembly of multiple polymer chains, or change the mechanical properties of a polymeric material.

Linear diblock copolymer chains in the form "hydrophilic-*b*-hydrophobic" are able to self-assemble into micellar nanoparticles in aqueous environments. In order to develop micelles whose formation can be reversibly controlled, polymer chemists have developed diblock copolymers possessing one block which is able to reversibly switch between hydrophilic and hydrophobic. This goal has been achieved by incorporating polymer chains which possess a stimuli-responsive hydrophobicity in response to changes in their environment within one block of the diblock copolymer.[28]
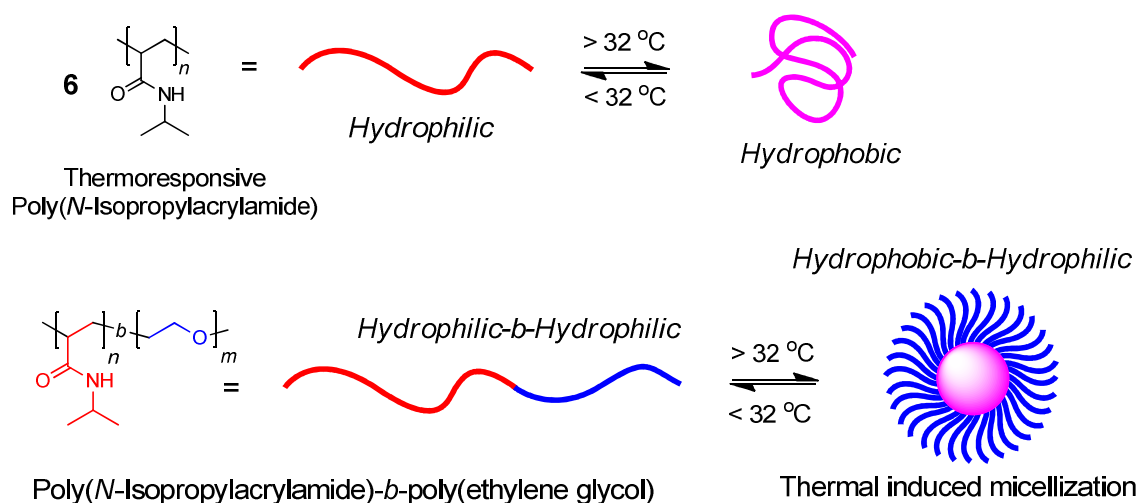
Figure 1.2 Thermally induced reversible micellization of poly(N-isopropylacrylamide)-*b*-poly(ethylene glycol).

The thermoresponsive nature of linear poly(*N*-isopropylacrylamide) (**6**) has been widely studied as it can undergo a temperature-induced coil to globule phase change (Figure 1.2) at 32 °C in water. The temperature at which this phase transition occurs is known as the lower critical solution temperature (LCST). Below this temperature, the polymer chains are hydrophilic on account of hydrogen-bonding between the amide functions situated along the polymer backbone and water molecules. Above this LCST these hydrogen-bonded interactions are broken and the water molecules move into the bulk

aqueous phase, causing the polymer chain to collapse and precipitate from solution. This process occurs when the entropic gain of the system associated with the water molecules returning the bulk solution outweighs the enthalpic contribution of water hydrogen-bonded to the polymer chain.[29] Diblock copolymers which incorporate thermoresponsive blocks such as poly(*N*-isopropylacrylamide)-*b*-poly(ethylene glycol)[30] are able to switch reversibly between hydrophilic-*b*-hydrophilic and hydrophobic-*b*-hydrophilic upon heating, a trigger which can be used to facilitate the self-assembly of multiple polymer chains into micelles (Figure 1.2). These nanoparticle-like species can convert back into linear polymer chains upon cooling. This thermally-induced change in polymer solubility has been used by several groups to facilitate reversible micellization of a wide range of diblock copolymers.[31, 32] Micellar systems which incorporate thermoresponsive characteristics have been shown to release encapsulated cargo upon micelle disassembly triggered by changes in temperature,[33-35] and have been extensively studied as potential vehicles for the controlled release pharmaceuticals.[36-38]
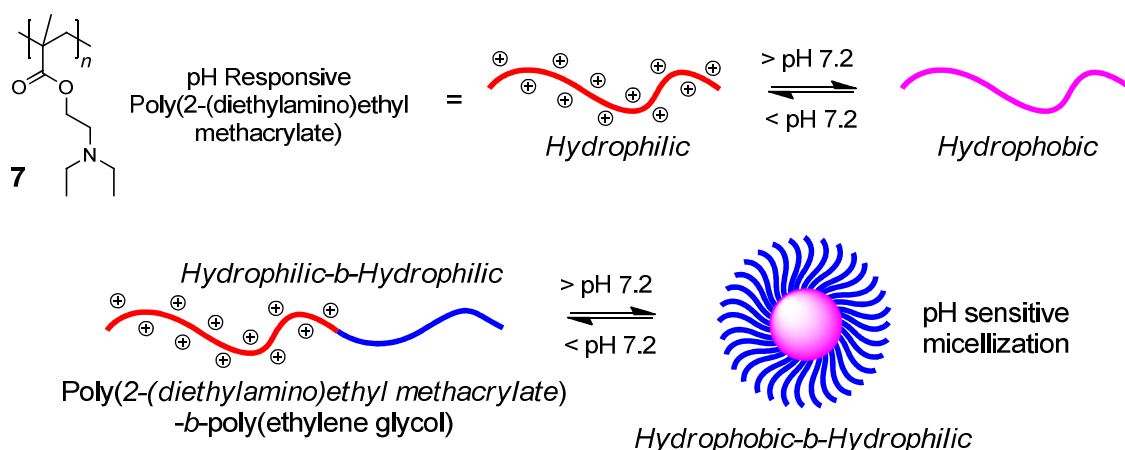
Figure 1.3 pH-Sensitive reversible micellization of poly(2-(diethylamino)ethyl methacrylate)-*b*-poly(ethylene glycol).

Linear polymer chains which possess acidic or basic functions are able to alter their charge and solubility in response to changes in pH. The pendant tertiary alkylamine functions in poly(2-(diethylamino)ethyl methacrylate) (**7**) are protonated below pH 7.2, and consequently the polymer chain is hydrophilic. Above pH 7.2, these polymer chains are deprotonated and become hydrophobic. Diblock copolymers which incorporate this pH-responsive polymer, such as poly(2-(diethylamino)ethyl methacrylate)-*b*-poly(ethylene glycol),[39] are able to switch between hydrophilic-*b*-hydrophilic and hydrophobic-*b*-hydrophilic upon changes in pH. Thus, changes in pH can be exploited

to trigger reversible aggregation of polymer chains into micellar aggregates (Figure 1.3). Polymeric systems incorporating pH responsive polymer chains have potential in the field of drug delivery,[40] as these triggers can be used to release encapsulated cargo in a specific biological environment which displays a pH which is less than the normal physiological pH (7.4), specifically cell endosomes which display a pH range of 5.0 – 6.0.[41, 42]

Whilst these non-covalently aggregated assemblies do possess stimuli-responsiveness, they do not possess chemical robustness as below their critical micellar concentration they can spontaneously disassemble into their component polymer chains. Another limitation is the relatively small selection of polymers which possess an innate stimuli-responsiveness. To circumvent these problems, polymer chemists have begun to investigate the incorporation of dynamic covalent bonds into polymeric nanoparticles, an approach which has drastically increased the stimuli-responsiveness of nanoparticles and allowed utilization of a greater selection of polymer classes. More importantly, the application of dynamic chemistries opens up the possibility to tune the nature of the desired response through the particular choice of dynamic covalent linkage utilized.

1.4   Dynamic Covalent Cross-Linked Polymeric Nanoparticles

The integration of dynamic bonds, whether they be non-covalent supramolecular interactions or dynamic covalent bonds, into polymeric nanoparticles and materials can endow polymeric systems with responsive and adaptive properties, in addition to driving the self-assembly process. The incorporation of dynamic bonds has led to the development[43] of materials possessing interesting and novel responsive and adaptive properties.

Polymer chemist have employed dynamic supramolecular interactions such as hydrogen bonding,[44] ion-dipole interactions[45] and metal-ligand interactions[46] to link multiple polymer chains together, resulting in dynamic polymeric nanoparticles.

An alternative and extremely attractive route towards stimuli-responsive polymeric assemblies is the incorporation of ideas from the field of dynamic covalent chemistry[47] (DCC) into polymer chemistry. DCC uses reversible covalent bond formation to link organic building blocks into larger structures. In addition to facilitating self-assembly, the reversible nature of the dynamic covalent linkages enables product assemblies to modify their constitutions by exchanging and reshuffling their building blocks.[48-50] Dynamic covalent bond forming reactions proceed under

equilibrium control, and the position of the resulting equilibrium is often sensitive to changes in pH, concentration, temperature and pressure. This responsive nature makes dynamic covalent bonds appealing linkages to incorporate into responsive and adaptive polymeric nanoparticles as their reversible nature instils the "intelligent" virtues of controlled assembly, adaptability, and self-repair into the resultant nanostructures. In effect, dynamic covalent interactions provide a mechanism for a polymeric assembly to reconfigure its covalent structure and therefore its functional or material properties. Importantly, the strength of the covalent bond ensures product assemblies possess chemical robustness, a feature not often present with non-covalent supramolecular interactions such as hydrogen bonding. Furthermore, as reversible covalent reactions are usually performed with the help of a suitable catalyst to aid kinetics, the option exists to halt these reversible processes and kinetically "fix" the products simply by quenching the catalyst.
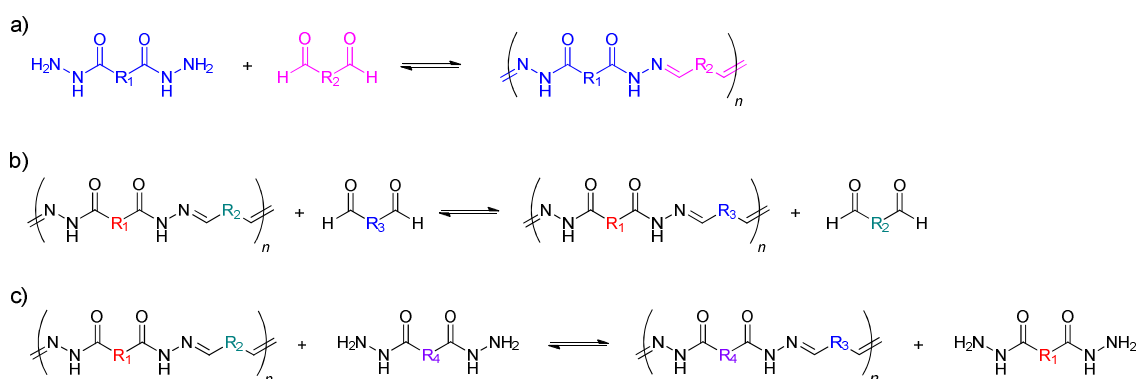
Scheme 1.2 (a) Dynamic poly(acylhydrazone) formation by condensation of a dihydrazide and a dialdehyde. Dynamic covalent polymer (dynamer) modification through (b) dialdehyde exchange and (c) dihydrazide exchange.

Arguably, the first application of so called 'dynamic covalent chemistry' in the field of polymer chemistry was the pioneering work of Lehn and Skene in 2004.[51] In this work the concept of linking multiple monomer units together through dynamic covalent bonds (Scheme 1.2) was presented, specifically the condensation of dihydrazide and dialdehyde monomer units to form a poly(acylhydrazone) (Scheme 1.2a). The authors have termed this class of dynamic polymer 'dynamers'. It was demonstrated that after initial condensation, different monomer units possessing alternative spacer units could be introduced into the polymer main chain through either dialdehyde (Scheme 1.2b) or dihydrazide exchange (Scheme 1.2c). This work demonstrated the great potential of dynamic covalent chemistry in the preparation polymeric materials which are able to incorporate or reshuffle components through an exchange pathway. The Lehn group

later demonstrated[52] that this dynamic hydrazone exchange mechanism could be utilized to change the mechanical properties of a dynamer-based polymeric film. A poly(acylhydrazone) was prepared initially from dihydrazide and dialdehyde monomer units which possessed highly flexible siloxane-derived spacer units. This dynamer formed a soft and flexible film after solvent evaporation, and it was then shown that this film could be re-dissolved and alternative dihydrazide and dialdehyde monomer units added which possessed rigid space units. After exchange and solvent evaporation, the newly formed film displayed rigid and hard mechanical properties. This work elegantly demonstrated the potential of dynamic covalent bonds in the preparation of responsive and adaptive polymeric materials which are able to change their mechanical strength.

The following section critically evaluates and summarises the recent development of polymeric nanoparticles which display stimuli-responsiveness through the incorporation of dynamic covalent bonds between multiple linear polymer chains.

1.4.1 *pH-Sensitive Imine Condensation*
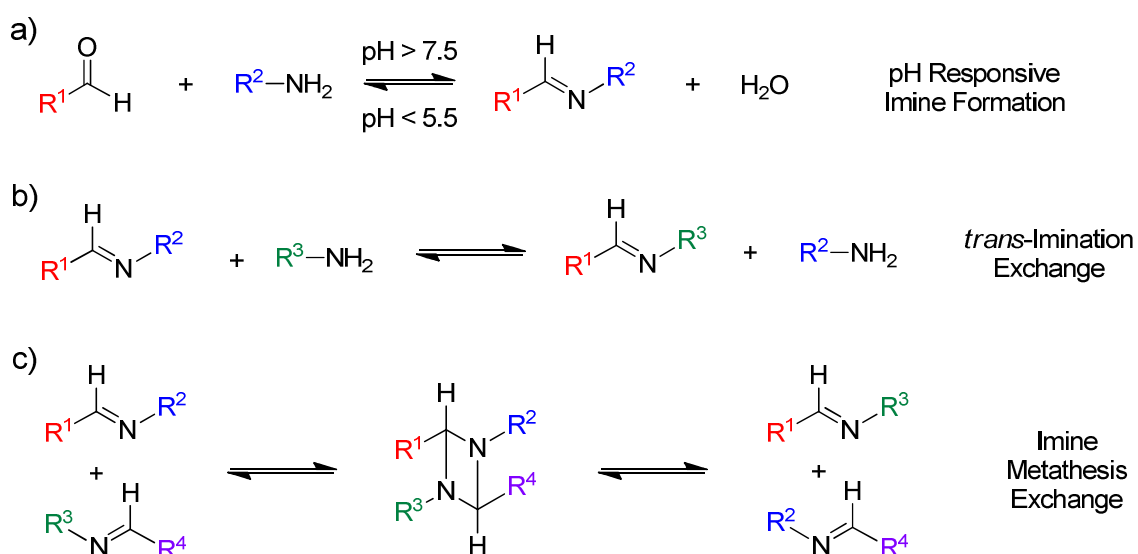
Scheme 1.3 Chemistry of the dynamic covalent imine bond.

The chemistry of the imine bond (Scheme 1.3) has been comprehensively studied[53, 54] and utilized in supramolecular chemistry.[55, 56] The formation of an imine bond from an aldehyde and amine (Scheme 1.3a) is pH sensitive in aqueous media, with imine formation favoured at high pH and disfavoured at low pH. The equilibrium position of imine formation is also sensitive to changes in concentration and temperature. Imine bonds can also undergo component exchange through *trans*-imination (Scheme 1.3b) and imine metathesis (Scheme 1.3c). These dynamic characteristics make imine

formation an attractive covalent linkage to incorporate into polymeric nanoparticles, and is a particularly appealing dynamic covalent reaction as it is possible to tune the stability of the imine bond by altering stereoelectronic characteristics of the reaction partners, in particular the carbonyl-derived part. The Lehn group performed a comprehensive study[57] of imine bond formation between 25 aldehydes and 13 imines, and it was clearly demonstrated that the equilibrium constant (K_{eq}) is pH dependent and that the pH at which hydrolysis occurs varies, and can thus be modulated through the selection of reaction partners.
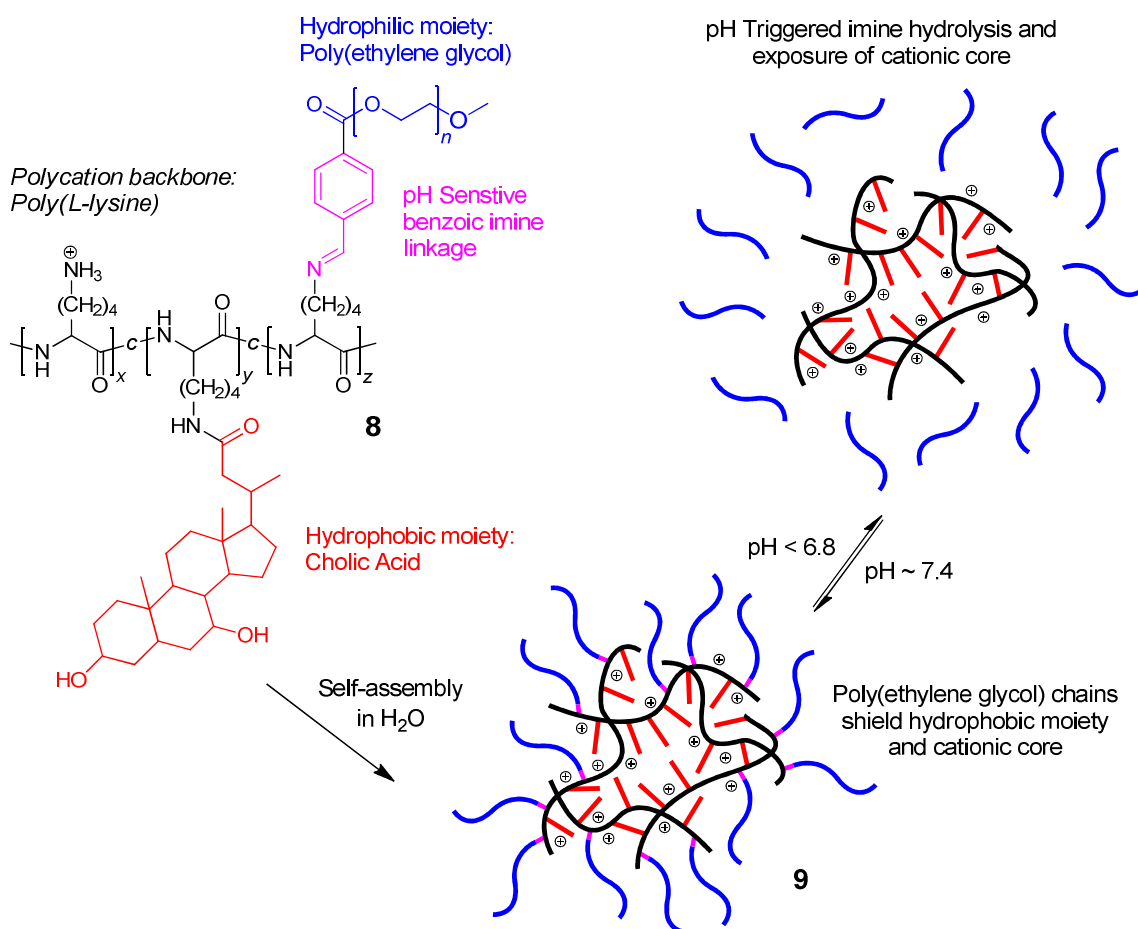
Figure 1.4 pH Triggered imine hydrolysis of aldehyde end-functionalized poly(ethylene glycol) from amine functional micellar assemblies based on cationic poly(L-lysine).

An early example of the exploitation of imine chemistry incorporated into polymeric nanoparticles was described[58] by the groups of Qu and Yang. This work utilizes (Figure 1.4) a cationic linear polymer building block based on poly(L-lysine) (**8**), which is functionalized through amide bond formation to introduce hydrophobic cholic acid residues, and then through imine bond formation with aldehyde end-functionalized hydrophilic poly(ethylene glycol) chains. These functional linear polymer building blocks were shown to self-assemble into micellar like architectures (**9**) in water on

account of the amphiphilic nature of the pendant functionalities. At physiological pH ~ 7.4 the imine bond is stable to hydrolysis and the poly(ethylene glycol) coronal arms remain attached to the core, protecting the cationic nature of the core and the covalently encapsulated cargo. A pH drop within the range of 5.0 – 6.0 similar to that found within an endosome, triggers imine bond hydrolysis, releasing the coronal arms and subsequently exposing cholic acid and the cationic amine functions. The resulting cationic polymer species is potentially membrane disruptive, and could be used as a drug delivery vehicle which destabilizes the endosomal membrane allowing the cargo to escape the endosome and enter the cell cytoplasm. This piece of work highlights the potential of the imine bond in dynamic covalent polymeric nanoparticles, demonstrating its potential to exploit the pH drop observed in the intracellular environment[41, 42] to expose covalently bound small molecules.

The reversible nature of the imine bond was further exploited[59] by this group. Aldehyde end-functionalized poly(ethylene glycol) was linked through imine bond formation to the hydrophobic small molecule $CH_3(CH_2)_{17}NH_2$ and the resulting amphiphilic species was shown to form micellar assemblies in water which disassemble at low pH on account of imine bond hydrolysis. This work further demonstrates that the introduction of a dynamic covalent linkage between two polymeric blocks can lead to stimuli-responsive micellar assemblies, which are able to disassemble in acidic conditions and subsequently release high value cargo.
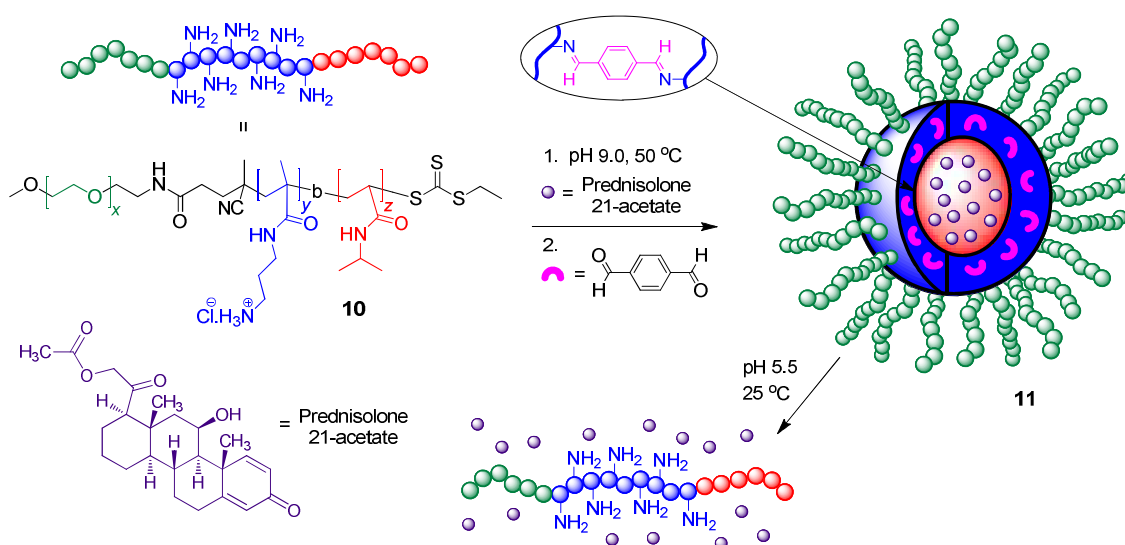
Figure 1.5 Imine shell cross-linked micellar assemblies possessing pH- and thermoresponsive characteristics.

The McCormick group have prepared[60] (Figure 1.5) a hydrophilic triblock copolymer (**10**) comprising poly(ethylene glycol)-*b*-poly(3-aminopropyl methacrylamide)-*b*-poly(*N*-isopropylacrylamide) (PEG-*b*-PAPMA-*b*-PNIPAm) via RAFT polymerization. This triblock copolymer was shown to form micellar assemblies (**11**) above the lower critical solution temperature (~ 37 °C) of the NIPAm block, which can encapsulate the hydrophobic drug molecule prednisolone 21-acetate (PA). The subsequent addition of the dialdehyde terephthaldicarboxaldehyde (TDA) cross-links the shell through imine bond formation with the amine functions of the poly(3-aminopropyl methacrylamide) block. The resulting micelle structures were shown to be both pH- and thermoresponsive. When the temperature is lowered to 25 °C the micelle core switches to hydrophilic and the slow release of the PA cargo is observed. Complete disassembly of the micelle is achieved through the adjustment of the pH to 5.5 at 25 °C, triggering imine hydrolysis and the burst release of PA. This cross-linked micellar system demonstrates how the thermoresponsive properties of poly(*N*-isopropylacrylamide) can be combined with the pH responsive and chemical robust nature of the dynamic covalent imine bond, affording a pH and temperature dual-stimuli responsive system. It is also highlighted how the rate of release of an encapsulated guest can be modulated, from a slow to a burst release, depending upon the combination of stimuli applied, and the likely potential application of this work lies in the field of controlled drug delivery.

1.4.2 *Redox-Responsive Disulfide Formation*
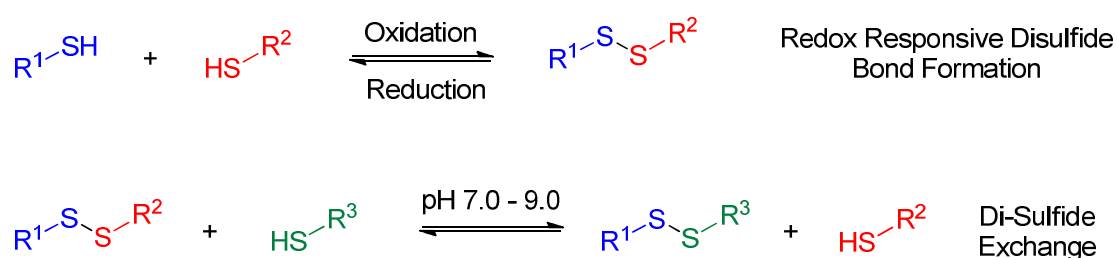
Scheme 1.4 Chemistry of the dynamic covalent disulfide bond.

The disulfide bond is a useful and widely-studied reaction in dynamic covalent chemistry[47] (Scheme 1.4). Disulfide bonds are particularity interesting as they are found in nature and play an important role in defining the tertiary and quaternary structure of many proteins[61] through intra- or intermolecular disulfide bond formation between thiol functional cysteine amino acid residues. The formation of the disulfide bond from its corresponding thiols is a redox sensitive process,[62] with formation occurring under

oxidative conditions and cleavage occurring under reductive conditions. Hydrogen peroxide[63] or iodine[64] in the presence of a base are both commonly used to promote disulfide bond formation, and reducing agents such as dithiothreitol, mercapoethanol and *tris*(carboxyethyl)phosphine[65, 66] are commonly used to reduce disulfide bonds. Cleavage can also be achieved using nucleophiles or electrophiles,[67, 68] or photochemically[69] or electrochemically.[70] Disulfide exchange reactions readily occur between pH 7 – 9, and this feature provides a mechanism to incorporate or release different components from polymeric nanoparticles. Much of the attention received by disulfide bonds is on account of their potential application in biomedical systems on account of the intracellular environment being highly reductive as a consequence of an increased concentration of glutathione, a biological reductant.[71, 72] This feature provides a route for disulfide cross-linked polymeric drug delivery vehicles to release their cargos within intracellular environments.

The groups of Matyjaszewski and Kataoka have utilized ATRP to prepare[73] biodegradable disulfide cross-linked nanogels under inverse miniemulsion conditions. These water-soluble nanogels are able to non-covalently encapsulate the anticancer drug doxorubicin, whose release within HeLa cancer cells is triggered by disulfide reduction caused by the presence of glutathione within the cell membrane. This work demonstrates how living radical polymerization techniques can be extended into inverse miniemulsion polymerization procedures in order to prepare nanogels possessing narrow distributions and the incorporation of diverse functionalities. The resulting nanogels retain the ATRP initiator functionality, which facilitates the polymerization of linear poly(styrene) coronal arms from the nanoparticle surface.[74] This post-formation functionalization would not be possible using traditional radical miniemulsion techniques. This body of work elegantly illustrates how advances in polymerization techniques can be combined with the reversible nature of the disulfide bond to afford highly novel and potentially very useful polymeric nanoparticles.

The Kataoka group have also investigated the incorporation of disulfide cross-links in the preparation of stimuli-responsive polymeric nanoparticles for potential applications as drug delivery vehicles. They have reported[75] the synthesis of poly(ethylene glycol)-*b*-(lysine) with thiol functions selectively introduced into the lysine repeat unit, through amide bond formation between the amine functions of lysine and 3-mercaptopropionic acid. This cationic diblock copolymer self-assembles through electrostatic interactions into a polyion complex (PIC) micelle with the anionic poly(α,β-aspartic acid). After self-assembly of the PIC micelle the thiol units within the

lysine core were oxidised to disulfide bonds. PIC micelle disassembly was then triggered through the addition of either glutathione or dithiothreitol. The introduction of dynamic covalent disulfide cross-links increases the stability of this PIC micelle, which would otherwise spontaneously disassemble below its critical micelle concentration (CMC) and thus greatly lowering its usefulness in the field of drug delivery. This work highlights how the reversibility and chemical robustness of the dynamic covalent disulfide bond can greatly increase the utility of polymeric nanoparticles which assemble non-covalently through ionic interactions.

Disulfide shell cross-linked micelles have been developed[76] by the groups of Armes and McCormick. They describe the synthesis of a poly(ethylene glycol)-b-(N,N'-dimethylacrylamide/ N-acryloxysuccinimide)-b-(N-isopropylacrylamide) triblock copolymer which forms micellar assemblies in water upon heating to 45 ºC on account of the thermoresponsive nature of poly(N-isopropylacrylamide), which when heated switches from hydrophilic to hydrophobic. The assembly process was performed in the presence of the drug dipyridamole, which was shown by fluorescence spectroscopy to non-covalently encapsulate within the micelle core. It was then shown that upon cooling to 25 ºC the micellar assemblies dissociate and release the encapsulated dipyridamole cargo. The addition of cystamine to the dipyridamole loaded micelles at 45 ºC, cross-links the micelle shell through amide bond formation at the active ester functions within the block containing the N-acryloxysuccinimide functions, thereby introducing disulfide linkages between multiple polymer chains. Micellar assemblies of this nature are named shell cross-linked (SCL) micelles. Upon cooling to 25 ºC, a temperature below the LCST of poly(N-isopropylacrylamide), these SCL micelles swell as a consequence of the hydrophilic nature of the core and subsequent influx of water molecules. It was demonstrated that the dipyridamole release can be triggered upon the addition of dithiothreitol, which cleaves the disulfide cross-links causing micelle disassembly. This particular system highlights the possibility to combine the inherent thermo-responsiveness of poly(N-isopropylacrylamide) with the redox-responsiveness of the disulfide bond to prepare dual-responsive micellar assemblies which possess increased stability on account of the covalent disulfide cross-links, and the ability to release encapsulated cargo with the application of either a change in temperature or addition of a reducing agent.
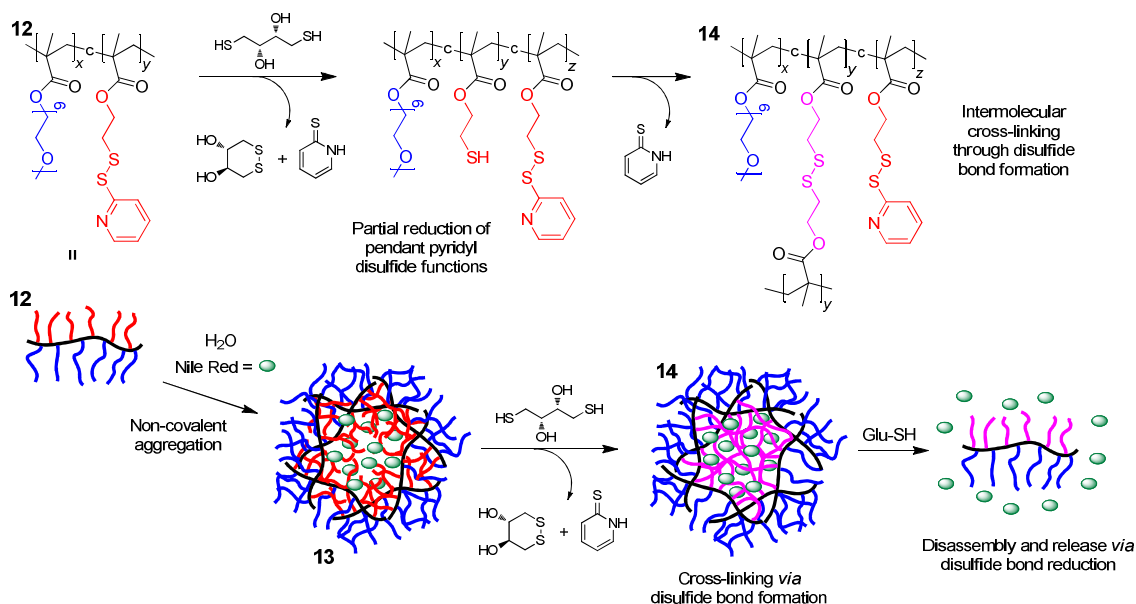
Figure 1.6 Formation of disulfide cross-linked nanogels and subsequent disassembly through disulfide bond reduction in the presence of glutathione.

The research group of Thayumanavan has developed (Figure 1.6) disulfide cross-linked polymeric nanogel assemblies[77-79] for application as drug delivery vehicles. Linear copolymer chains (**12**) possessing hydrophilic (oligoethylene glycol methacrylate) and hydrophobic (2-pyridyldisulfide ethylmethacrylate) monomer units were shown to non-covalently aggregate into nano-sized polymeric assemblies (**13**) upon heating in aqueous media as a consequence of the thermoresponsive nature of the oligoethylene glycol methacrylate monomer units. The addition of a deficient amount of dithiothreitol (DTT) reduces a portion of the pyridyldisulfide functions present upon the polymer chains to alkylthiols, which then intermolecularly cross-link with the remaining pyridyldisulfide functions. The resulting cross-linked nanogel assemblies (**14**) were shown to be very stable at lower temperatures on account of the covalent cross-links, and are shown to non-covalently encapsulate the hydrophobic small molecule fluorescent probe Nile Red. The triggered release of the encapsulated Nile Red cargo is achieved through exposure to the biologically-active reducing agent glutathione, which cleave the disulfide cross-links and triggers the disassembly of the nanogel into water-soluble linear polymer chains. This polymeric system is highly sophisticated, and the Thayumanavan group have demonstrated the capability to tune the rate of release, adjust the nanoparticle size and adorn the nanoparticle periphery through post-formation functionalization. It was shown that the rate of cargo release is dependent upon the concentration of glutathione, and the kinetics of cargo release can therefore be tuned by adjusting the density of disulfide cross-links, either by altering the amount of 2-pyridyldisulfide ethylmethacrylate in the linear polymer building block or by adjusting

the amount of DTT added. The hydrodynamic radius of the cross-linked nanoparticles can be tuned from 10 – 200 nm through altering the ratio of the hydrophilic and hydrophobic monomer units in the linear polymer building blocks, or by altering the overall length of the polymer building blocks. Particle size is very important in the field of drug delivery as it plays a crucial role in cell permeability and retention.[80] It was also demonstrated that excess pyridyldisulfide functions not employed in cross-linking can be used as handles for the post-functionalization of the nanogel assemblies, which were adorned with thiol modified peptides. The ability to perform post-functionalization is very important as biomolecules conjugated onto the nanoparticle periphery may increase specificity in cell targeting. Taken together, all of these features may increase the utility of nanogels in the field of drug delivery.

These examples highlight the chemical robustness and redox-responsive nature of nanoparticles which possess dynamic covalent disulfide cross-links. Disulfide bond formation is currently intensively investigated in the preparation of polymeric drug delivery vehicles, as the intracellular environment is known to be highly reductive.[81] The reducing agent glutathione has an intracellular concentration of 3 mM, which is 300 times greater than its concentration in blood which is approximately 10 µM. It is therefore widely hypothesized that polymeric nanoparticles possessing disulfide cross-links will only disassemble and release their encapsulated cargo within the intracellular environment, ensuring that drugs are only released within cells where they are required and not in the extracellular environment.

1.4.3 *pH-Dependent Acetal Hydrolysis*
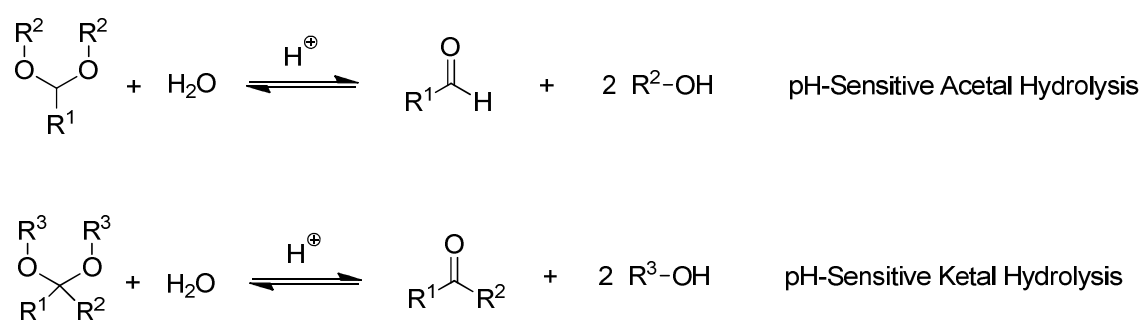
Scheme 1.5 Acetal and ketal hydrolysis.

Acetal formation between an aldehyde and two primary alcohols, or ketal formation between a ketone and two primary alcohols is often performed in organic solvents under acidic conditions. The resulting acetal/ketal functionality will readily hydrolyse

(Scheme 1.5) back to its component partners in aqueous media, and the rate of this hydrolysis is pH sensitive. This pH-responsive hydrolysis makes the incorporation of acetal/ketal functional groups within polymeric nanoparticles very appealing, as their acid catalysed hydrolysis can be utilized to trigger nanoparticle disassembly and subsequent cargo release within low pH environments. It is also possible to tune their stability by altering the electronic characteristics of the component aldehydes and alcohols. This feature could prove very useful in the field of controlled drug delivery, as certain tissue targets display low pH, such as inflammatory tissues and the phagolysosomes of antigen presenting cells.[82, 83]

This acetal/ ketal cross-links have been extensively exploited to introduce stability and pH-responsiveness into polymeric nanoparticles. However, as acetal/ketal formation does not readily proceed in aqueous environments, the incorporation of cross-linking acetal/ketal functions must be performed post-formation of the polymeric nanoparticle. This goal is often achieved through the addition of an acetal/ ketal-containing di-functional cross-linker, adding an undesirable layer of complexity. The polymer building blocks must incorporate a functionality which can be used to introduce the di-functional linker, and amide bond formation between diamino functional linkers and pendant activated esters is therefore often employed. These property prevents polymeric nanoparticles which disassemble through acetal/ ketal hydrolysis from re-assembling through subsequent acetal formation, resulting in a "one-use" disassembly pathway with no possibility for reformation. This is in contrast with imine or disulfide cross-linked nanoparticles, as these dynamic covalent bond forming reactions are completely reversible in aqueous environments and their formation/ disassembly can be reversibly cycled.

The Fréchet group have developed[84] acrylamide-based nanogels which possess acetal cross-links. These were achieved through the copolymerization of acrylamide monomer units and a di-acrylamide cross-linker which cross-links the growing polymer chains. This copolymerization was performed in the presence of the fluorescently labelled protein (Bovine Serum Albumin (BSA)). The di-acrylamide cross-linker contains an acetal linkage, thereby introducing the desired pH-sensitivity acetal linkages. They have demonstrated that under acidic conditions acetal hydrolysis occurs which triggers nanogel disassembly into linear polymer chains, a process which results in protein release from the nanogel interior. It was shown that disassembly and protein release occurs on a faster time scale at pH 5.0 compared to physiological pH of 7.4.

This piece of work is an early example of an acid degradable polymeric nanoparticle which utilizes acetal cross-links.

The Bulmus research group have also investigated[85] the potential of acetal cross-links to prepare pH-sensitive polymeric nanoparticles. Utilizing RAFT polymerization, the diblock copolymer poly(hydroxyethyl acrylate)-*b*-poly(*n*-butyl acrylate) was synthesised and shown to self-assemble into micellar assemblies in aqueous environments. The micelle cores were then cross-linked through the subsequent polymerization of a divinyl acetal-containing monomer. This post-micellization cross-linking polymerization was made possible as a consequence of the RAFT CTA dithiocarbonate functionality retention after isolation and purification of the initial diblock copolymer. It was also demonstrated that these cross-linked micelles were able to non-covalently encapsulate the drug doxorubicin within the hydrophobic micelle cores. The degradation of the cross-linked micelles and doxorubicin release was achieved through acetal hydrolysis, and the disassembly process was studied at pH 5.0 and pH 7.4. After 70 h, it was observed that approximately 70% and 30 % of encapsulated doxorubicin was released at pH 5.0 and 7.4, respectively. This work again demonstrates the great utility of living radical polymerization techniques, specifically the ability to cross-link multiple chains by continuing the polymerization process after self-assembly has occurred. This highly useful feature has been utilized by the Bulmus group to simultaneously stabilise the micellar assemblies and introduce stimuli-responsive characteristics.
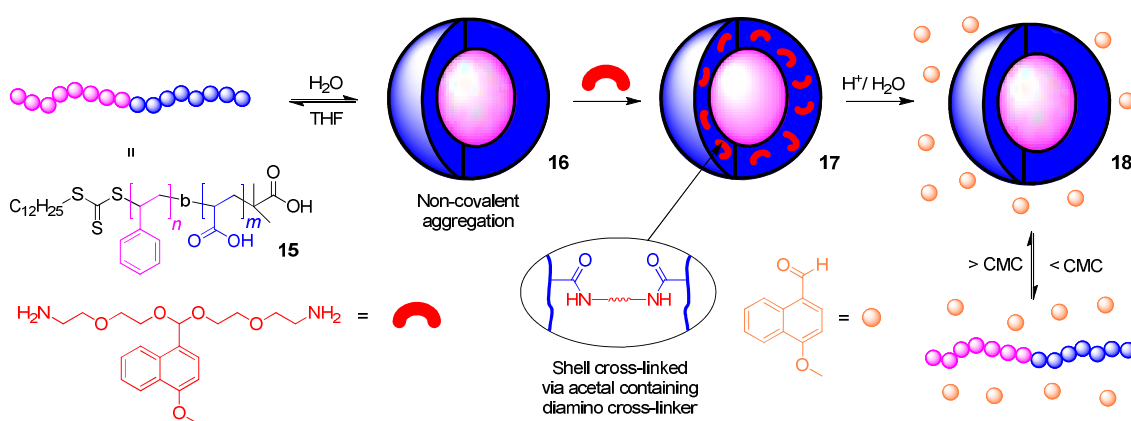
Figure 1.7 Shell cross-linked micelles possessing acid sensitive acetal linkages.

Acetal hydrolysis has also been utilized by Wooley and co-workers to prepare[86] micelles whose shells are cross-linked through acetal bonds (Figure 1.7). These micelles (**16**) were prepared through the micellization of poly(styrene)-*b*-(acrylic acid) (**15**) in

water, followed by shell cross-linking (**17**) *via* amide bond formation using a diamine cross-linker which contains an acetal linkage. At pH 5.0 acetal hydrolysis readily occurs (**18**), releasing the fluorescent molecule 4-methoxy-1-naphthaldehyde which was a by-product of acetal hydrolysis and chosen to help monitor the disassembly process. At physiological pH (7.4) acetal hydrolysis was shown to occur at a slower rate. Indeed, it was observed that acetal hydrolysis occurred with a 7-fold faster rate at pH 5.0, a feature which could make these nanoparticles potentially very useful in the field of controlled drug delivery. This work also exemplifies the utility of small molecule cross-linkers incorporating a specific molecule which upon release can play an important role monitoring the disassembly process. This concept could be extended further if the cross-linker were to incorporate a small molecule pharmaceutical, allowing the cross-linking process to be exploited to also introduce the desired cargo, in addition to imparting stimuli-responsiveness.
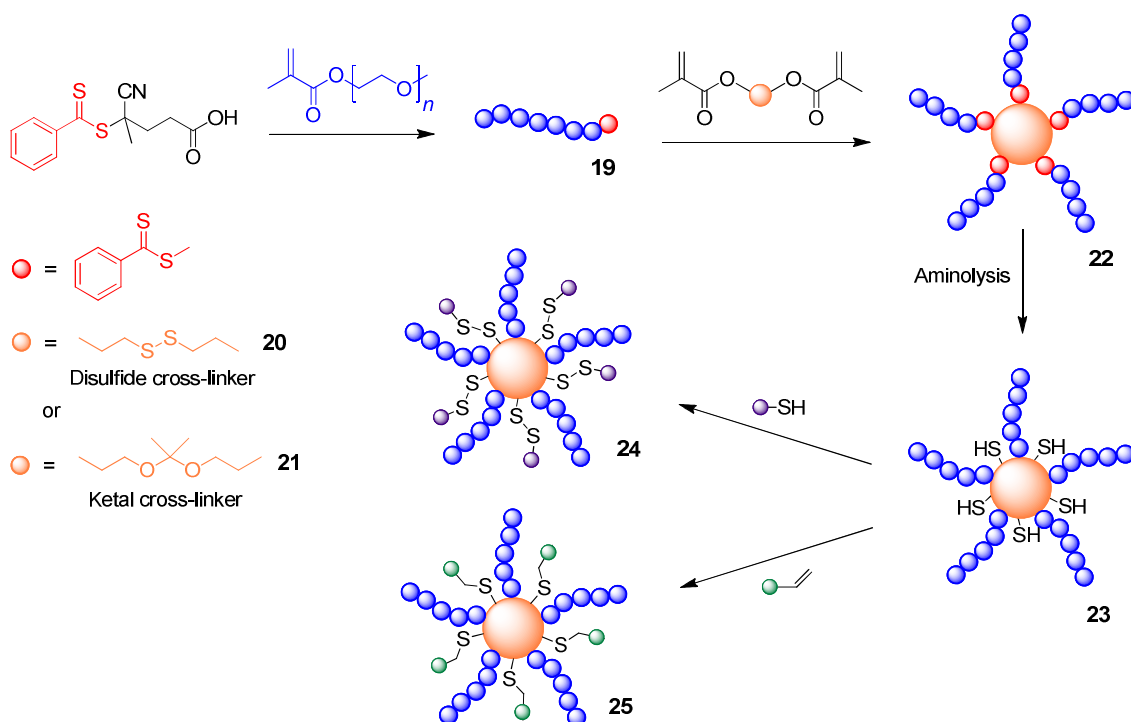
Figure 1.8 The formation of core cross-linked star polymers through the incorporation of either acetal or disulfide containing dimethacrylate monomer units during polymerization.

The groups of Haddleton and Davis have developed[87] stimuli-responsive biodegradable core cross-linked star (CCS) polymers (**22**, Figure 1.8). RAFT polymerization techniques were employed to synthesise poly(OEGMA) (**19**), which forms the coronal arms of the CCS polymers. The polymerization is then continued in the presence of dimethacrylate monomer units to cross-link the growing polymer chains into CCS polymers. Two different cross-linkers have been employed containing either a disulfide (**20**) or ketal (**21**) linkage, resulting in the formation of two types of CCS polymer

22

possessing either redox- or pH-responsive degradability on account of either disulfide or ketal cross-links present within their cores. These CCS polymers also possess dithiocarbonate functionalities from the retention of the RAFT chain transfer agent and aminolysis of these dithiocarbonate groups to thiol functions (**23**) permits post-formation functionalization through either disulfide bond formation (**24**) or thiol-ene click chemistry[88] (**25**). This feature has been exploited to tag these CCS polymers with fluorescent pyridyl disulfide appendages. The disassembly of the ketal CCS polymers was found to be pH-sensitive, with complete disassembly occurring within 12 h and 1 h, at pH 5.0 and 2.0 respectively. At pH 7.0 the CCS polymers were found to be stable for over 48 h. The disulfide CCS polymers were shown to disassemble over 1h in the presence of the reducing agent tributyl phosphine. The work demonstrates that traditional "arm first" CCS formation techniques can be evolved to introduce dynamic covalent cross-links between the growing polymer chains, and that living radical polymerization techniques introduce the possibility of post-polymerization functionalization at specific sites as a consequence of CTA functionality retention.
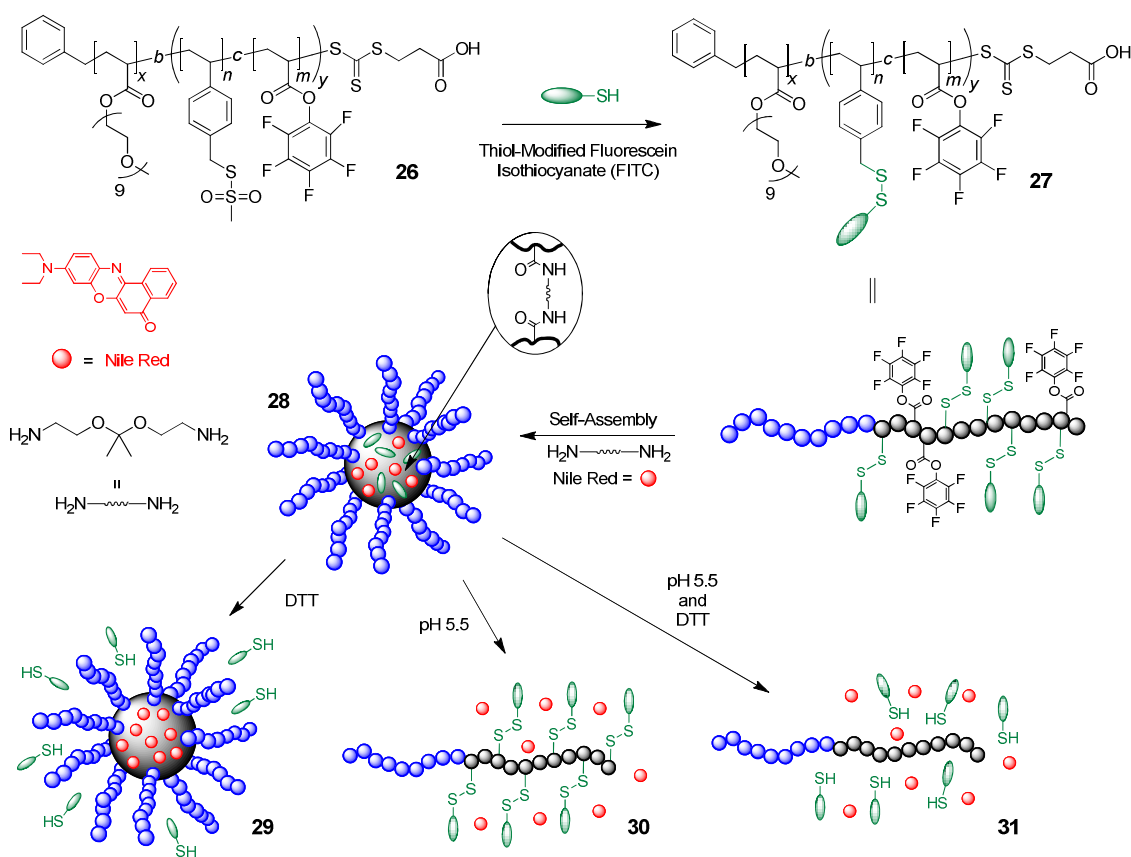
Figure 1.9 Formation of acetal cross-linked nanoparticles which can non-covalently encapsulate Nile Red while covalently encapsulating a thiol-modified fluorescein isothiocyanate (FITC) through disulfide bond formation.

The Davis research group has prepared[89] ketal cross-linked nanoparticles (**28**, Figure 1.9) which are able to incorporate and release both hydrophilic and hydrophobic small molecule guests simultaneously. These polymeric nanoparticles were prepared by synthesising linear diblock copolymer building blocks which possess a hydrophilic block, composed of OEGMA monomer units, and a functional block containing vinyl benzyl chloride and pentafluorophenyl acrylate co-monomers. The vinyl benzyl chloride monomer units within the functional block were then substituted using sodium methanethiosulfonate, yielding copolymer chains with methanethiosulfonate pendant functionality (**26**). The hydrophilic guest, a thiol-modified fluorescein isothiocyanate (FITC), was then covalently bound through disulfide bond exchange with the methanethiosulfonate functional groups (**27**). The resulting FITC functional polymer chains were then shown to self-assemble into micellar type aggregates in water. The self-assembly process was performed in the presence of the hydrophobic guest Nile Red, which was non-covalently encapsulated within the hydrophobic core. After self-assembly was achieved, a diamine cross-linker featuring a central ketal group was employed to intermolecularly cross-link the micellar cores (**28**) through amide bond formation with the activated esters of the pentafluorophenyl monomer units, introducing the desired ketal functionality. The polymeric nanoparticles were able to release FITC through disulfide reduction with the application of dithiothreitol (**29**), whilst maintaining the structural integrity of the nanoparticles. It was also possible to apply a low pH (**30**), triggering ketal hydrolysis and releasing Nile Red, or release both the guest molecules with the application of both reducing agent and low pH to cleave simultaneously the disulfide and ketal cross-links and triggering disassembly (**31**). This novel dynamic covalent polymeric nanoparticle utilizes two orthogonal reversible covalent bonds to yield a dual-stimuli responsive system, which is able to release its cargo in response to changes in redox potential or pH. The two distinct stimuli can be applied in three different combinations, with each combination affording a different outcome.

1.4.4 *Boronic Ester Formation and Hydrolysis*
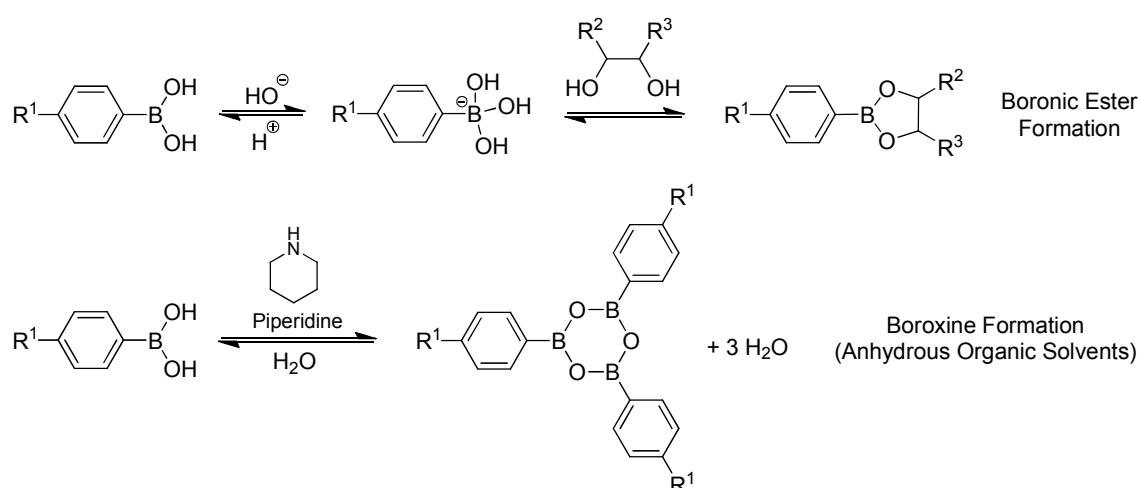
Scheme 1.6 Boronic ester formation between a boronic acid and a 1,2-diol and boronic acid trimerization in the presence of a Lewis base to form a cyclic boroxine.

Boronic acids are a very useful and well studied functional group in organic chemistry,[90, 91] finding numerous applications in catalysis,[92] asymmetric synthesis[93] and novel polymeric structures and materials.[94-96] The empty *p*-orbital on the boron atom endows it with Lewis acidity and permits sp^2 to sp^3 interconversion of its hybridization. In basic conditions the reversible reaction between a boronic acid and a hydroxide anion occurs, affording a tetrahedral boron anion which can then reversibly react with a 1,2- or 1,3-diol to form a cyclic boronic ester (Scheme 1.6). In acidic conditions the hydrolysis of the boronic ester back to the boronic acid is favourable. In anhydrous organic solvents and in the presence of a Lewis base such as piperidine, boronic acids can trimerize to form a six-membered boroxine (Scheme 1.6), a process which is reversible upon the addition of water. As a consequence of these useful properties, boronic acids have attracted much attention in biomedical applications,[97, 98] and in particular, they have been utilized to sense carbohydrates by reacting with 1,2-diols found in naturally occurring sugars.[99, 100]

Boronic acid containing-polymers have great potential in the field of stimuli-responsive polymeric nanoparticles. The Jäkle group has prepared[101] poly(styreneboronic acid)-*b*-polystyrene (PSBA-*b*-PS) diblock copolymers which were shown to non-covalently aggregate in aqueous environments into micellar assemblies on account of the amphiphilicity of the linear diblock copolymers. This micellar system utilizes the pH-sensitive sp^2 to sp^3 interconversion of boronic acids to trigger structural changes in micelle morphology. At high pH, when sp^3 hybridization is favourable, the

formation of spherical micelles is observed as a consequence of high interface curvature, caused by the electrostatic repulsion of the $B(OH)_3^-$ groups. At low pH, when sp^2 hybridization is favourable, worm-like assemblies were observed as the neutral $B(OH)_2$ functions do not induce any repulsion, reducing the interface curvature. This early boronic acid containing polymeric system does not utilize pH-sensitive formation of dynamic covalent boronic esters to trigger a structural change, however it does emphasises the versatility and potential of boronic acids in polymeric nanoparticles as a consequence of the pH-induced switch in hybridization.
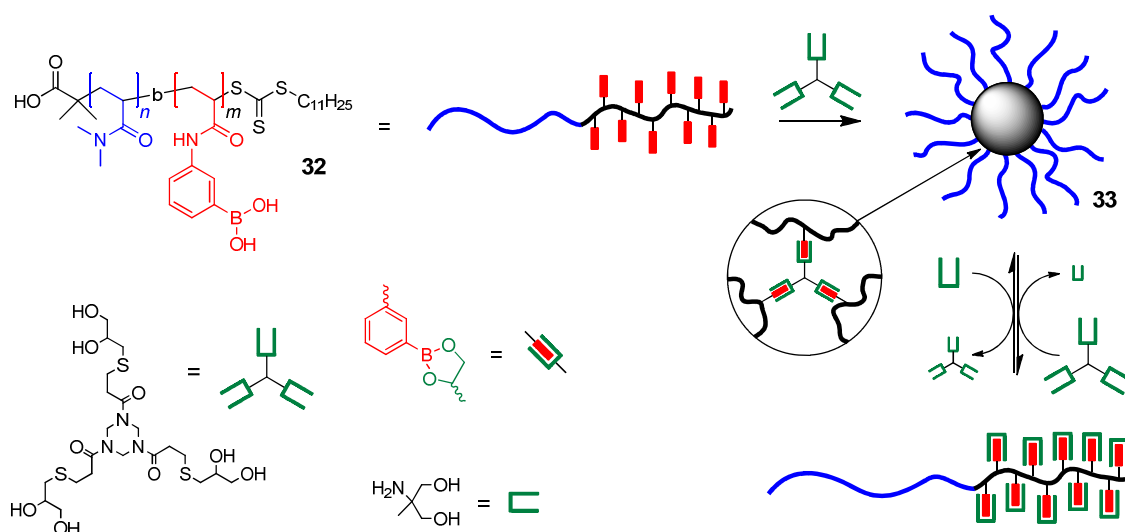
Figure 1.10 Star polymer formation *via* boronic ester formation between pendant boronic acid functions along a diblock copolymer chain and 1,2-diols within multifunctional small molecule cross-linkers.

The Sumerlin research group has focused on utilising the dynamic nature of boronic esters to prepare dynamic covalent cross-linked polymeric nanoparticles. The group has demonstrated[102] that boronic acid end-functionalized polymers prepared by RAFT can form three-arm star polymers as a consequence of boroxine cyclisation of the polymer end-groups in the presence of the Lewis base piperidine. The hydrolysis-triggered disassembly back to linear polymer chains was achieved through the addition of water. In subsequent work the Sumerlin group has also prepared[103, 104] (Figure 1.10) diblock copolymers containing pendant boronic acid functions within one of the blocks (**32**), and shown that these linear polymer chains can self-assemble into core cross-linked star polymers (**33**) through boronic ester formation with multifunctional small molecule 1,2- and 1,3-diols. Disassembly of the core cross-linked star polymers is achieved through the subsequent addition of an excess of monofunctional 1,2- and 1,3-diols, which exchange through a *trans*-esterification process, effectively capping the boronic acids

and cleaving the intermolecular cross-links. This piece of work demonstrates how boronic acid containing polymers can be used to prepare chemoresponsive polymeric nanoparticles which reconfigure their structural properties in the presence of naturally occurring 1,2- and 1,3-diols, such as sugars, polysaccharides, and nucleic acids, and the authors speculate this feature could potentially be exploited in the field of drug delivery.

1.4.5 *Thermally-Responsive TEMPO-Based Alkoxyamines*
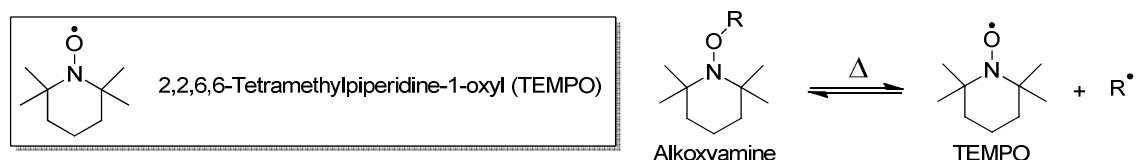
Scheme 1.7 The stable 2,2,6,6,-tetramethypiperidine-1-oxyl (TEMPO) radical and its reversible thermally-induced cleavage from a corresponding alkoxyamine.

2,2,6,6-Tetramethylpiperidine-1-oxyl (TEMPO) (Scheme 1.7) is a stable radical on account of the steric protection afford by the four adjacent methyl groups, derivatives of which are often referred to as a *nitroxyl* or *nitroxide* radicals. TEMPO has been extensively studied[105-107] as a radical trap with carbon-centred radicals, and derivatives of TEMPO have also been recently studied[108] for the same application. TEMPO has also found applications in synthesis[109] and catalysis.[110, 111] More recently TEMPO-based alkoxyamine derivatives have been used to mediate polymerizations, furnishing polymers with narrow polydispersity indices and desired end-group functionality, and this particular class of living radical polymerizations (LRP) has been named nitroxide-mediated polymerization (NMP).[13, 112-114]
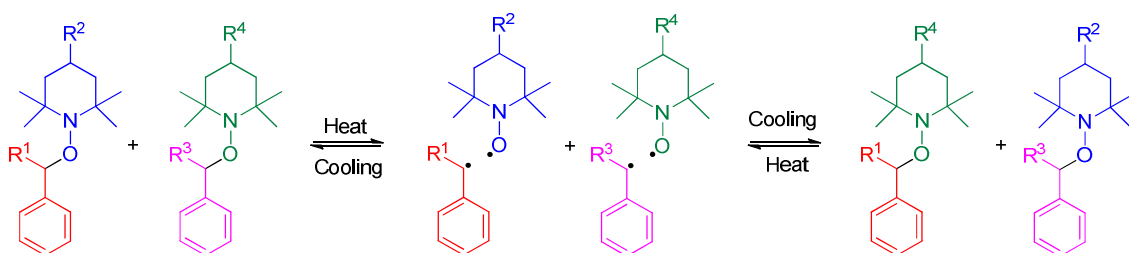
Scheme 1.8 Thermally-induced radical crossover reaction of alkoxyamine TEMPO derivatives utilized by the groups of Otsuka and Takahara.

The groups of Otsuka and Takahara have pioneered the use of TEMPO-based alkoxyamine derivatives in the preparation of thermally-dynamic polymeric systems (Scheme 1.8). The central C–O bonds within these alkoxyamine derivatives behave as

27

typical covalent bonds under ambient conditions. Upon heating this bond breaks homolytically and a styryl radical and a TEMPO-based radical are formed, and different components can exchange via radical crossover processes. The Japanese group have focused on employing these thermally dynamic functionalities as linkages within the main chain of linear polymers or between multiple polymer chains within polymeric nanoparticles, and have developed a host of polymeric materials and nanoparticles incorporating this thermally responsive linkage. Their early work in this field focused on preparing[115] dynamic covalent polymer chains incorporating thermally-dynamic TEMPO-based alkoxyamine within the main chain (**34**, Figure 1.11). These TEMPO containing monomer units can readily dissociate upon heating and recombine to form polymer chains of varying lengths. This early example demonstrates how linear polymer chains can reconfigure their structural properties at elevated temperatures through thermally exchangeable radical crossover reactions, which then become fixed at ambient conditions. Such thermally responsive polymers could find application in the field of self-healing materials, and Otsuka and Takahara have recently reviewed the current progress and potential applications in the field of dynamic covalent polymer chains.[116]
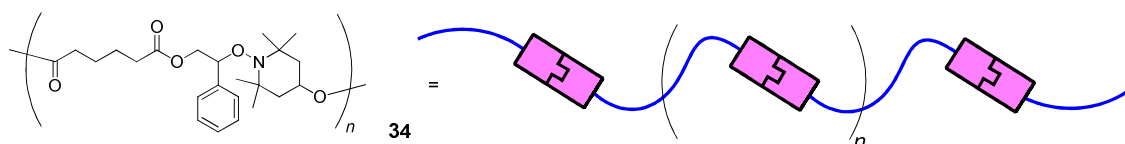
Figure 1.11 Dynamic covalent linear polymer chains incorporating a TEMPO derivative within the main chain.

Otsuka and Takahara have also utilized the thermoresponsive nature of 2,2,6,6-tertramethylpyperidine-1-oxy (TEMPO) based alkoxyamine derivatives to prepare[26] core cross-linked star (CCS) polymers (**36**, Figure 1.12). Linear diblock copolymer building blocks (**35**) which possess an inert block composed of methyl methacrylate, and a reactive block which contains complementary pendant alkoxyamine derivatives have been synthesised by ATRP. These pendant functionalities within the reactive block can undergo radical crossover reactions upon thermal stimulation, which facilitates the cross-linking of multiple polymer chains into CCS polymeric nanoparticles, whilst the inert blocks discourages macroscopic gelation. These CCS polymers become dynamic when heated and fixed when cooled, and this thermoresponsive nature can be used to trigger disassembly upon the addition of a small molecule TEMPO-based alkoxyamine,

which competes through a radical crossover reaction above 110 ºC. This group have also exploited this dynamic reaction to cross-link multiple linear polymer chains into star-like nanogel assemblies,[23, 117-119] discrete spherical nanoparticles[27] and macroscopically cross-linked organo-[120] and hydrogels.[121]
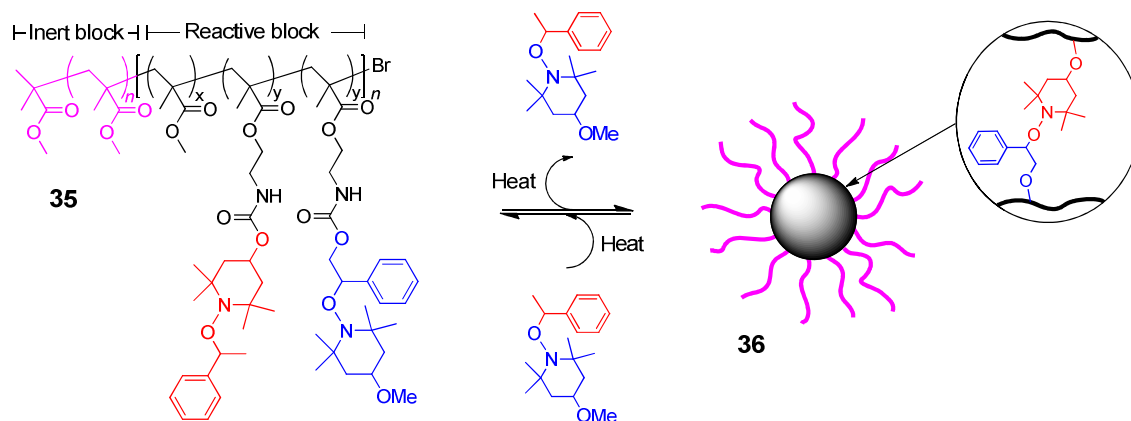
Figure 1.12 Core cross-linked star polymer formation via a TEMPO-based thermally exchangeable radical crossover reaction between multiple linear copolymer building blocks.

The research of Otsuka and Takahara elegantly demonstrates how previously-identified reversible reactions can be incorporated into polymeric systems to afford thermo- and chemoresponsive polymeric nanoparticles and materials. The application of alkoxyamine radical crossover reactions within polymeric nanoparticles is very interesting as the linkages are only reversible above 100 ºC, and consequently, these species possess covalent stability at lower temperatures. Otsuka and Takahara have recently demonstrated that this chemistry can be taken into aqueous environments[121] by employing 2-(dimethylamino)ethyl methacrylate monomer units, which are extremely hydrophilic after protonation with hydrochloric acid. However, as a consequence of the elevated temperatures required to promote structural reorganisation, applications in biological environments are arguably very unlikely.

1.4.6 *Photoresponsive Diels-Alder 2+2 Addition*
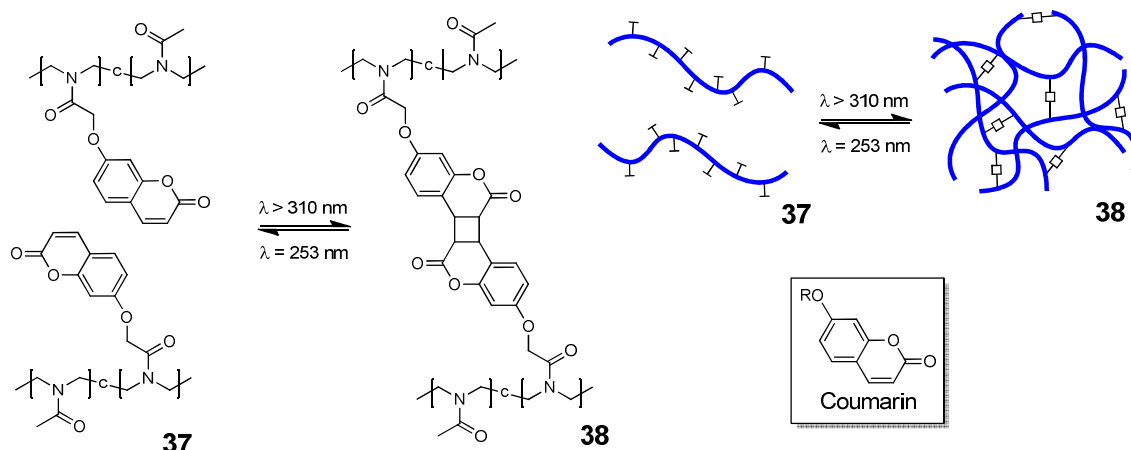
Figure 1.13 Photoresponsive polymeric networks via cross-linking through 2+2 cycloadditions of multiple polymer chains containing pendant coumarin functionalities.

Coumarin is known to undergo a photoreversible [2+2] cycloaddition dimerization upon ultraviolet radiation.[122, 123] This reversible covalent bond forming reaction has been exploited by the Saegusa group who have incorporated[124] coumarin units onto a polyoxazoline linear chain scaffold (**37**). This material is able to reversibly undergo a solution to gel (sol-gel) transition upon UV radiation at different wavelengths (Figure 1.13). Upon irradiation above 310 nm multiple polymer chains are cross-linked through the formation of cyclobutane rings, forming a macroscopically cross-linked gel (**38**). The degradation of these macroscopic gels can be triggered through cleavage of the cyclobutane cross-links through irradiation at 253 nm. Other photoresponsive chemistries have been incorporated into polymeric systems which can undergo gel-sol transitions for applications in biomedical devices.[125] This chemistry could also be employed to develop photoresponsive polymeric nanoparticles.

1.5   Conclusions

The field of responsive and adaptive polymeric nanoparticles is continuing to attract a great deal of attention. The development of living radical polymerization techniques has given polymer chemists the tools to prepare polymer building blocks with a high level of molecular precision, most significantly the incorporation of diverse functionalities along the polymer backbone and chain terminus. These developments have resulted in a vast array of novel polymeric building blocks, which can be used in the self-assembly of polymeric nanoparticles. With the aims of developing highly sophisticated polymeric

nanoparticles possessing the ability to change their structure/ physical properties or release components in response to a given stimuli, polymer chemists have looked to incorporate dynamic covalent bonds into or between multiple polymer chains, an approach which has immense possibilities, most notably in the field of controlled and targeted drug delivery, on account of the reversible virtues and chemical robustness of dynamic covalent bonds. While several dynamic covalent polymeric nanoparticles have already been prepared, there is still a huge amount of research to be carried out in this field. The continued utilization of dynamic covalent chemistry will furnish polymeric nanoparticles which possess multiple responsive characteristics with the ability to perform a combination of structural or physical changes in response to triggered changes in their environment.

1.6   References

1.   D. Roy, J. N. Cambre and B. S. Sumerlin, *Prog. Polym. Sci.*, 2010, **35**, 278-301.
2.   G. Pasparakis and M. Vamvakaki, *Polym. Chem.*, 2011, **2**, 1234-1248.
3.   J. M. Spruell and C. J. Hawker, *Chem. Sci.*, 2011, **2**, 18-26.
4.   K. E. Uhrich, S. M. Cannizzaro, R. S. Langer and K. M. Shakesheff, *Chem. Rev.*, 1999, **99**, 3181-3198.
5.   W. B. Liechty, D. R. Kryscio, B. V. Slaughter and N. A. Peppas, *Annu. Rev. Chem. Biomol. Eng.*, 2010, **1**, 149-173.
6.   L. Zhang, F. X. Gu, J. M. Chan, A. Z. Wang, R. S. Langer and O. C. Farokhzad, *Clin. Pharmacol. Ther.*, 2008, **83**, 761-769.
7.   S. Ganta, H. Devalapally, A. Shahiwala and M. Amiji, *J. Control. Release*, 2008, **126**, 187-204.
8.   E. B. Murphy and F. Wudl, *Prog. Polym. Sci.*, 2010, **35**, 223-251.
9.   C. J. Kloxin, T. F. Scott, B. J. Adzima and C. N. Bowman, *Macromolecules*, 2010, **43**, 2643-2653.
10.   W. A. Braunecker and K. Matyjaszewski, *Prog. Polym. Sci.*, 2007, **32**, 93-146.
11.   G. Moad, E. Rizzardo and S. H. Thang, *Aust. J. Chem.*, 2005, **58**, 379-410.
12.   K. Matyjaszewski and J. H. Xia, *Chem. Rev.*, 2001, **101**, 2921-2990.
13.   C. J. Hawker, A. W. Bosman and E. Harth, *Chem. Rev.*, 2001, **101**, 3661-3688.
14.   J. Chiefari, Y. K. Chong, F. Ercole, J. Krstina, J. Jeffery, T. P. T. Le, R. T. A. Mayadunne, G. F. Meijs, C. L. Moad, G. Moad, E. Rizzardo and S. H. Thang, *Macromolecules*, 1998, **31**, 5559-5562.
15.   G. Moad, E. Rizzardo and S. H. Thang, *Aust. J. Chem.*, 2006, **59**, 669-692.
16.   G. Moad, E. Rizzardo and S. H. Thang, *Aust. J. Chem.*, 2009, **62**, 1402-1472.
17.   M. A. Tasdelen, M. U. Kahveci and Y. Yagci, *Prog. Polym. Sci.*, 2011, **36**, 455-567.
18.   C. Boyer, M. H. Stenzel and T. P. Davis, *J. Polym. Sci., Part A*, 2011, **49**, 551-595.
19.   G. Riess, *Prog. Polym. Sci.*, 2003, **28**, 1107-1170.
20.   R. K. O'Reilly, C. J. Hawker and K. L. Wooley, *Chem. Soc. Rev.*, 2006, **35**, 1068-1083.
21.   H. Gao and K. Matyjaszewski, *J. Am. Chem. Soc.*, 2007, **129**, 11828-11834.

22. H. F. Gao and K. Matyjaszewski, *Macromolecules*, 2008, **41**, 1118-1125.
23. Y. Amamoto, M. Kikuchi, H. Masunaga, S. Sasaki, H. Otsuka and A. Takahara, *Macromolecules*, 2010, **43**, 1785-1791.
24. A. W. Jackson and D. A. Fulton, *Chem. Commun.*, 2011, **47**, 6807-6809.
25. A. W. Jackson, C. Stakes and D. A. Fulton, *Polym. Chem.*, 2011, **2**, 2500-2511.
26. Y. Amamoto, Y. Higaki, Y. Matsuda, H. Otsuka and A. Takahara, *J. Am. Chem. Soc.*, 2007, **129**, 13298-13304.
27. Y. Higaki, H. Otsuka and A. Takahara, *Macromolecules*, 2006, **39**, 2121-2125.
28. C. d. l. H. Alarcon, S. Pennadam and C. Alexander, *Chem. Soc. Rev.*, 2005, **34**, 276-285.
29. H. G. Schild, *Prog. Polym. Sci.*, 1992, **17**, 163-249.
30. M. D. C. Topp, P. J. Dijkstra, H. Talsma and J. Feijen, *Macromolecules*, 1997, **30**, 8518-8520.
31. C. M. Schilli, M. F. Zhang, E. Rizzardo, S. H. Thang, Y. K. Chong, K. Edwards, G. Karlsson and A. H. E. Muller, *Macromolecules*, 2004, **37**, 7861-7866.
32. F. Kohori, K. Sakai, T. Aoyagi, M. Yokoyama, Y. Sakurai and T. Okano, *J. Control. Release*, 1998, **55**, 87-98.
33. J. E. Chung, M. Yokoyama, M. Yamato, T. Aoyagi, Y. Sakurai and T. Okano, *J. Control. Release*, 1999, **62**, 115-127.
34. J. C. Leroux, E. Roux, D. Le Garrec, K. L. Hong and D. C. Drummond, *J. Control. Release*, 2001, **72**, 71-84.
35. S. H. Qin, Y. Geng, D. E. Discher and S. Yang, *Adv. Mater.*, 2006, **18**, 2905-2909.
36. L. A. Lyon, Z. Y. Meng, N. Singh, C. D. Sorrell and A. S. John, *Chem. Soc. Rev.*, 2009, **38**, 865-874.
37. M. Nakayama and T. Okano, *J. Drug Delivery Sci. Technol.*, 2006, **16**, 35-44.
38. H. Wei, S. X. Cheng, X. Z. Zhang and R. X. Zhuo, *Prog. Polym. Sci.*, 2009, **34**, 893-910.
39. J. F. Tan, P. Ravi, H. P. Too, T. A. Hatton and K. C. Tam, *Biomacromolecules*, 2005, **6**, 498-506.
40. M. Oishi and Y. Nagasaki, *React. Funct. Polym.*, 2007, **67**, 1311-1329.
41. D. Schmaljohann, *Adv. Drug Delivery Rev.*, 2006, **58**, 1655-1670.
42. Y. Bae, S. Fukushima, A. Harada and K. Kataoka, *Angew. Chem., Int. Ed.*, 2003, **42**, 4640-4643.
43. R. J. Wojtecki, M. A. Meador and S. J. Rowan, *Nat. Mater.*, 2011, **10**, 14-27.
44. E. M. Todd and S. C. Zimmerman, *J. Am. Chem. Soc.*, 2007, **129**, 14534-14535.
45. F. Huang, D. S. Nagvekar, C. Slebodnick and H. W. Gibson, *J. Am. Chem. Soc.*, 2004, **127**, 484-485.
46. L. Munuera and R. K. O'Reilly, *Dalton Trans.*, 2010, **39**, 388-391.
47. S. J. Rowan, S. J. Cantrill, G. R. L. Cousins, J. K. M. Sanders and J. F. Stoddart, *Angew. Chem., Int. Ed.*, 2002, **41**, 898-952.
48. P. T. Corbett, J. Leclaire, L. Vial, K. R. West, J. L. Wietor, J. K. M. Sanders and S. Otto, *Chem. Rev.*, 2006, **106**, 3652-3711.
49. J. M. Lehn, *Chem. Soc. Rev.*, 2007, **36**, 151-160.
50. J. M. Lehn, *Prog. Polym. Sci.*, 2005, **30**, 814-831.
51. W. G. Skene and J. M. P. Lehn, *Proc. Natl. Acad. Sci. U. S. A.*, 2004, **101**, 8270-8275.
52. T. Ono, S. Fujii, T. Nobori and J. M. Lehn, *Chem. Commun.*, 2007, 46-48.
53. R. W. Layer, *Chem. Rev.*, 1963, **63**, 489-510.
54. S. Patai, *Ed. The Chemistry of the Carbon-Nitrogen Double Bond; Interscience: London*, 1968.

55. C. D. Meyer, C. S. Joiner and J. F. Stoddart, *Chem. Soc. Rev.*, 2007, **36**, 1705-1723.

56. M. E. Belowich and J. F. Stoddart, *Chem. Soc. Rev.*, 2012, **41**, 2003-2024.

57. C. Godoy-Alcantar, A. K. Yatsimirsky and J. M. Lehn, *J. Phys. Org. Chem.*, 2005, **18**, 979-985.

58. J. Gu, W.-P. Cheng, J. Liu, S.-Y. Lo, D. Smith, X. Qu and Z. Yang, *Biomacromolecules*, 2007, **9**, 255-262.

59. C. X. Ding, J. X. Gu, X. Z. Qu and Z. Z. Yang, *Bioconjugate Chem.*, 2009, **20**, 1163-1170.

60. X. W. Xu, J. D. Flores and C. L. McCormick, *Macromolecules*, 2011, **44**, 1327-1334.

61. J. M. Thornton, *J. Mol. Biol.*, 1981, **151**, 261-287.

62. J. K. Howie, J. J. Houts and D. T. Sawyer, *J. Am. Chem. Soc.*, 1977, **99**, 6323-6326.

63. Y. Wang and J. H. Espenson, *J. Org. Chem.*, 2000, **65**, 104-107.

64. C. C. Silveira and S. R. Mendes, *Tetrahedron Lett.*, 2007, **48**, 7469-7471.

65. J. A. Burns, J. C. Butler, J. Moran and G. M. Whitesides, *J. Org. Chem.*, 1991, **56**, 2648-2650.

66. J. C. Han and G. Y. Han, *Anal. Biochemistry*, 1994, **220**, 5-10.

67. A. J. Parker and N. Kharasch, *Chem. Rev.*, 1959, **59**, 583-628.

68. J. L. Kice, *Acc. Chem. Res.*, 1968, **1**, 58-64.

69. C. W. Bookwalter, D. L. Zoller, P. L. Ross and M. V. Johnston, *J. Am. Soc. Mass Spectrom.*, 1995, **6**, 872-876.

70. T. B. Christensen and K. Daasbjerg, *Acta. Chem. Scand.*, 1997, **51**, 307-317.

71. M. J. Heffernan and N. Murthy, *Ann. Biomed. Eng.*, 2009, **37**, 1993-2002.

72. A. Bernkop-Schnurch, *Adv. Drug Delivery Rev.*, 2005, **57**, 1569-1582.

73. J. K. Oh, D. J. Siegwart, H. I. Lee, G. Sherwood, L. Peteanu, J. O. Hollinger, K. Kataoka and K. Matyjaszewski, *J. Am. Chem. Soc.*, 2007, **129**, 5939-5945.

74. J. K. Oh, C. B. Tang, H. F. Gao, N. V. Tsarevsky and K. Matyjaszewski, *J. Am. Chem. Soc.*, 2006, **128**, 5578-5584.

75. Y. Kakizawa, A. Harada and K. Kataoka, *J. Am. Chem. Soc.*, 1999, **121**, 11247-11248.

76. Y. T. Li, B. S. Lokitz, S. P. Armes and C. L. McCormick, *Macromolecules*, 2006, **39**, 2726-2728.

77. J. H. Ryu, R. T. Chacko, S. Jiwpanich, S. Bickerton, R. P. Babu and S. Thayumanavan, *J. Am. Chem. Soc.*, 2010, **132**, 17227-17235.

78. S. Jiwpanich, J. H. Ryu, S. Bickerton and S. Thayumanavan, *J. Am. Chem. Soc.*, 2010, **132**, 10683-10685.

79. J. H. Ryu, S. Jiwpanich, R. Chacko, S. Bickerton and S. Thayumanavan, *J. Am. Chem Soc.*, 2010, **132**, 8246-8247.

80. H. Maeda, J. Wu, T. Sawa, Y. Matsumura and K. Hori, *J. Control. Release*, 2000, **65**, 271-284.

81. A. Meister and M. E. Anderson, *Annu. Rev. Biochem.*, 1983, **52**, 711-760.

82. G. Helmlinger, A. Schell, M. Dellian, N. S. Forbes and R. K. Jain, *Clin. Cancer Res.*, 2002, **8**, 1284-1291.

83. A. S. Trevani, G. Andonegui, M. Giordano, D. H. Lopez, R. Gamberale, F. Minucci and J. R. Geffner, *J. Immunology*, 1999, **162**, 4849-4857.

84. N. Murthy, Y. X. Thng, S. Schuck, M. C. Xu and J. M. J. Frechet, *J. Am. Chem. Soc.*, 2002, **124**, 12398-12399.

85. Y. Chan, T. Wong, F. Byrne, M. Kavallaris and V. Bulmus, *Biomacromolecules*, 2008, **9**, 1826-1836.

86. Y. L. Li, W. J. Du, G. R. Sun and K. L. Wooley, *Macromolecules*, 2008, **41**, 6605-6607.
87. J. A. Syrett, D. M. Haddleton, M. R. Whittaker, T. P. Davis and C. Boyer, *Chem. Commun.*, 2011, **47**, 1449-1451.
88. C. E. Hoyle and C. N. Bowman, *Angew. Chem., Int. Ed.*, 2010, **49**, 1540-1573.
89. H. T. T. Duong, C. P. Marquis, M. Whittaker, T. P. Davis and C. Boyer, *Macromolecules*, 2011, **44**, 8008-8019.
90. J. P. Lorand and J. O. Edwards, *J. Org. Chem.*, 1959, **24**, 769-774.
91. A. L. Korich and P. M. Iovine, *Dalton Trans.*, 2010, **39**, 1423-1431.
92. H. C. Zheng, R. McDonald and D. G. Hall, *Chem. Eur. J.*, 2010, **16**, 5454-5460.
93. N. A. Petasis, *Aust. J. Chem.*, 2007, **60**, 795-798.
94. F. Cheng and F. Jakle, *Polym. Chem.*, 2011, **2**, 2122-2132.
95. K. Severin, *Dalton Trans.*, 2009, **27**, 5254-5264.
96. F. Jakle, *J. Inorg. Organomet. Polym. Mater.*, 2005, **15**, 293-307.
97. J. N. Cambre and B. S. Sumerlin, *Polymer*, 2011, **52**, 4631-4643.
98. P. C. Trippier and C. McGuigan, *Med. Chem. Commun.*, 2010, **1**, 183-198.
99. W. Wang, X. M. Gao and B. H. Wang, *Curr. Org. Chem.*, 2002, **6**, 1285-1317.
100. M. Dowlut and D. G. Hall, *J. Am. Chem. Soc.*, 2006, **128**, 4226-4227.
101. Y. Qin, V. Sukul, D. Pagakos, C. Z. Cui and F. Jakle, *Macromolecules*, 2005, **38**, 8987-8990.
102. P. De, S. R. Gondi, D. Roy and B. S. Sumerlin, *Macromolecules*, 2009, **42**, 5614-5621.
103. J. N. Cambre, D. Roy, S. R. Gondi and B. S. Sumerlin, *J. Am. Chem. Soc.*, 2007, **129**, 10348-10349.
104. A. P. Bapat, D. Roy, J. G. Ray, D. A. Savin and B. S. Sumerlin, *J. Am. Chem. Soc.*, 2011, **133**, 19832-19838.
105. A. L. J. Beckwith, V. W. Bowry and K. U. Ingold, *J. Am. Chem. Soc.*, 1992, **114**, 4983-4992.
106. V. W. Bowry and K. U. Ingold, *J. Am. Chem. Soc.*, 1992, **114**, 4992-4996.
107. I. W. C. E. Arends, P. Mulder, K. B. Clark and D. D. M. Wayner, *J. Phys. Chem.*, 1995, **99**, 8182-8189.
108. M. V. Ciriano, H.-G. Korth, W. B. van Scheppingen and P. Mulder, *J. Am. Chem. Soc.*, 1999, **121**, 6375-6381.
109. T. Vogler and A. Studer, *Synthesis*, 2008, **13**, 1979-1993.
110. P. L. Bragd, H. van Bekkum and A. C. Besemer, *Top. Catal.*, 2004, **27**, 49-66.
111. T. Fey, H. Fischer, S. Bachmann, K. Albert and C. Bolm, *J. Org. Chem.*, 2001, **66**, 8154-8159.
112. M. K. Georges, R. P. N. Veregin, P. M. Kazmaier and G. K. Hamer, *Macromolecules*, 1993, **26**, 2987-2988.
113. D. Greszta and K. Matyjaszewski, *Macromolecules*, 1996, **29**, 7661-7670.
114. C. J. Hawker, G. G. Barclay, A. Orellana, J. Dao and W. Devonport, *Macromolecules*, 1996, **29**, 5245-5254.
115. H. Otsuka, K. Aotani, Y. Higaki and A. Takahara, *Chem. Commun.*, 2002, 2838-2839.
116. T. Maeda, H. Otsuka and A. Takahara, *Prog. Polym. Sci.*, 2009, **34**, 581-604.
117. Y. Amamoto, T. Maeda, M. Kikuchi, H. Otsuka and A. Takahara, *Chem. Commun.*, 2009, 689-691.
118. Y. Amamoto, M. Kikuchi, H. Otsuka and A. Takahara, *Polym. J.*, 2010, **42**, 860-867.
119. Y. Amamoto, M. Kikuchi, H. Otsuka and A. Takahara, *Macromolecules*, 2010, **43**, 5470-5473.

120. Y. Amamoto, M. Kikuchi, H. Masunaga, S. Sasaki, H. Otsuka and A. Takahara, *Macromolecules*, 2009, **42**, 8733-8738.
121. J. Su, Y. Amamoto, M. Nishihara, A. Takahara and H. Otsuka, *Polym. Chem.*, 2011, **2**, 2021-2026.
122. L. H. Leenders, E. Schouteden and F. C. De Schryver, *J. Org Chem.*, 1973, **38**, 957-966.
123. N. Yonezawa, T. Yoshida and M. Hasegawa, *J. Chem. Soc., Perkin Trans. 1*, 1983, **5**, 1083-1086.
124. Y. Chujo, K. Sada and T. Saegusa, *Macromolecules*, 1990, **23**, 2693-2697.
125. I. Tomatsu, K. Peng and A. Kros, *Adv. Drug Delivery Rev.*, 2011, **63**, 1257-1266.

Chapter 2

Dynamic Covalent Diblock Copolymers

Table of Contents:

2.1   Abstract

Aldehyde- or alkoxyamine-containing trithiocarbonate chain transfer agents were prepared and used to mediate the synthesis of a series of polymers end-functionalized with aldehyde or alkoxyamine functions, utilising reversible addition-fragmentation polymerization techniques. Aldehyde end-functionalized polymers were shown to link through oxime bond formation with alkoxyamine end-functionalized polymers forming diblock copolymers. The dynamic nature of the oxime bond linking these polymer blocks together was demonstrated through a simple exchange reaction with a small molecule alkoxyamine. A diblock copolymer prepared from the self-assembly of an aldehyde end-functionalized poly(isoprene) with an alkoxyamine end-functionalized poly(styrene) was shown to undergo further hierarchical self-assembly into micellar aggregates in DMF. It was shown that the addition of an excess of a small molecule alkoxyamine triggered the disassembly of these micelles.

2.2   Introduction
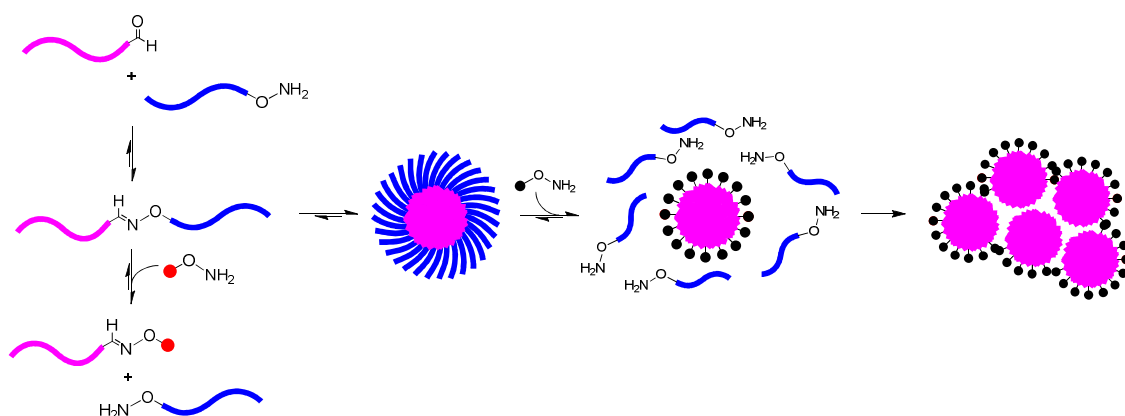
Figure 2.1 Formation of dynamic covalent diblock copolymers, subsequent assembly into micellar aggregates and disassembly through addition of a small molecule alkoxyamine.

Block copolymers have been extensively studied over recent decades, with their ability to act as building blocks for the self-assembly of nano-scale objects such as micelles and vesicles[1, 2] being of particular interest as these species can be used as dispersants[3] and emulsifiers.[4] More recently, there has been a large effort in the development of micellar systems for the targeted and controlled intracellular delivery of pharmaceuticals.[5, 6]

To increase the utility of self-assembled micellar aggregates, polymer chemists have employed dynamic and reversible supramolecular interactions such as hydrogen-

bonding,[7-10] metal-ligand interactions,[11-14] or a combination of both[15] to link polymer blocks together. Recent advances have also seen the utilization of the macrocyclic host cucurbit[8]uril as a supramolecular "handcuff" to link polymer chains into supramolecular diblock copolymers in water,[16] and pseudorotaxane formation has also been utilized[17] to link polymer blocks end-functionalized with either crown ethers or secondary ammonium salts. In addition to facilitating self-assembly, supramolecular interactions can impart dynamic behaviour into the resultant block copolymer assemblies, which are also incorporated into their supramolecular aggregates.

After a survey of the current literature (Chapter 1), we became intrigued by the possibility of using ideas from the field of dynamic covalent chemistry (DCC)[18] to develop responsive and adaptive polymeric nanoparticles. It was hypothesized that diblock copolymers where the polymer blocks are joined through a dynamic covalent bond would be able to reshuffle and exchange their blocks through a dynamic exchange pathway, this adaptive capability could be exploited to trigger micelle decomposition and subsequent cargo release. The synthetic strategy described utilizes reversible addition-fragmentation chain transfer (RAFT) polymerization to prepare end-functionalized polymers, employing thiocarbonylthio-containing chain transfer agents (CTAs) to mediate the polymerization process. It is well understood that these CTAs can be modified to incorporate a wide range of functionalities, which are then transferred to the resulting polymer chain terminus.[19] This chapter describes the synthesis of aldehyde and alkoxyamine functional RAFT chain transfer agents which were then used to prepare end-functionalized linear polymer chains possessing these functionalities. These polymer building blocks were shown to link together through a *single dynamic covalent oxime bond*, and their subsequent aggregation into micellar assemblies (Figure 2.1) is demonstrated. There has been impressive work describing micellization of dynamic covalent surfactants,[20, 21] however, this work describes the first examples of dynamic covalent block copolymers of a truly polymeric nature.

2.3   Results and Discussion

2.3.1   *Synthesis of Modified Chain Transfer Agents*

Oxime exchange was chosen as our dynamic covalent reaction to link preformed polymer blocks into diblock copolymers, as it is a well-studied and successful reaction in dynamic covalent chemistry.[18, 22] The equilibrium position of the reaction between an aldehyde and an alkoxyamine lies very much on the side of the resulting oxime bond. This feature was especially important for the work described in this chapter, as it was desirable to maximise the amount of component mono-block polymer chains converted into diblock copolymers, as any unreacted polymer chains could precipitate out of solution during micellization if not linked to a solubilising polymer block. To prepare polymer chains end-functionalized with either alkoxyamine or aldehyde groups, we utilized reversible addition-fragmentation transfer (RAFT) polymerization techniques.[23-26] RAFT is a living radical polymerization technique which allows access to a range of well-defined polymer structures possessing high levels of end-group fidelity, and is mediated by a chain transfer agent (CTA) typically based on dithioesters or trithiocarbonates. The use of modified CTAs allows the preparation of polymers end-functionalized with a specific functional group and overcomes the limitations of post-polymerization strategies. This approach has been used by the group of Sumerlin to prepare[27] α-azido terminal polymers, the group of Maynard to prepare pyridyl disulfide[28] and alkoxyamine[29] terminal polymers and the Pan group to prepare[30] *mono*-biotinylated polymers. Thus, 4-carboxybenzaldehyde was refluxed in toluene with an excess of thionyl chloride after evaporation to dryness the resulting crude acid chloride was reacted with triethylene glycol to prepare 2-[2-(2-hydroxyethoxy)ethoxy]ethyl-4-formylbenzoate (**1**, Scheme 2.1) in a yield of 50 %. The aldehyde-containing chain transfer agent (**2**) was then prepared (Scheme 1) in a yield of 59% via a carbodiimide-mediated coupling between the chain transfer agent *S*-1-dodecyl-*S'*-(α,α'-dimethyl-α''-acetic acid)trithiocarbonate[31] (DDMAT) and **1**. 6-Bromo-hexan-1-ol was *boc*-protected with *N-boc*-hydroxylamine to afford *N*-Boc-6-aminoxyhexan-1-ol (**3**, Scheme 2.1) in a yield of 64 %. The desired alkoxyamine-containing chain transfer agent (**4**) was prepared (Scheme 2.1) in a yield of 57 % from a carbodiimide-mediated coupling between DDMAT and **3** followed by acid-catalyzed removal of the Boc protecting group proceeding with a yield of 55 % after purification. ^{1}H NMR and FTIR

spectroscopies and mass spectrometry confirmed the identity of both modified chain transfer agents (**2** and **4**).
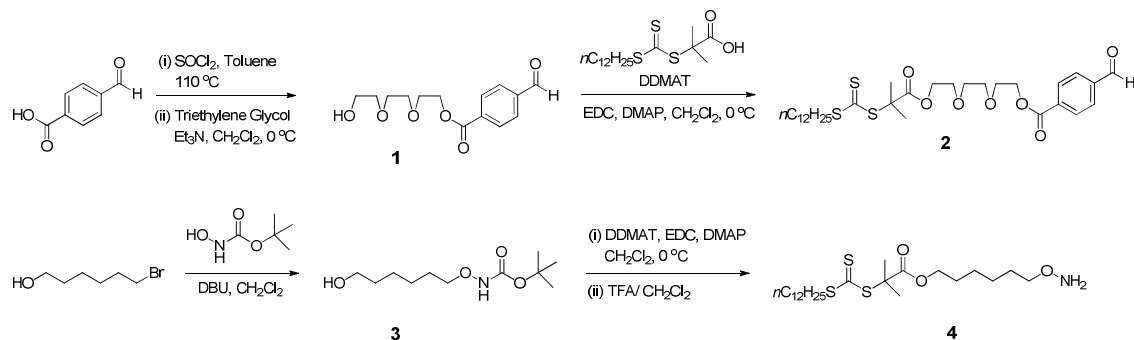
Scheme 2.1 Synthesis of modified chain transfer agents **2** and **4**.

2.3.2   *Synthesis of End-Functionalized Polymers*

Polymerizations of styrene, isoprene, and methyl methacrylate mediated by RAFT chain transfer agents **2** and **4** afforded a range of aldehyde or alkoxyamine-terminated polymers (Scheme 2.2, Table 2.1). The RAFT polymerizations of styrene were performed in DMF at 70 °C using a range of reagent stoichiometries (Table 2.1, entries **P1a**-**P1d** and **P5a-c**) yielding well-defined polymers in all cases.
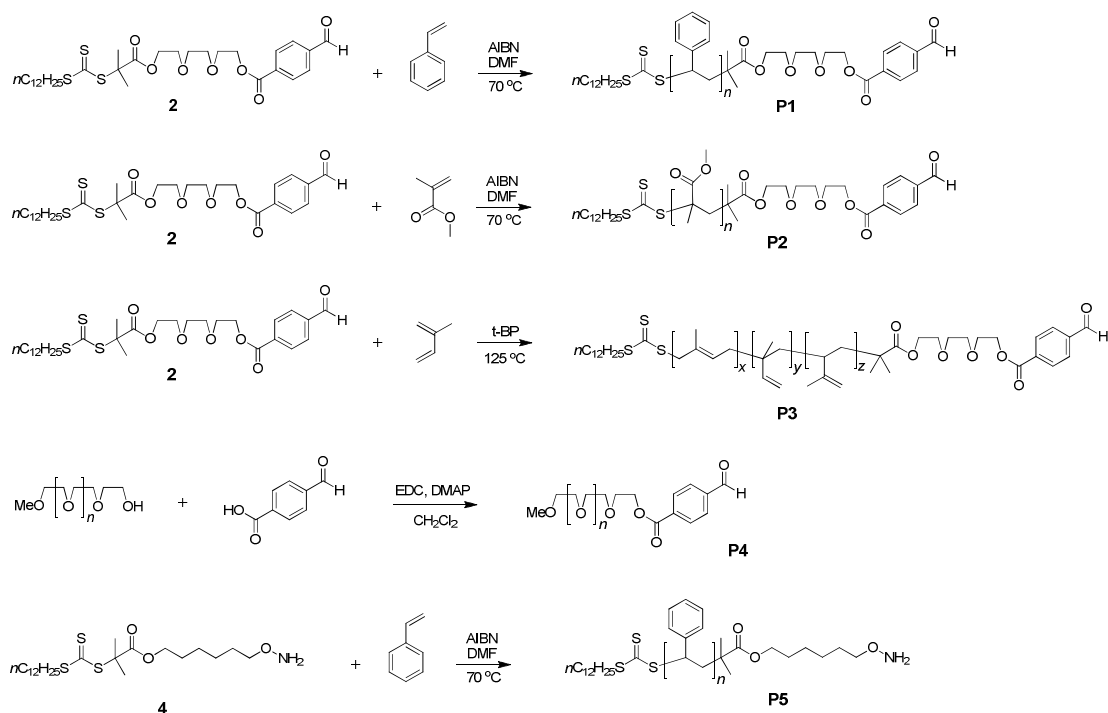
Scheme 2.2 Synthesis of aldehyde- or alkoxyamine end-functionalized polymers **P1**-**P5**.

polymer	chain transfer agent	monomer	initiator	temp (°C)	time (h)	M_n^a (g mol^{-1})	M_n^b (g mol^{-1})	M_w^b (g mol^{-1})	PDI^b (M_w/M_n)
P1a	**1** (1 eq)	styrene (100 eq)	AIBN (0.2 eq)	70	3	1,750	1,950	2,100	1.08
P1b	**1** (1 eq)	styrene (100 eq)	AIBN (0.1 eq)	70	14	5,100	4,800	5,050	1.05
P1c	**1** (1 eq)	styrene (100 eq)	AIBN (0.2 eq)	70	24	6,250	6,100	6,600	1.08
P1d	**1** (1 eq)	styrene (200 eq)	AIBN (0.1 eq)	70	26	9,800	9,000	10,700	1.19
P2	**1** (1 eq)	MMA (200 eq)	AIBN (0.1eq)	70	24	13, 550	11,850^c	16,000^c	1.35
P3	**1** (1 eq)	isoprene (500 eq)	t-BP (0.2 eq)	125	45	18,300	14,600^c	19,100^c	1.31
P4	-	-	-	25	72	5,000	4,900	5,450	1.11
P5a	**2** (1 eq)	styrene (200 eq)	AIBN (0.1 eq)	70	16	5,050	5,450	5,650	1.04
P5b	**2** (1 eq)	styrene (100 eq)	AIBN (0.2 eq)	70	21	6,350	6,200	6,400	1.03
P5c	**2** (1 eq)	styrene (300 eq)	AIBN (0.2 eq)	70	23	10,750	12,700	14,950	1.18

Table 2.1 Selection of aldehyde or alkoxyamine end-functionalized polymers **P1**-**P5**. ^{a} As determined by ^{1}H NMR spectroscopy. ^{b} As determined by gel permeation chromatography in THF. ^{c} Calculated by multi-angle light scattering.

Pseudo-first-order rate plots for styrene mediated by chain transfer agents **2** and **4** were performed. The plots obtained (Figure 2.2) from this brief kinetic study were linear, suggesting a constant concentration of radicals during the polymerizations. The polymerization of methyl methacrylate to afford **P2** was performed in DMF at 70 °C under near identical conditions to those used for polystyrene **P1**. The RAFT polymerization of isoprene to afford **P3** was performed using the method of Wooley and co-workers[32] using *tert*-butyl peroxide as initiator at 125 °C in the absence of solvent. All RAFT polymers were characterized by GPC analysis (Figure 2.3), indicating unimolecular weight distributions and low polydispersities in all cases. The degree of polymerization values calculated from NMR spectroscopy matched well those found by GPC. Polymer **P4** was prepared by EDC-mediated esterification of commercially available poly(ethylene glycol) monomethyl ether (M_w = 5,000 Da) with 4-formylbenzoic acid. The presence of the aldehyde or alkoxyamine end groups in polymers **P1-P5** was confirmed by ^{1}H NMR spectroscopy. Polymers possessing aldehyde end groups (**P1-P4**) each displayed singlets at 10.10-10.12 ppm, corresponding to the formyl (C*H*O) proton, and triplets at 3.29 ppm, corresponding to the SC*H$_2$* group. Those polymers possessing alkoxyamine end-groups (**P5a-c**) each displayed signals at 5.34 ppm corresponding to CH$_2$ON*H$_2$* and triplets at 3.29 ppm corresponding to SC*H$_2$* group. The degree of end-functionalization of all RAFT polymers (**P1-P3**, **P5**) was estimated from ^{1}H NMR spectroscopy to be ~ 80-90 % and the degree of end-functionalization of polymer **P4** to be ~95%.
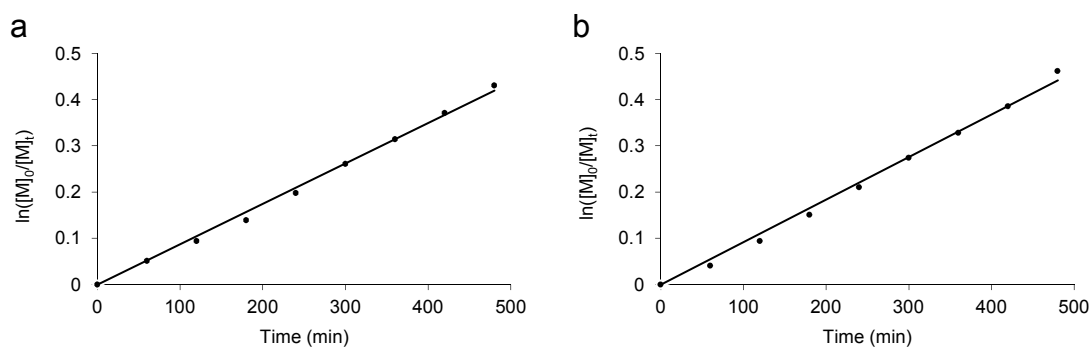
Figure 2.2 (a) First order kinetics plot of styrene polymerization in DMF facilitated by chain transfer agent **2** and AIBN as the radical initiator (70 °C, $[M]_0$: $[2]_0$: $[AIBN]_0$ = 100: 1: 0.2), (b) First order kinetics plot of styrene polymerization in DMF facilitated by chain transfer agent **4** and AIBN as the radical initiator (70 °C, $[M]_0$: $[4]_0$: $[AIBN]_0$ = 100: 1: 0.2). Monomer conversion monitored in comparison to solvent by ^{1}H NMR, aliquots of reaction periodically withdrawn and quenched by rapid cooling before NMR analysis.
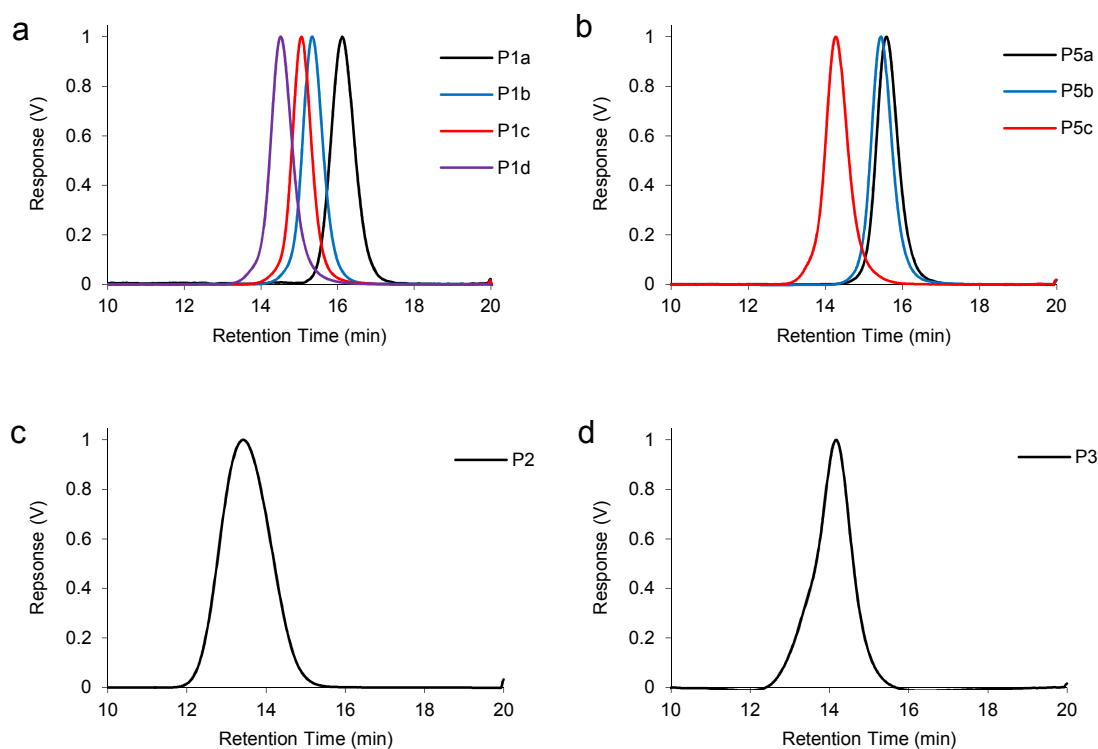
Figure 2.3 Gel permeation chromatography – multi-angle laser light scattering analysis (GPC-MALLS) traces for (a) **P1a-d**, (b) **P5a-c**, (c) **P2** and (d) **P3**.

2.3.3 *Dimerisation of Chain Transfer Agents*

As a first step toward dynamic covalent diblock copolymers, we studied initially the dimerization of the modified CTAs **2** and **4** to form the oxime-linked dimer **5** (Scheme 2.3). TFA catalyst (20 mol %) was added to a 1: 1 mixture of **2** and **4** (*c* = 30 mM of each component) in CDCl$_3$ and the solution allowed to come to equilibrium (< 30 min).

43

^{1}H NMR spectroscopy showed (Figure 2.4a) a significant reduction in the intensity of the signal corresponding to the aldehyde proton (H$_a$) of **2** and the appearance of a *trans*-oxime (H$_{a'}$) signal at 8.14 ppm. The ^{1}H NMR signal corresponding to the *cis*-oxime proton overlaps with aromatic signals of compound **3**. It is reasonable to assume that most of the oxime exists as its thermodynamically most stable *trans*-isomer. These changes were accompanied by a reduction in intensity of the aromatic signals (H$_c$) of **2** at 8.21 and 7.95 ppm and the appearance of signals corresponding to the aromatic moiety of oxime **5** (H$_{c'}$) at 8.03 and 7.66 ppm. Further evidence for the formation of **5** was obtained from electrospray mass spectrometry of this solution, which showed a signal at *m/z* =1090.51, indicating the presence of the oxime-linked dimer **5** at equilibrium. To demonstrate the dynamic nature of oxime **5**, 4 equiv of 2-aminooxymethynapthalene **6** was added (Scheme 2.3), and the solution was left to re-equilibrate. ^{1}H NMR spectroscopic analysis (Figure 2.4b) shows the appearance of a signal at 5.41 ppm, corresponding to the C*H$_2$*ON protons of oxime **7** (H$_{e'}$) and an equal increase in the intensity of the signal corresponding to the C*H$_2$*ONH$_2$ protons of **4** (H$_{f,g}$). This observation indicates the presence of oxime **7** and confirms the dynamic nature of the oxime bond. The NMR spectroscopic and mass spectrometry studies also indicate that the trithiocarbonate moieties of all species in solution were found to remain intact and appear not to be susceptible to nucleophilic attack by the alkoxyamine nitrogen under the reaction conditions. These same experiments were repeated in DMF-d_7 with essentially identical outcomes, and the equilibrium constant (K$_{eq}$ = [**5**][H$_2$O]/[**2**][**4**]) in this solvent for the formation of oxime **5** from starting materials **2** and **4** was determined by ^{1}H NMR spectroscopy in DMF-d_7 at 25 °C to be 361, assuming the concentration of water equals the concentration of oxime. The water signal unfortunately is obscured by other signals in the spectrum to allow its accurate integration. These experiments confirm that the reaction between an aldehyde and an alkoxyamine is dynamic and the equilibrium lies almost completely on the side of the oxime.
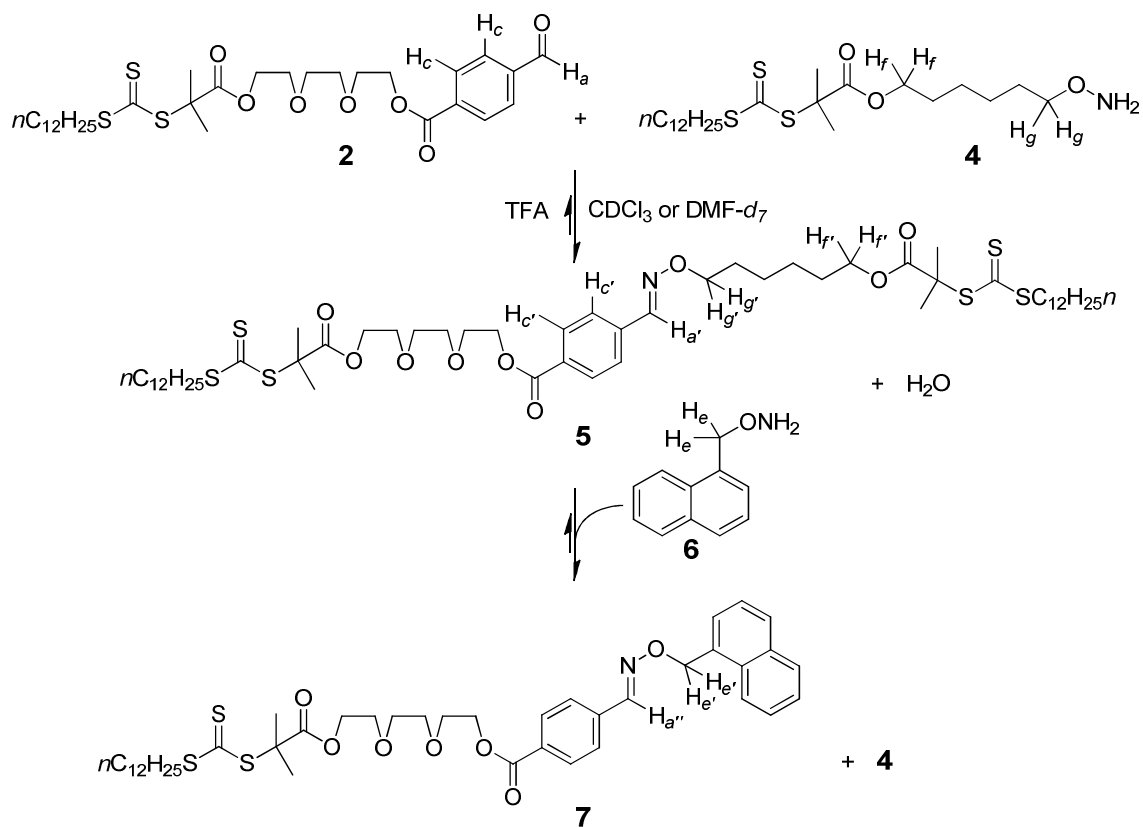
Scheme 2.3 Dimerization of modified CTAs **2** and **4** to form oxime **5** and subsequent re-equilibration upon the addition of 2-aminooxymethylnapthalene **6** into Oxime **7**.
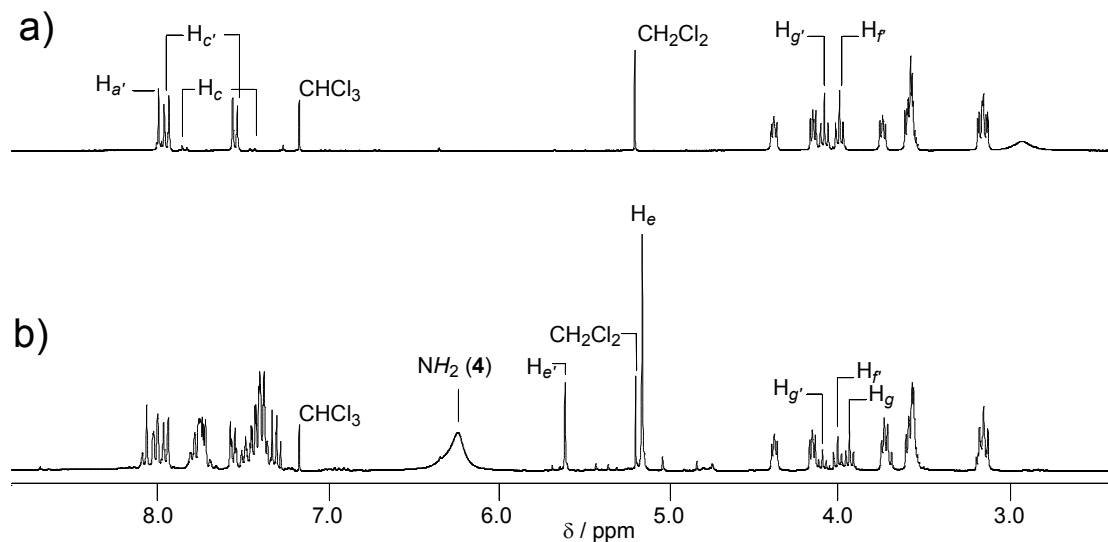
Figure 2.4 (a) Partial ^{1}H NMR spectra (300 MHz, CDCl$_3$) displaying dimerization between modified chain transfer agents **2** + **4** to afford dimer **5** linked via oxime formation, (b) Partial ^{1}H NMR spectra (300 MHz, CDCl$_3$) displaying the re-equilibration of oxime **5** to oxime **7** upon the addition of alkoxyamine (**6**).

2.3.3 *Formation of Dynamic Covalent Diblock Copolymers*

To investigate the formation of a dynamic covalent block copolymer, **P1b** (M_n = 4,800 Da) and **P5b** (M_n = 6,200 Da) were mixed in DMF-d_7 (5 mM each) and TFA added (10 mol %), and the reaction allowed to reach equilibrium. The solution was analyzed by ^{1}H NMR spectroscopy (Figure 2.5), which displayed the appearance of a signal at 8.35 ppm corresponding to the oxime linkage of **P1b**-Dyn*b*-**P5b** (M_n = 11,000 Da) and a reduction in the intensity of the signal at 10.21 ppm corresponding to the formyl proton in **P1b**. Under these conditions, equilibrium was reached in ~ 24 h. We propose the notation "Dyn*b*" to highlight the presence of a dynamic covalent bond linking the polymer blocks together. Dimerization of **P1b** and **P5b** to form **P1b**-Dyn*b*-**P5b** was also investigated by GPC (Figure 2.6), which shows the appearance of a peak at 14.29 min, corresponding to the block copolymer **P1b**-Dyn*b*-**P5b** and the reduction in area of the peak at 15.10 min corresponding to both **P1b** and **P5b**.
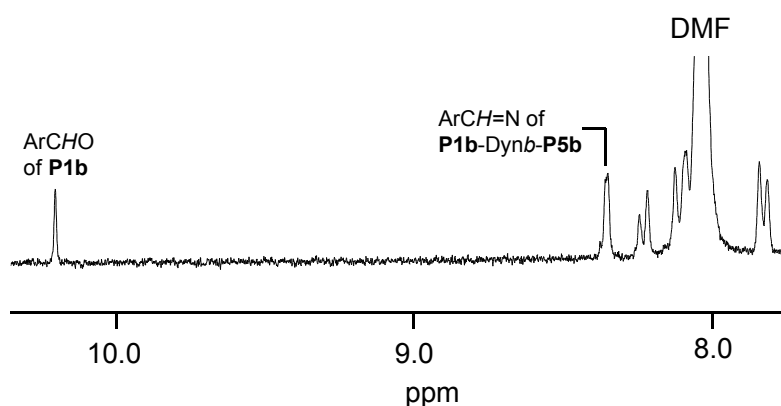
Figure 2.5 Partial ^{1}H NMR spectra (300 MHz, DMF-d^7) displaying dimerization between **P1b** and **P5b** to afford oxime-linked dynamic covalent diblock copolymer **P1b**-Dyn*b*-**P5b**.
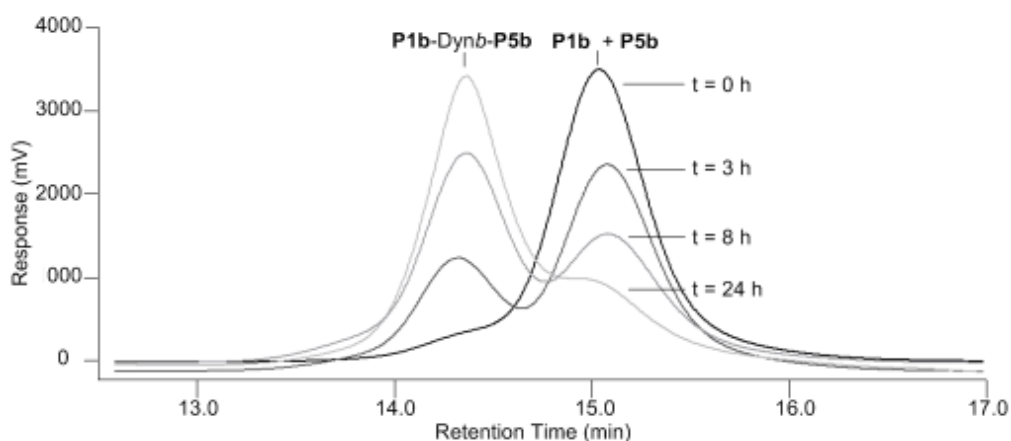
Figure 2.6 Gel permeation chromatography (THF, 1.0 mL/ min) traces of the dimerization process of **P1b** and **P5b** into **P1b**-Dyn*b*-**P5b** at t = 0, 3, 8, and 24 h. Traces were recorded on a UV detector at 254 nm.

To demonstrate the dynamic and reversible nature of the oxime linkage, excess 1-aminooxyhexane (10 equiv) was added to a solution of **P1b**-Dyn*b*-**P5b** at equilibrium with its component polymer blocks in the presence of TFA. GPC analysis (Figure 2.7) displayed the complete disappearance of the peak at 14.29 min and an increase in the area of the peak at 15.10 min, a process which took 4 d to reach completion. This observation suggests that 1-aminooxyhexane competes with the alkoxyamine end group of **P5b** to form an oxime linkage with **P1b**, resulting in the re-equilibration of the diblock copolymer **P1b**-Dyn*b*-**P5b** into **P5b** and hexyloxime-capped **P1b**. The results of the ^{1}H NMR spectroscopic and GPC analysis suggest that polymer chains can be linked through a dynamic covalent bond to form a diblock copolymer which displays dynamic behaviour, i.e. the ability to undergo component exchange.
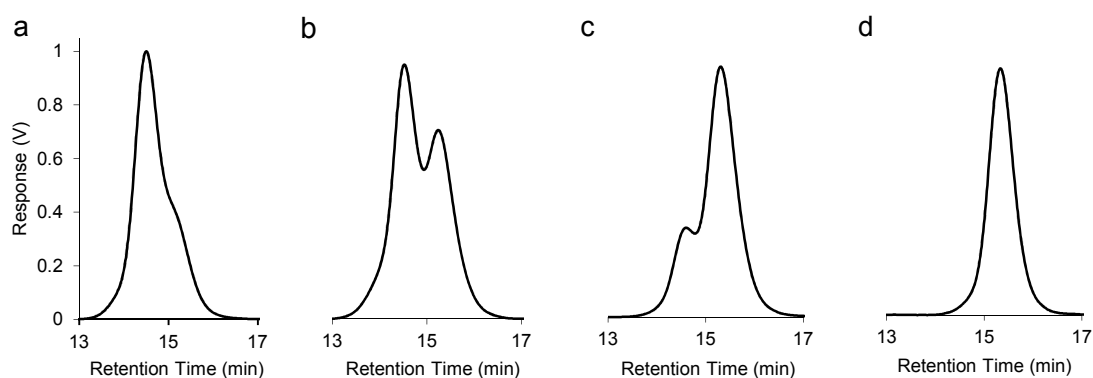
Figure 2.7 Gel permeation chromatography traces for **P1b**-Dyn*b*-**P5b** re-equilibration with 1-aminooxyhexane after (a) 24 h, (b) 48 h, (c) 72 h and (d) 96 h. Traces were recorded on a differential refractive index detector.

polymer blocks	block copolymers	theoretical M_n (Da) of block copolymer[a]	association constant
P1b + P5b	**P1b**-Dyn*b*-**P5b**	11,000	5.44[b]
P1c + P5c	**P1c**-Dyn*b*-**P5c**	18,800	2.45[b]
P2 + P5c	**P2**-Dyn*b*-**P5c**	24,550	2.66[b]
P3 + P5c	**P3**-Dyn*b*-**P5c**	27,300	2.07[c]
P4 + P5b	**P4**-Dyn*b*-**P5b**	11,100	6.61[c]

Table 2.2 Preparation of a selection of homo- and heterodynamic covalent diblock copolymers (5 mM of each block). [a] Calculated by addition of the M_n values (as determined by GPC or multi-angle light scattering) of each polymer block. [b] Calculated in DMF-d_7. [c] Calculated in THF-d_8.

A series of end-functionalized polymer building blocks were reacted to form dynamic covalent diblock copolymers and characterized under equilibrium conditions (Table 2.2). The equilibrium constants for the dimerization of all polymer blocks were determined from ^{1}H NMR spectroscopy and were found to be considerably lower than those for the dimerization of **2** + **4**. This significant reduction in equilibrium constant is

presumably on account of the steric bulk of the polymer blocks hindering the linking of the chain ends. The association constant is higher for those diblock copolymers with lower theoretical molecular weights, and the fact that not all polymer chains contain the desired end-groups as a consequence of less than 100 % end-group fidelity in the RAFT process.

2.3.4 *Self-Assembly and Triggered Disassembly of Micelles*

To investigate the potential of dynamic covalent diblock copolymers to form micellar aggregates, we focused on the **P3**-Dyn*b*-**P5c** system formed at equilibrium from the dimerization of the polystyrene block **P5c** and the polyisoprene block **P3** in DMF, which is a selective solvent for the polystyrene block. The self-assembly into micelles of polystyrene-*b*-polyisoprene diblock copolymers in organic solvents which are selective for one of the blocks is well-known,[33, 34] and this aggregation process is thought to be enthalpy-driven.[35] Under the conditions studied, any micelles formed should possess polyisoprene chains at their core surrounded by a corona of polystyrene chains. On account of the poor solubility of **P3** in DMF, both **P3** and **P5c** were dissolved in CH_2Cl_2 (concentration of each block =2 mM) and TFA was added (10 mol %). DMF was added, and a portion of this stock solution was filtered and further diluted in DMF (concentration of each block ~ 4 µM). Dynamic light scattering measurements indicated the formation of a tertiary structure with a calculated hydrodynamic radius of 29.6 ± 1.8 nm. Regularization analysis of the light scattering data displays (Figure 2.8a) a narrow mono-modal particle size distribution. Control experiments using THF, which is selective for both blocks, revealed a hydrodynamic radius of 8-10 nm which indicates only the presence of non-aggregated polymer mono- and diblocks. Further evidence for the formation of a tertiary structure was obtained from GPC analysis (Figure 2.8b), which displayed a peak at 12.00 min, corresponding to a very high molecular weight aggregate. To trigger the decomposition of the micelles, a large excess of **6** was added, and the re-equilibration process was monitored over the course of several days. Surprisingly, GPC analysis (Figure 2.8b) displays a peak at 8.50 min, which is indicative of high molecular weight aggregates. Calibration of our GPC system (DMF, 1 mL/ min, 40 °C) with polystyrene standards of masses up to 6.3 MDa (retention time 9.20 min) affords a linear calibration curve. The observed decomposition product (retention time 8.50 min) is therefore probably of even higher mass, although it is not known with certainty whether this measurement is within the exclusion limits of our

GPC setup. This observation was further supported by dynamic light scattering measurements (Figure 2.9a) which show an apparent increase in the hydrodynamic radius of the system to 70-85 nm. Furthermore, even after several days no precipitation of the polyisoprene cores was observed. These observations suggest the formation of metastable aggregates of collapsed polyisoprene cores in DMF, which is a poor solvent for polyisoprene, formed when the individual polystyrene and polyisoprene blocks begin to phase separate,[36] and support the hypothesis that the addition of the small molecule alkoxyamine **6** has indeed triggered the decomposition of the micelles. To further support this hypothesis, a simple control experiment was performed. Following the same procedure for the formation of micelles, a solution of polyisoprene (**P3**) was prepared and analyzed by DLS. This sample was found to display very similar DLS characteristics (Figure 2.9b) as the sample prepared by the small molecule-induced decomposition of **P3**-dyn*b*-**P5c** (Figure 2.9a).
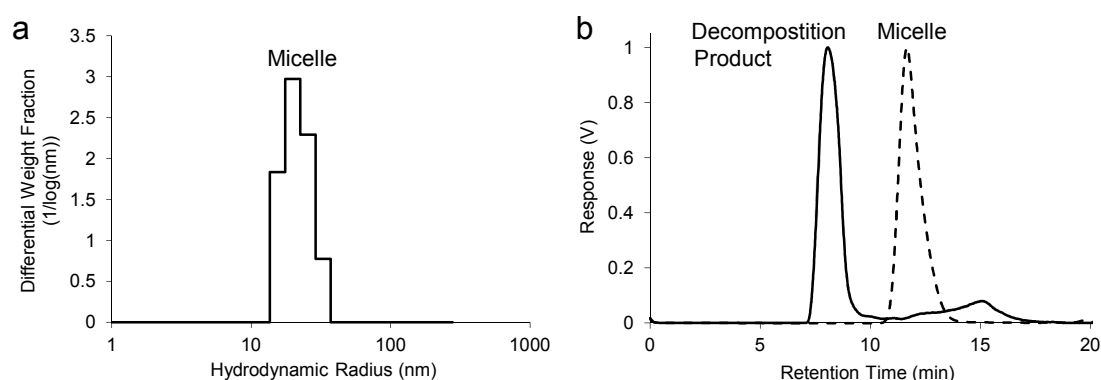
Figure 2.8 (a) Regularization analysis of dynamic light scattering data of micelles formed from **P3**-Dyn*b*-**P5c** in DMF, (b) Gel permeation chromatographic traces of the micellar aggregates formed from dynamic covalent diblock copolymer **P3**-Dyn*b*-**P5c** (dotted line) and trace of the decomposition products (solid line). GPC was performed in DMF at 1 mL/min at 40 °C and recorded using a light scattering detector measuring the scattered light at 90°.
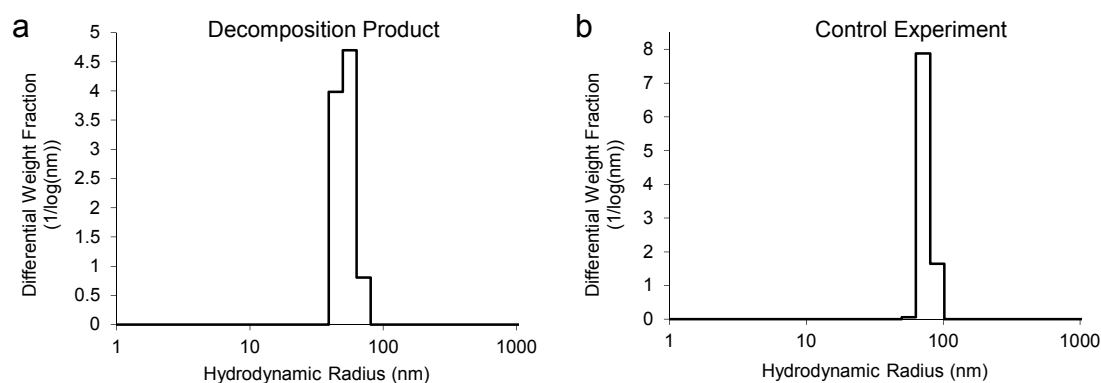
Figure 2.9 (a) Regularization analysis of dynamic light scattering data of micelle decomposition product after addition of small molecules alkoxyamine, (b) Regularization analysis of dynamic light scattering data of **P3** control experiment. Sample prepared under identical conditions to micelle assembly without the presence of **P5c**.

2.4   Conclusions

We have utilized RAFT polymerization techniques to prepare a series of polymer building blocks possessing either aldehyde or alkoxyamine functions as end-groups. We have demonstrated that these polymers can link together through dynamic covalent oxime bonds to form dynamic covalent diblock copolymers and highlighted the dynamic nature of these species. The ability of a dynamic covalent diblock copolymer formed from polystyrene and polyisoprene blocks to aggregate into higher order micellar structures has been demonstrated, and we have shown how its disassembly can be triggered by the addition of a small molecule alkoxyamine. One limitation of this system is that oxime bond is only dynamic through the addition of a small molecule alkoxyamine which can compete through a *trans*-imination exchange mechanism. The oxime bond is very hydrolytically stable and the equilibrium cannot be affected through changes in temperature or pH, a more dynamic covalent bond such as an imine or disulfide could potentially result in a more responsive system. Furthermore, for this system to be completely reversible the competing small molecules would have to be removed, which is experimentally very difficult. However, we believe that the utilization of dynamic covalent linkages between polymer blocks may lead to the development of new dynamic functional materials and complements alternative systems that utilize non-covalent or metal-ligand interactions to link polymer chains together. In particular, our approach may allow for the preparation of kinetically stable micelles which possess the ability to alter the polymer block composition of their coronal polymer chains while their core polymer chains remain within the core.

2.5   Experimental

All chemicals were purchased from Sigma-Aldrich or Alfa Aesar and were used as received without further purification. ^{1}H and ^{13}C NMR spectra were recorded on a Bruker Advance 300 spectrometer at 300 and 75 MHz, respectively, with the residual solvent signal as an internal standard. FT-IR spectroscopy was performed on a Varian 800 FT-IR instrument (Varian Inc.). High-resolution mass spectrometry was performed on a Waters LCT premier mass spectrometer (Waters Inc.). Gel permeation chromatography (GPC) was conducted on a Varian ProStar instrument (Varian Inc.) equipped with a Varian 325 UV-vis dual wavelength detector (254 nm), a Viscotek 3580 differential RI detector, and a pair of PL gel 5 µm Mixed D 300 × 7.5 mm

columns with guard column (Polymer Laboratories Inc.) in series. Near monodisperse polystyrene standards (Polymer Laboratories) were used for calibration. Data collection was performed with Galaxie software (Varian Inc.) and chromatograms analyzed with the Cirrus software (Varian Inc.). Dynamic and static light scattering was performed on a Dawn Heleos II instrument (Wyatt Technology Corp.), and data collection and analysis were performed with Astra software (Wyatt Technology Corp.).

2-[2-(2-Hydroxyethoxy) ethoxy]ethyl-4-formylbenzoate (1)

Thionyl chloride (27.94 g, 0.237 mol) in toluene (30 mL) was added to a solution of 4-carboxybenzaldehyde (4.44 g, 0.029 mol) in toluene (20 mL). The reaction was heated under reflux at 110 °C for 3 h. After this time the reaction was evaporated to dryness to afford the crude 4-formylbenzoylchloride which was used without purification. A solution of Et_3N (6.0 g, 0.059 mol) and triethylene glycol (31.1 g, 0.207 mol) in CH_2Cl_2 (40 mL) was cooled to 0 °C in an ice bath while stirring under a nitrogen atmosphere. To this solution the crude 4-formylbenzoylchloride (4.99 g, 0.0296 mol) in CH_2Cl_2 (50 mL) was added dropwise over 30 min and the reaction was left to stir overnight at room temperature. The reaction mixture was evaporated to dryness and the residue was dissolved in EtOAc (50 mL) and washed with saturated $NaHCO_3$ solution. The organic layer was dried over $MgSO_4$, filtered and evaporated to dryness to obtain crude oil which was purified by column chromatography [SiO_2, EtOAc-Hexane (3:1)] to yield the title product as a pale yellow oil (4.68 g, 50 %): ^1H NMR ($CDCl_3$): δ 3.57 (m, 2H), 3.67 (m, 6H) , 3.82 (m, 2H), 4.49 (m, 2H), 7.91 (d, 2H, J = 8.0 Hz), 8.18 (d, 2H, J = 8.0 Hz), 10.06 (s, 1H). ^{13}C NMR ($CDCl_3$): δ 62.1, 64.8, 69.5, 70.8, 71.1, 72.9, 129.7, 130.2, 135.5, 139.8, 165.8, 191.6. FT-IR (wavenumber, cm^{-1}): 3490 (O-H), 2920 (C-H, alkyl), 2855 (C-H, alkyl), 1702 (C=O), 1453 (C=C, aromatic), 1385 (C=C, aromatic), 1202 (C-H, aromatic). $HRMS^+$ $C_{14}H_{18}O_6$; Theoretical: 283.1182 Actual: 283.1189.

Aldehyde-functionalized chain transfer agent (2)

A solution of *S*-1-dodecyl-*S*'-(α,α-dimethyl-α''-acetic acid)trithiocarbonate (DDMAT, 0.63 g, 1.73 mmol) and 2-[2-(2-hydroxyethoxy)ethoxy]ethyl-4-formylbenzoate (**1**, 0.49 g, 1.73 mmol) in CH_2Cl_2 (20 mL) was cooled to 0 °C in an ice bath whilst stirring under a nitrogen atmosphere. A solution of EDC (0.37 g, 1.91 mmol) and DMAP (0.23 g, 1.91 mmol) in CH_2Cl_2 (10 mL) was added dropwise. The reaction mixture was stirred

51

overnight at room temperature, then evaporated to dryness to afford a crude yellow oil which was purified by column chromatography [SiO$_2$, Hexane-EtOAc (3:1)] to yield the title product as a yellow oil (0.65 g, 59 %): ^{1}H NMR (CDCl$_3$): δ 0.86 (t, 3H, J = 7 Hz), 1.25 (m, 18H), 1.68 (m, 8H), 3.24 (t, 2H, J = 7.5 Hz), 3.66 (m, 6H), 3.85 (m, 2H), 4.24 (m, 2H), 4.50 (m, 2H), 7.95 (d, 2H, J = 9.0 Hz), 8.21 (d, 2H, 9.0 Hz), 10.10 (s, 1H). ^{13}C NMR (CDCl$_3$): δ 14.2, 22.9, 25.5, 25.7, 28.3, 29.2, 29.4, 29.6, 29.7, 29.8, 29.9, 30.9, 32.2, 37.3, 56.4, 64.9, 65.3, 69.3, 69.5, 71.1, 129.7, 130.6, 135.6, 139.8, 165.8, 172.9, 191.4, 206.1. FT-IR (wavenumber, cm^{-1}): 2981 (C-H, alkyl), 2923 (C-H, alkyl), 1726 (C=O), 1463 (C=C, aromatic), 1383 (C=C, aromatic), 1270 (C-H, aromatic). HRMS$^+$ C$_{31}$H$_{48}$O$_7$S$_3$Na; Theoretical: 651.2460 Actual: 651.2463.

N-Boc-6-aminoxyhexan-1-ol (3)

1,8-Diazabicyclo[5.4.0]undec-7-ene (0.677 mL, 4.52 mmol) was added dropwise over 10 min to a solution of *N-boc*-hydroxylamine (0.50 g, 3.75 mmol) and 6-bromo-hexan-1-ol (0.819 g, 4.52 mmol) in CH$_2$Cl$_2$ (20 mL). The reaction mixture was left to stir overnight at room temperature, then transferred into a separating funnel and CH$_2$Cl$_2$ (100 mL) added. The organic layer was washed with 1 M HCl (50 mL) and saturated NaCl$_{(aq)}$ (50 mL) then dried over MgSO$_4$, filtered and evaporated to dryness to afford a yellow oil which was purified by column chromatography [SiO$_2$, Hexane-EtOAc (3:2)] to yield the title product as a pale yellow oil (0.565 g, 64 %): ^{1}H NMR (CDCl$_3$): δ 1.38 (m, 4H), 1.45 (s, 9H), 1.57 (m, 4H), 3.61 (t, 2H, J = 6.5 Hz), 3.83 (t, 2H, J = 6.5 Hz), 7.28 (s, 1H). ^{13}C NMR (CDCl$_3$): δ 25.3, 28.3, 28.8, 33.1, 60.6, 63.1, 81.8, 157.2, 171.2. FT-IR (wavenumber, cm^{-1}): 3450 (O-H), 3230 (N-H), 2981 (C-H, alkyl), 1716 (C=O). HRMS$^+$ C$_{11}$H$_{23}$NO$_3$K; Theoretical: 256.1525 Actual: 256.1529.

Alkoxyamine-functionalized chain transfer agent (4)

A solution of *S*-1-dodecyl-*S'*-(α,α-dimethyl-α''-acetic acid)trithiocarbonate (DDMAT, 0.78 g, 2.14 mmol) and *N*-Boc-6-aminoxy hexan-1-ol (**3**, 0.50 g, 2.14 mmol) in CH$_2$Cl$_2$ (20 mL) was cooled to 0 ˚C in an ice bath whilst stirring under a nitrogen atmosphere. A solution of EDC (0.452 g, 2.35 mmol) and DMAP (0.29 g, 2.35 mmol) in CH$_2$Cl$_2$ (10 mL) was added dropwise and the reaction mixture stirred overnight at room temperature. The reaction mixture was evaporated to dryness and the crude yellow oil purified by column chromatography [SiO$_2$, Hexane-EtOAc (9:1)] to yield the *Boc-*

protected oxylamine chain transfer agent as a yellow oil (0.707 g, 57 %): ^{1}H NMR (CDCl$_3$): δ 0.87 (t, 3H, J = 7.0 Hz), 1.36 (m, 18H), 1.48 (s, 9H), 1.64 (m, 16H), 3.26 (t, 2H, J = 7.5 Hz), 3.83 (t, 2H, J = 6.0 Hz), 4.08 (t, 2H, J = 6.5 Hz), 7.10 (s, 1H). ^{13}C NMR (CDCl$_3$): δ 14.2, 22.9, 25.8, 25.9, 26.1, 28.3, 28.6, 28.7, 29.2, 29.4, 29.6, 29.7, 29.8, 29.9, 31.8, 32.2, 37.3, 56.5, 66.2, 77.7, 81.7, 157.1, 173.1. FT-IR (wavenumber, cm^{-1}): 2981 (C-H, alkyl), 2925 (C-H, alkyl), 1733 (C=O).

Boc-protected oxylamine chain transfer agent (0.350 g, 0.60 mmol) was dissolved in CH$_2$Cl$_2$ (3 mL) and TFA (3 mL). The reaction mixture was left to stir at room temperature for 30 min, and the solution was evaporated to dryness to afford a yellow oil. The crude product was purified by column chromatography [SiO$_2$, Hexane-EtOAc (4:1)] to yield the title product as a yellow oil (0.158 g, 55%): ^{1}H NMR (CDCl$_3$): δ 0.87 (t, 3H, J = 6.5 Hz), 1.25 (m, 18H), 1.68 (m, 16H), 3.26 (t, 2H, J = 7.5 Hz), 3.64 (t, 2H, J = 6.5 Hz), 4.08 (t, 2H, J = 6 Hz), 5.35 (s, 2H). ^{13}C NMR (CDCl$_3$): δ 14.2, 22.9, 25.8, 26.0, 26.2, 28.2, 28.7, 28.8, 29.2, 29.4, 29.6, 29.7, 29.8, 29.9, 32.2, 37.3, 56.5, 66.2, 76.2, 173.1. HRMS$^+$ C$_{23}$H$_{45}$S$_3$O$_3$N; Theoretical: 480.2640 Actual: 480.2646.

Aldehyde end-functionalized poly(styrene) (P1a-d).

To a small schlenk tube the chain transfer agent **2** (1 eq) and AIBN (0.1 eq - 0.2 eq) was added. Styrene (100 – 200 eq) was then added followed by DMF (200 eq). The reaction mixture was degassed five times then the vessel was back filled with nitrogen and purged with N$_2$ and allowed to warm to room temperature. The reaction mixture was placed in an oil bath at 70 ˚C. The polymerization was quenched after a predetermined time and solvent removed on the rotary evaporator. The resulting yellow oil was dissolved in a minimal amount of THF and added dropwise to ice cold methanol. The polymer precipitate was then isolated by filtration and dried under high vacuum. Polymers **P1a-d** were obtained as pale yellow solids with yields typically between 60 and 80 %. ^{1}H NMR (CDCl$_3$): δ 0.88 – 1.01 (br, dodecyl of the chain terminus), 1.45 (br, CHC*H*$_2$, polymer backbone), 1.88 (br, C*H*CH$_2$, polymer backbone), 3.29 (br, S*CH*$_2$, of the chain terminus) 6.59 (br, Ar, polymer backbone), 7.06 (br, Ar, polymer backbone), 7.95 (d, Ar, of the chain terminus), 8.21 (d, Ar, of the chain terminus), 10.12 (s, C*H*O, of the chain terminus).

*Alkoxyamine end-functionalized poly(styrene) (**P5a-c**)*

To a small schlenk tube the chain transfer agent **4** (1 eq) and AIBN (0.1 eq - 0.2 eq) was added. Styrene (100 – 200 eq) was then added followed by DMF (200 eq). The reaction mixture was degassed five times then the vessel was back filled with nitrogen and purged with N_2 and allowed to warm to room temperature. The reaction mixture was placed in an oil bath at 70 ˚C. The polymerization was quenched after predetermined time and solvent removed on the rotary evaporator. The resulting yellow oil was dissolved in minimal amount of THF and added dropwise to ice cold methanol. The polymer precipitate was then isolated by filtration and dried under high vacuum. Polymers **P5a-c** were obtained as pale yellow solids with yields typically between 70 and 80 %. ^{1}H NMR (CDCl$_3$): δ 0.88 – 1.01 (br, dodecyl of the chain terminus), 1.45 (br, CHC*H$_2$*, polymer backbone), 1.88 (br, C*H*CH$_2$, polymer backbone), 3.29 (br, SC*H$_2$*, of the chain terminus), 5.35 (br, CH$_2$ON*H$_2$*, of the chain terminus) 6.59 (br, Ar, polymer backbone), 7.06 (br, Ar, polymer backbone).

*Aldehyde-end functionalized poly(methyl methacrylate) (**P2**)*

The chain transfer agent **2** (118 mg, 0.188 mmol) and AIBN (3.08 mg, 18.8 μmol) were added to a small schlenk tube. Methyl methacrylate (1.88 g, 18.8 mmol) was then added followed by DMF (1.9 mL). The reaction mixture was degassed five times then the vessel was back filled with nitrogen and purged with N_2 and allowed to warm to room temperature. The reaction mixture was placed in an oil bath at 70 ˚C. The polymerization was quenched after 16 h and solvent removed on the rotary evaporator. The resulting yellow oil was dissolved in minimal amount of THF and added dropwise to ice cold hexane. The polymer precipitate was then isolated by filtration and dried under high vacuum. Polymer **P2** was obtained as pale yellow solid in a yield of 81 %. ^{1}H NMR (CDCl$_3$): δ 0.92 (br, CH$_2$C(C*H$_3$*)C, polymer backbone), 1.80 (br, C*H$_2$*C(CH$_3$)C, polymer backbone), 3.59 (br, C(O)OC*H$_3$*, polymer backbone), 8.01 (d, Ar, of the chain terminus), 8.21 (d, Ar, of the chain terminus), 10.11 (s, C*H*O, of the chain terminus).

Aldehyde-end functionalized poly(isoprene) (P3)

The chain transfer agent **2** (94 mg, 0.15 mmol) and *tert*-butyl peroxide (4.4 mg, 0.03 mmol) were placed in a small schlenk tube fitted with a Young's tap. Isoprene (5.09g, 0.0748 mol) was then added and the reaction mixture was degassed five times and the vessel was back filled with nitrogen and purged with N_2 and allowed to warm to room temperature. The system was then sealed and placed in an oil bath at 125 ˚C. The polymerization was quenched after 45 h and the reaction mixture was evaporated to dryness on the rotary evaporator. The resulting yellow oil was dissolved in minimal amount of CH_2Cl_2 and added dropwise to ice cold methanol. Evaporation to dryness and further drying under high vacuum afforded polymer **P3** as a yellow oil in a yield of 83 %. ^{1}H NMR (CDCl$_3$): δ 0.8 – 1.0 (br, dodecyl of the chain terminus), 1.60 (br, C*H*$_3$, polymer backbone), 2.00 (br, C*H*$_2$, polymer backbone), 3.35 (br, SC*H*$_2$, of the chain terminus), 4.0 – 4.1 (br, C*H*, polymer backbone), 4.6 – 4.8 (br, 3,4-C(CH$_3$)-C*H*$_2$, polymer backbone), 4.8 – 5.1 (br, 1,2-CH=C*H*$_2$, polymer backbone), 5.1 – 5.3 (br, 1,4-CH$_2$-C(CH$_3$)-C*H*-CH$_2$, polymer backbone) 5.70 – 5.85 (1,2-C*H*=CH$_2$, polymer backbone), 7.95 (d, Ar, of the chain terminus), 8.22 (d, Ar, of the chain terminus) 10.12 (s, C*H*O, of the chain terminus). ^{1}H NMR spectroscopic analysis confirmed the distribution of monomers units to be 10:19:230 for the 1,2-, 3,4- and 1,4- conformations respectively.

Aldehyde end-functionalized poly(ethylene glycol) (P4)

Poly(ethylene glycol) monomethyl ether M_w = 5,000 g mol^{-1} (Sigma Aldrich) (3.65g, 0.731 mmol) was dissolved in CH_2Cl_2 (50 mL). 4-Carboxybenzaldehyde (0.548g, 3.65 mmol), DMAP (0.464 g, 3.80 mmol) and EDC (0.728 g, 3.80 mmol) were added and the reaction mixture was stirred at room temperature for 72 h and then evaporated to dryness. The crude product was dissolved in CH_2Cl_2 (10 mL) and this solution was added dropwise to ice cold diethyl ether. The precipitated solids were isolated by filtration and dried under high vacuum. Polymer **P4** was obtained as a white solid in a 20 % yield. ^{1}H NMR (CDCl$_3$): δ 3.61 (br, 4H, C*H*$_2$-C*H*$_2$O, polymer backbone), 7.95 (d, Ar, of the chain terminus), 8.21 (d, Ar, of the chain terminus), 10.10 (s, C*H*O, of the chain terminus).

General Procedure for Dynamic Covalent Diblock Copolymers

The appropriate aldehyde terminated polymer (**P1a-d**, **P2**, **P3**, **P4**) and alkoxyamine terminated polymer (**P5a-c**) were dissolved in DMF-d^7 (5 mM of each polymer) for ^{1}H NMR spectroscopic analysis or THF (5 mM of each polymer) for GPC analysis. To each solution TFA (10 - 20 mol %) was added. Samples were analyzed at regular intervals during the dimerization process after predetermined times.

Procedure for Dynamic Covalent Diblock Copolymer Re-Equilibration

To a solution of **P1b**-Dyn*b*-**P5b** (5 mM of each polymer block in THF) was added 1-aminooxyhexane (10 eq, per aldehyde function). The solution was stirred at room temperature and monitored periodically by gel permeation chromatography.

*Micellization of Dynamic Covalent Diblock Copolymer (**P3**-Dynb-**P5c**)*

P3 poly(isoprene) (78.8 mg, 1 eq) and **P5c** poly(styrene) (64.7 mg, 1 eq) were dissolved in CH$_2$Cl$_2$ (2 mL) and TFA (0.25 μL, 0.75 eq) was added. The reaction mixture was left to stir at room temperature for 24 h. After this time DMF (8 mL) was added dropwise over 10 min. 2 mL of this stock solution (0.4 mM) was filtered through 0.45 μM nylon syringe filter and diluted in DMF to prepare a range of solutions (0.2 mM – 4μM) for DLS and GPC analysis.

Procedure for Micelle Decomposition

2-Aminooxymethylnapthalene (50 eq per aldehyde function) was added to a solution of **P3**-Dyn*b*-**P5c** (2 mM of each polymer block in DMF). The reaction was left to stir for 5 days before filtration through a 0.45 μM nylon syringe filter and analysis by gel permeation chromatography.

2.6   References

1.   S. Forster and T. Plantenberg, *Angew. Chem., Int. Ed.*, 2002, **41**, 689-714.
2.   G. Riess, *Prog. Polym. Sci.*, 2003, **28**, 1107-1170.
3.   H.-i. Shin, B. G. Min, W. Jeong and C. Park, *Macromol. Rapid Commun.*, 2005, **26**, 1451-1457.

4. S. Fujii, Y. Cai, J. V. M. Weaver and S. P. Armes, *J. Am. Chem. Soc.*, 2005, **127**, 7304-7305.

5. K. Kataoka, A. Harada and Y. Nagasaki, *Adv. Drug Delivery Rev.*, 2001, **47**, 113-131.

6. G. Gaucher, M. H. Dufresne, V. P. Sant, N. Kang, D. Maysinger and J. C. Leroux, *J. Control. Release*, 2005, **109**, 169-188.

7. X. W. Yang, F. J. Hua, K. Yamato, E. Ruckenstein, B. Gong, W. Kim and C. Y. Ryu, *Angew. Chem., Int. Ed.*, 2004, **43**, 6471-6474.

8. W. H. Binder, S. Bernstorff, C. Kluger, L. Petraru and M. J. Kunz, *Adv. Mater.*, 2005, **17**, 2824-2828.

9. A. Noro, Y. Nagata, A. Takano and Y. Matsushita, *Biomacromolecules*, 2006, **7**, 1696-1699.

10. K. E. Feldman, M. J. Kade, T. F. A. de Greef, E. W. Meijer, E. J. Kramer and C. J. Hawker, *Macromolecules*, 2008, **41**, 4694-4700.

11. B. G. G. Lohmeijer and U. S. Schubert, *Angew. Chem., Int. Ed.*, 2002, **41**, 3825-3829.

12. B. Z. Chen and H. F. Sleiman, *Macromolecules*, 2004, **37**, 5866-5872.

13. G. C. Zhou and Harruna, II, *Macromolecules*, 2005, **38**, 4114-4123.

14. A. O. Moughton and R. K. O'Reilly, *J. Am. Chem. Soc.*, 2008, **130**, 8714-8725.

15. A. V. Ambade, S. K. Yang and M. Weck, *Angew. Chem., Int. Ed.*, 2009, **48**, 2894-2898.

16. U. Rauwald and O. A. Scherman, *Angew. Chem., Int. Ed.*, 2008, **47**, 3950-3953.

17. H. W. Gibson, A. Farcas, J. W. Jones, Z. X. Ge, F. H. Huang, M. Vergne and D. M. Hercules, *J. Polym. Sci., Part A*, 2009, **47**, 3518-3543.

18. S. J. Rowan, S. J. Cantrill, G. R. L. Cousins, J. K. M. Sanders and J. F. Stoddart, *Angew. Chem., Int. Ed.*, 2002, **41**, 898-952.

19. M. A. Tasdelen, M. U. Kahveci and Y. Yagci, *Prog. Polym. Sci.*, 2011, **36**, 455-567.

20. R. Nguyen, L. Allouche, E. Buhler and N. Giuseppone, *Angew. Chem., Int. Ed.*, 2009, **48**, 1093-1096.

21. C. B. Minkenberg, L. Florusse, R. Eelkema, G. J. M. Koper and J. H. van Esch, *J. Am. Chem. Soc.*, 2009, **131**, 11274-11275.

22. P. T. Corbett, J. Leclaire, L. Vial, K. R. West, J. L. Wietor, J. K. M. Sanders and S. Otto, *Chem. Rev.*, 2006, **106**, 3652-3711.

23. G. Moad, E. Rizzardo and S. H. Thang, *Aust. J. Chem.*, 2006, **59**, 669-692.

24. G. Moad, E. Rizzardo and S. H. Thang, *Aust. J. Chem.*, 2009, **62**, 1402-1472.

25. S. Perrier and P. Takolpuckdee, *J. Polym. Sci., Part A*, 2005, **43**, 5347-5393.

26. J. Chiefari, Y. K. Chong, F. Ercole, J. Krstina, J. Jeffery, T. P. T. Le, R. T. A. Mayadunne, G. F. Meijs, C. L. Moad, G. Moad, E. Rizzardo and S. H. Thang, *Macromolecules*, 1998, **31**, 5559-5562.

27. S. R. Gondi, A. P. Vogt and B. S. Sumerlin, *Macromolecules*, 2007, **40**, 474-481.

28. K. L. Heredia, T. H. Nguyen, C. W. Chang, V. Bulmus, T. P. Davis and H. D. Maynard, *Chem. Commun.*, 2008, 3245-3247.

29. J. T. Kopping, Z. P. Tolstyka and H. D. Maynard, *Macromolecules*, 2007, **40**, 8593-8599.

30. C. Y. Hong and C. Y. Pan, *Macromolecules*, 2006, **39**, 3517-3524.

31. J. T. Lai, D. Filla and R. Shea, *Macromolecules*, 2002, **35**, 6754-6756.

32. D. S. Germack and K. L. Wooley, *J. Polym. Sci., Part A*, 2007, **45**, 4100-4108.

33. C. Booth, T. D. Naylor, C. Price, N. S. Rajab and R. B. Stubbersfield, *J. Chem. Soc., Faraday Trans. 1*, 1978, **74**, 2352-2362.

34.   P. Bahadur, N. V. Sastry, S. Marti and G. Riess, *Colloids and Surfaces*, 1985, **16**, 337-346.

35.   C. Price, *Pure Appl. Chem.*, 1983, **55**, 1563-1572.

36.   P.-G. Gennes, *Scaling Concepts in Polymer Physics; Cornell University Press: Ithaca, NY*, 1970, 113-123.

Chapter 3

Imine Cross-Linked Star Polymer and Nanogel Nanoparticles

This chapter is based on the following publications:

A. W. Jackson and D. A. Fulton, "The formation of core cross-linked star polymers containing cores cross-linked by dynamic covalent imine bonds", *Chem. Commun.*, 2010, **46**, 6051 – 6053.

A. W. Jackson, C. Stakes and D. A. Fulton, "The formation of core cross-linked star polymer and nanogel assemblies facilitated by the formation of dynamic covalent imine bonds", *Polym. Chem.*, 2011, **2**, 2500 – 2511.

Table of Contents:

3.1   Abstract

Reversible addition-fragmentation chain transfer (RAFT) polymerization has been utilized to prepare diblock copolymer chains possessing 'inert' blocks of polystyrene and 'reactive' blocks displaying aldehyde or amino functional groups. These polymer chains were shown to cross-link through the formation of imine bonds in organic solvents to form kinetically stable polymer nanoparticles possessing core-cross-linked star (CCS) polymer architectures. RAFT polymerization was utilized to prepare methacrylate copolymers possessing only 'reactive' blocks, and these copolymers were shown to cross-link through the formation of imine bonds in organic solvents to form polymer assemblies possessing nanogel architectures. Both cross-linking procedures displayed a size-dependency upon the concentration at which the cross-linking reactions are performed. Both the CCS polymers and nanogels underwent structural reconfiguration to linear polymer chains through component exchange facilitated by trans-imination with a small molecule amine.

3.2   Introduction

Polymeric nanoparticles represent an important class of polymer materials, finding application in numerous technological applications such as electronics,[1] coatings,[2] and drug delivery.[3] Recent developments have seen the incorporation of dynamic interactions into polymeric nanoparticles, which has led to the emergence of impressive new materials possessing thermoresponsive,[4] chemoresponsive,[5] mechanoresponsive,[6] photoresponsive,[7] electroresponsive[8] or self-healing properties.[9]

It was hypothesized here that dynamic covalent imine bond formation could be employed to facilitate the assembly of complementary aldehyde- and amine-functional linear polymer building blocks into nanoparticle-like assemblies. The condensation between an aldehyde and an amine to afford an imine proceeds readily in organic solvents, making imine bond formation particularly appealing as the cross-linking reaction in organic media. This approach does not rely upon non-covalent self-assembly, and instils chemical robustness on account of the covalent nature of the imine bond. It was hypothesized that polymer nanoparticles which incorporate imine linkages would be able to reversibly switch between nano-sized assemblies and linear polymer chains via a *trans*-imination pathway upon the addition of a small molecule amine. This chapter describes the incorporation of multiple imine cross-links into two classes of

interesting and potentially useful polymer architectures which can be considered as nanoparticles, namely, core cross-linked star (CCS) polymers[10, 11] and nanogels.[12]

CCS polymers are a class of nano-sized polymer assembly whose structural features are defined by a core consisting of a network of cross-linked polymer chains surrounded by a corona of polymeric arms. Much of the interest in CCS polymers is as a consequence of their architectures, possessing cores which can be utilized as carriers for small molecules such as drugs or fragrances, and coronal chains which help to solubilise and shield the cargo from its external environment. CCS polymers also possess solubilities and viscosities similar to linear polymers of relatively low molecular weight, which make them potentially very useful in a diverse range of fields, most notably drug delivery[13] as well as imaging[14] and catalysis.[15-17] The CCS polymers presented here are constructed (Figure 3.1) from linear diblock copolymer chains possessing an ''inert'' block which prevents macroscopic cross-linking, and a ''reactive'' block which contains aldehyde or amine functions which facilitate cross-linking of polymer chains through reversible imine bond formation.

Nanogels can be considered as CCS polymers without coronal arms, consisting only of a spherical network of cross-linked polymer chains. This class of polymer architecture has been extensively investigated as drug delivery carriers on account of their high stabilities and loading capacities.[18] The nanogels presented here were prepared (Figure 3.1) by cross-linking "reactive" linear copolymer chains possessing aldehyde or amine functions, with a lower functional density required to prevent macroscopic gelation as these polymer chains do not possess an "inert" block.
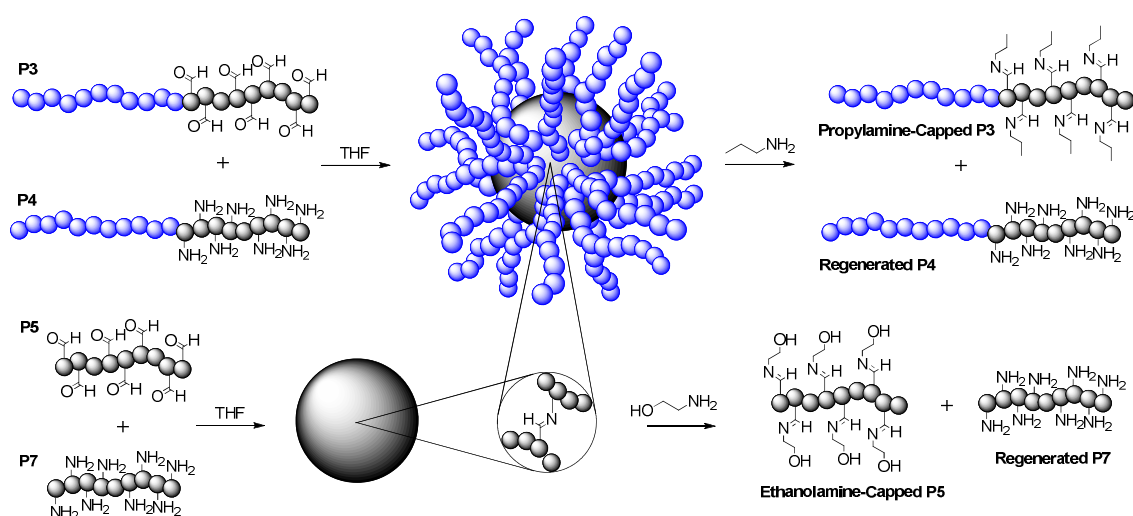
Figure 3.1 Formation of dynamic covalent core cross-linked star polymers and nanogel nanoparticles facilitated by the cross-linking of polymer chains through the formation of imine bonds, followed by reconfiguration back to linear polymer chains through *trans*-imination.

3.3   Results and Discussion

3.3.1   *Styrenic Aldehyde/ Amine-Functional Diblock Copolymers*
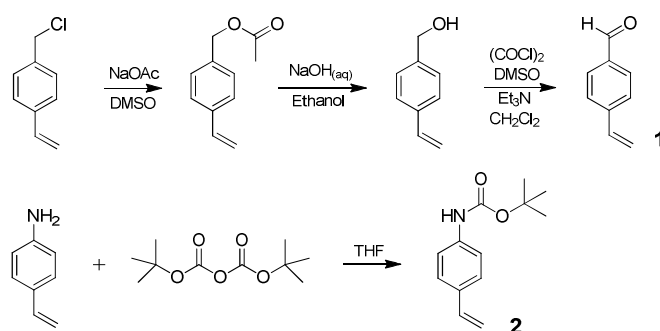
Scheme 3.1 Synthesis of aldehyde- and *boc*-amino-functional styrenic monomers **1** and **2**.

The first part of this project focused on investigating the formation of CCS polymers from pre-formed linear polymer chains. 4-Vinylbenzaldehyde (**1**) was prepared[19] (Scheme 3.1) in three synthetic steps. 4-Vinylbenzyl chloride which was initially converted to 4-vinylbenzyl acetate through reaction with sodium acetate in DMSO at 45 °C and treatment of this crude product with $NaOH_{(aq)}$ furnished 4-vinylbenzyl alcohol which was converted to the desired product **1** via a Swern oxidation. *N*-Boc-4-aminostyrene (**2**) was prepared[20] by treating 4-aminostyrene with di-*tert*-butyldicarbonate in THF.
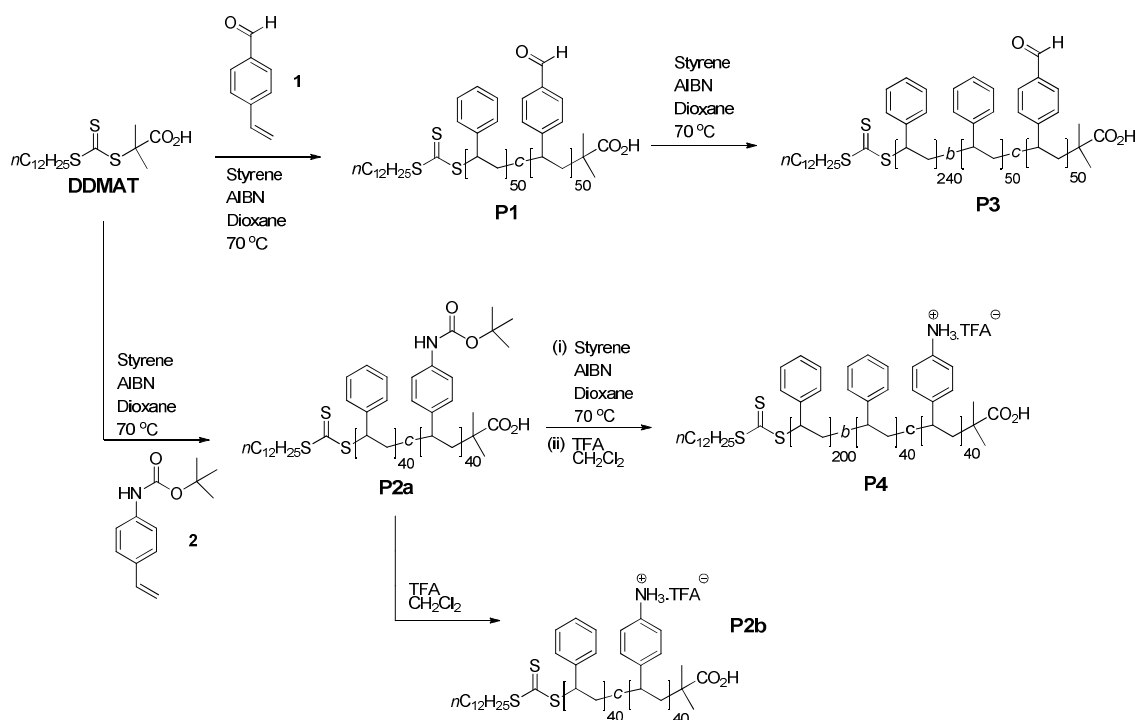
Scheme 3.2 Synthetic route to aldehyde- and amine-functional styrenic diblock copolymers.

The two functional styrenic monomers **1** and **2** were then used to prepare diblock copolymers incorporating the desired functionality. The polymers **P3** and **P4** were prepared by RAFT polymerization, which was utilized throughout this study on account of its versatility and experimental simplicity. The RAFT chain transfer agent *S*-1-dodecyl-*S'*-(α,α-dimethyl-α''-acetic acid)trithiocarbonate[21] (DDMAT) was used (Scheme 3.2) to mediate the copolymerization of a 1:1 mixture of styrene and 4-vinylbenzaldehyde (**1**) at 70 ˚C in dioxane to afford **P1**, which after purification, *via* precipitation in hexane, was used as a macro-CTA and extended via RAFT polymerization with styrene at 70 ˚C in dioxane to afford **P3** which features a 'reactive block' featuring approximately 50 aldehyde functions and an 'inert' block of polystyrene. Comparison of the GPC trace of the chain-extended polymer **P3** with the macro-CTA **P1** (Figure 3.2a) indicates complete and successful chain extension. The copolymer **P2a** was prepared (Scheme 3.2) via RAFT polymerization of a 1:1 mixture of *N*-boc-4-aminostyrene (**2**) and styrene at 70 ˚C in dioxane, which was then used as a macro-CTA and extended via RAFT polymerization with styrene at 70 ˚C in dioxane to afford, after the removal of the protecting groups, **P4**. Again, comparison of the GPC trace of the chain-extended polymer **P4** with the macro-CTA **P2a** (Figure 3.2b) indicates complete and successful chain extension. The shoulder present in the GPC trace for **P4** is probably on account of the noticeable increase in viscosity of the polymerization mixture as the reaction proceeds, which may adversely affect the kinetics of the polymerization process. A sample of the copolymer **P2a** was also subjected to acidic conditions to remove the protecting groups to yield **P2b**. All polymers **P1** – **P4** were characterized by ^{1}H NMR spectroscopy and gel permeation chromatography (GPC) (Table 3.1). The PDIs were found to be < 1.40, indicating all polymerizations proceeded with acceptable levels of control. The values of hydrodynamic radius (R_h), as determined by online dynamic light scattering measurements are consistent with linear polymer chains and indicate that there is no aggregation between the polymers dissolved in THF.
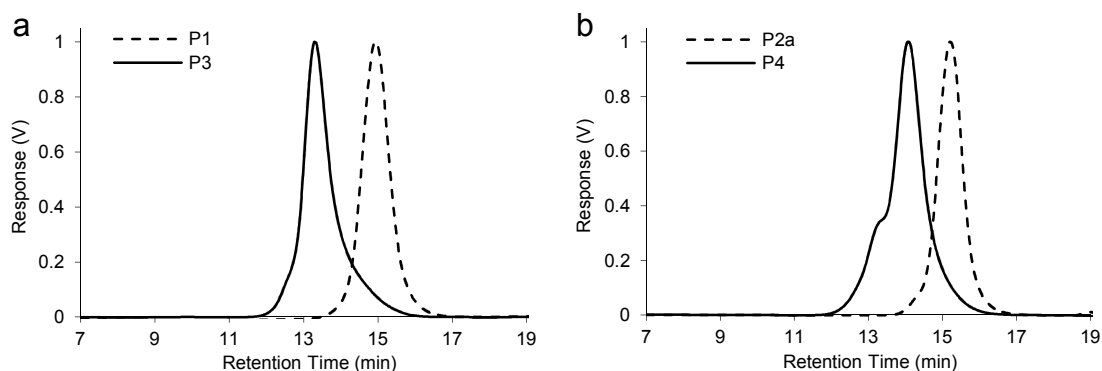
Figure 3.2 (a) Differential refractive index (dRI) GPC traces (THF 1.0 mL/ min) of **P1** and resulting diblock copolymer **P3** after chain extension, (b) dRI GPC traces (THF 1.0 mL/ min) of **P2a** and resulting diblock copolymer **P4** after chain extension.

polymer	$M_n{}^a$ (g mol^{-1})	$M_n{}^b$ (g mol^{-1})	$M_w{}^b$ (g mol^{-1})	PDI^b (M_w/M_n)	$R_h{}^c$ (nm)
P1	12,200	9,200	10,750	1.17	2.5
P2a	13,300	7,350	8,300	1.13	2.4
P2b	13,800	8,000	9,000	1.13	2.6
P3	37,200	32,000	43,300	1.35	4.5
P4	30,100	20,250	28,350	1.40	5.2

Table 3.1 Characterization of polymer **P1** – **P4**. . ^{a} As determined by ^{1}H NMR spectroscopy. ^{b} As determined by gel permeation chromatography in THF (1.0 mL/ min) calibrated against polystyrene standards. ^{c} As determined by online dynamic LS measurements.

3.3.2   *Polystyrene-Based Core Cross-Linked (CCS) Polymers*

The diblock copolymers **P3** and **P4** were then used as components for the self-assembly of CCS polymers. These were prepared by mixing equimolar solutions of **P3** and **P4** in THF in the presence of TFA catalyst at a range of different concentrations (0.5 – 5.0 wt % with respect to total polymer concentration), and the resulting solutions were left to equilibrate overnight before analysis (Table 3.2) by gel permeation chromatography– multiangle laser light scattering (GPC–MALLS) which also permits the measurement of M_w and the radius of gyration (R_g). Online dynamic light scattering measurements also furnished the hydrodynamic radius (R_h). No macroscopic gelation was observed in any of these experiments, an observation which suggests the 'inert' blocks are successfully preventing macroscopic cross-linking of the polymer chains at the concentrations studied.

exp. no.	total diblock copolymer wt %	$M_n{}^a$ (g mol^{-1})	$M_w{}^a$ (g mol^{-1})	PDI^a (M_w/M_n)	average no. of polymer chains per assembly^c	$R_g{}^a$ (nm)	$R_h{}^b$ (nm)	structure sensitive ρ parameter (R_g/R_h)
1	0.5	379,600	399,600	1.05	11	13.3	11.7	1.14
2	1	493,000	515,100	1.04	14	13.1	12.5	1.05
3	2	967,000	1,175,000	1.22	33	19.5	14.8	1.32
4	3	1,337,000	1,651,000	1.23	46	27.7	17.7	1.56
5	4	2,401,000	3,034,000	1.26	85	44.9	26.0	1.73
6	5	5,235,000	6,808,000	1.30	190	61.9	34.4	1.80

Table 3.2 Characterization of styrenic CCS polymers. ^{a} As determined by online static light scattering in THF (1.0 mL/ min) using experimentally determined dn/dc value (0.204 mL/ g). ^{b} As determined by online dynamic light scattering in THF (1.0 mL/ min). ^{c} Calculated by dividing M_w for CCS polymers by the average M_w of **P3** and **P4**.

All GPC traces (Figure 3.3a) display disappearance of the peaks at ~ 14 min corresponding to diblock copolymers **P3** and **P4**, and the appearance of major peaks at lower elution volumes indicative of the formation of high molecular weight aggregates of polymer chains. These experiments indicate a dependence (Figure 3.3b) of the M_w of the CCS polymers formed upon the concentrations of the starting diblock polymers used, indicating CCS polymers of a desired size can be prepared simply by altering the concentration of polymer building blocks in the self-assembly reaction.
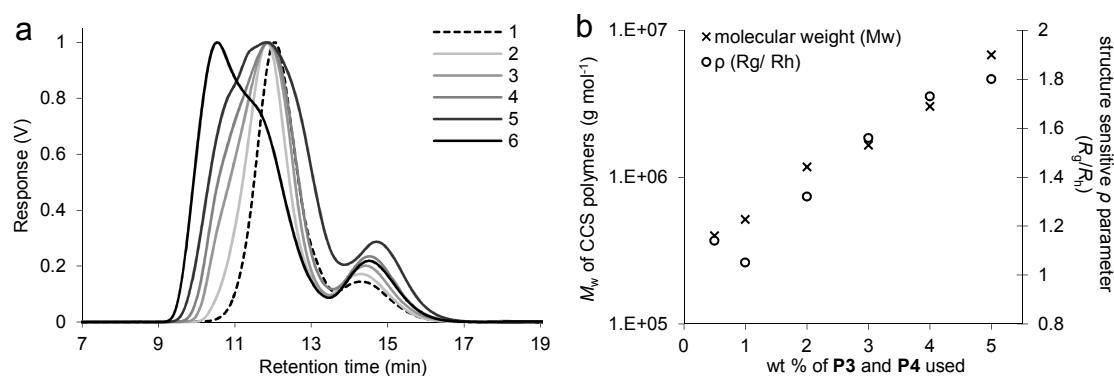
Figure 3.3 (a) Differential refractive index (dRI) GPC traces for experiments **1**, **3** and **6** in THF (1.0 mL/ min). Traces for experiments **2**, **4** and **5** have been omitted for clarity, (b) The dependence of M_w and ρ of the CCS polymers obtained from cross-linking equimolar amounts of polymers **P3** and **P4** at different concentrations.

The M_w measurements as determined by GPC-MALLS were consistently larger than those determined by calibration against PS standards, an observation consistent with the character of CCS polymers, which are more compact than their linear counterparts with the same molecular weights, suggesting that the CCS polymers prepared possess a cross-linked branched structure. Further evidence supporting the CCS polymer

architecture can be obtained from the structure sensitive ρ parameter ($\rho = R_g/R_h$) defined by Burchard and co-workers.[22] Those CCS polymers prepared at lower concentrations (0.5 and 1.0 wt %, Table 3.2, entries **1 - 2**) possess ρ values ~ 1.1, which is consistent[23] with monodisperse regular star architectures and suggests that these lower concentrations are the optimum to form the most monodisperse species. The upward trend (Figure 3.3b) in ρ values for those CCS polymers prepared at higher concentrations (Table 3.2, entry **3 - 6**) indicates increasing polydispersity, which may be as a consequence of a degree of star-star couplings.

To investigate whether the CCS polymers are prone to re-equilibration, solutions of CCS polymers containing sufficient TFA to ensure *trans*-imination could occur were stored for one week at concentrations lower and higher than the concentration at which they were prepared. Subsequent GPC analysis showed no change suggesting that the CCS polymers formed are kinetically very stable and do not 'shrink' or 'grow' in response to concentration changes. This is most probably due to the fact that each polymer chain is incorporated through potentially 40-50 imine bonds. While the imine bonds are under dynamic equilibrium, release of a single chain would require all of the dynamic cross-links to momentarily lie on the side of products simultaneously. Therefore, it is highly unlikely that a single polymer chain could be released. These observations suggest that the products formed are under kinetic control.

Interestingly, all dRI GPC traces (Figure 3.3a) displayed the presence of a minor species eluting after ~ 14.5 min. An analytical sample of this species was isolated (Figure 3.4a) from experiment **3** by GPC and analyzed by matrix-assisted laser desorption ionization–time of flight (MALDI–TOF) mass spectrometry (Figure 3.5a). The mass spectrum suggests the presence of an aggregate with a molecular weight of approximately 60 – 65 kDa, strongly suggesting the formation of a 2–armed CCS polymer (Figure 3.4b) formed by the cross-linking between a single **P3** chain and a single **P4** chain. The mass spectroscopic evidence is, to the best of our knowledge, arguably the most convincing to date supporting the formation of 2-armed CCS polymers as a by-product during the formation of CCS polymers. Based on GPC chromatograms, Qiao and co-workers have postulated[24] the formation of 2-armed CCS polymers as a minor component of polymers prepared through so-called 'arm-first' methods[10, 11] employing irreversible cross-linking of the polymer chains. Further analysis of the GPC traces for cross-linking experiments **1 – 6** (Figure 3.3a) also reveals a concentration dependence for the 2-armed species, as it appears that increased concentrations of 2-armed species are formed at higher initial concentrations of

polymers **P3** and **P4**. This concentration dependence suggests that the cross-linking of polymers **P3** and **P4** to form multi- and 2-armed species proceeds under kinetic control. It is likely that the formation of multi-armed species is a slower process than the formation of the 2-armed species simply because larger numbers of polymer chains are required to aggregate, and thus their concentration will decrease relative to the 2-armed species in the product distribution at higher starting concentrations.
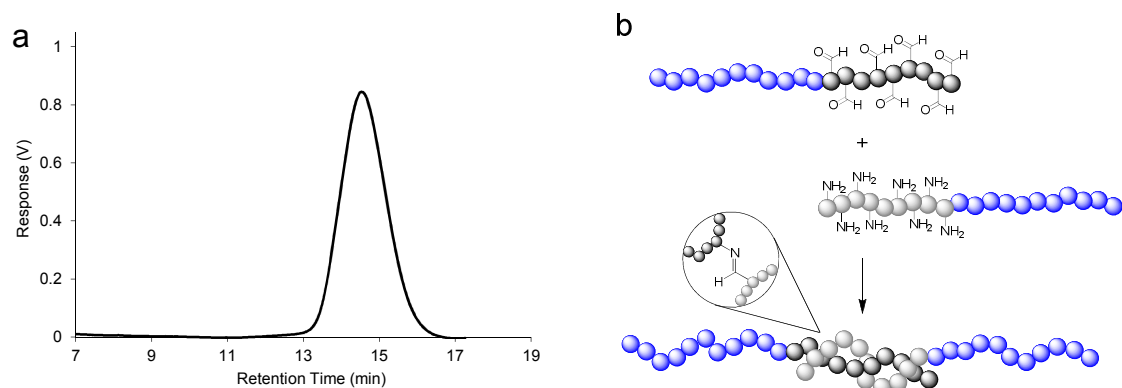
Figure 3.4 (a) Differential refractive index (dRI) GPC trace of purified minor peak from experiment **3**, (b) Formation of 2-armed core cross-linked star polymer.
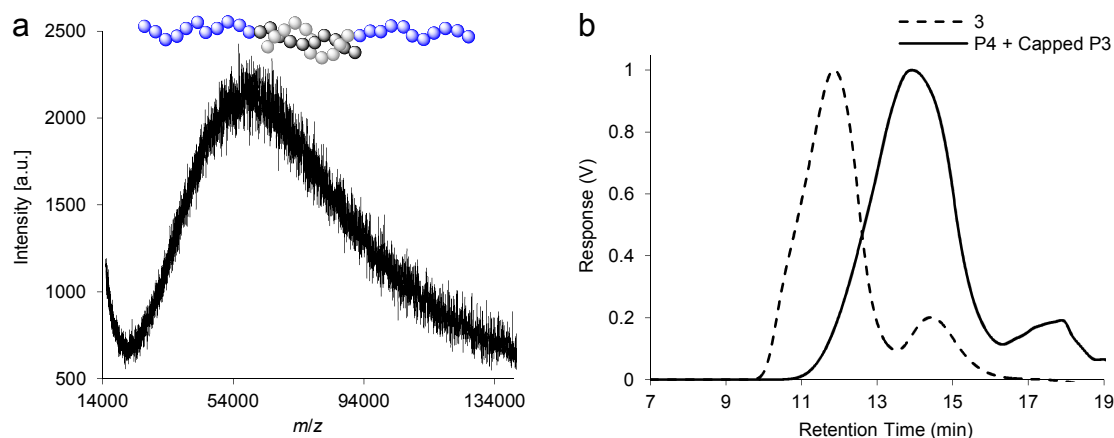
Figure 3.5 (a) The MALDI-TOF mass spectrum of the minor product of polymer cross-linking, which suggests this species is a 2–arm core cross-linked star polymer, (b) Differential refractive index (dRI) GPC traces indicating the decomposition of the CCS polymers prepared in Table 3.1 experiment **3** (dashed line) into block copolymers (solid line) after the addition of propylamine.

To demonstrate the potential of these CCS polymers to undergo structural reconfiguration upon exposure to a chemical stimulus, a large excess of propylamine was added to a solution of CCS polymers (as prepared in Table 3.1, experiment **3**) and the resulting mixture left to re-equilibrate overnight before GPC analysis (Figure 3.5b). The chromatogram obtained displayed the loss of the peak at ~11.5 min corresponding to CCS polymers and the appearance of a peak at ~14.0 min which corresponds to

diblock copolymers. This observation confirms that all the imine bonds present within the CCS polymer have undergone *trans*-imination reactions, resulting in disassembly of the CCS polymer species and the generation of **P4** and a derivative of **P3** where all aldehydes are have transformed into propylimines. Alkyl-derived imines are thermodynamically more stable than aniline-derived imines, providing a driving force for *trans*-imination to occur. We do not envisage that the products of the CCS polymer disassembly can easily be reconverted back into CCS polymers, as this transformation would effectively require the removal of propylamine from the system. The ability to induce a significant change in polymer assembly architecture as demonstrated here is potentially very useful because dramatic structural reconfiguration is likely to be accompanied by a significant change in the properties of the polymer, *e.g.* mechanical strength or viscosity.

The importance of the "inert" block in the formation of discrete CCS polymers was emphasized by a cross-linking experiment involving polymers **P1** and **P2b** which do not possess "inert" blocks. Equimolar solutions of **P1** and **P2b** in THF were combined in the presence of TFA catalyst at either 0.5 or 5 wt % and left to equilibrate. After approximately 15 min (5 wt %) or 2 h (0.5 wt %) a gel-like material was obtained (Figure 3.6a) suggesting the formation of a macroscopic cross-linked gel. This gel could potentially hold promise as a so-called covalently adaptable network[25] (CAN), constituting a new class of materials possessing adaptive and responsive properties on account of their dynamic imine cross-links.
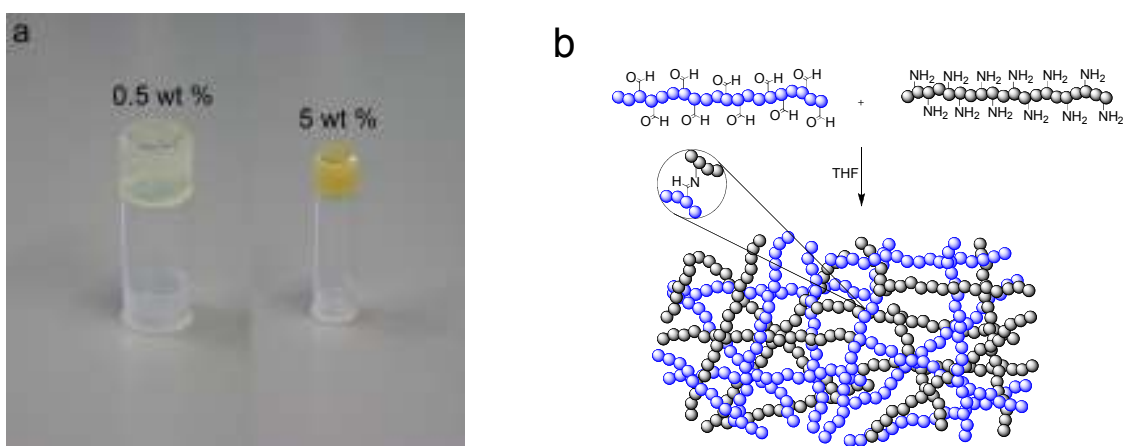
Figure 3.6 (a) Photographs of vial inversion test after cross-linking between **P1** and **P2b** at 0.5 and 5 wt %, (b) Cross-linking between aldehyde and amine-functional copolymers to form a macroscopic cross-linked organogel.

Results from our experiments suggest that an 'inert' block is required to promote the formation of CCS polymer species, and that in the absence of an inert block the polymer chains will cross-link to form macroscopic gels (Figure 3.6b). The propensity of polymers **P1** and **P2b** to cross-link into gels, however, may also be as a consequence of the relatively high density of aldehyde and amino groups within the polymer. Work by the group of Otsuka and Takahara suggests[26] that polymer chains without 'inert' blocks can cross-link to form polymeric nanogel architectures. This work utilizes cross-linking through a radical cross-over reaction, and the reactive functional group density within these polymers is much lower than the 1: 1 ratio of amine/aldehyde: styrene used in our own polymers **P1** and **P2b**. We therefore set out to investigate if it would be possible to form nanogel architectures by cross-linking through imine bonds polymer chains when the reactive functional group density is lowered to 1: 8.

3.3.3   *Aldehyde/ Amine Functional Methyl Methacrylate Copolymers*
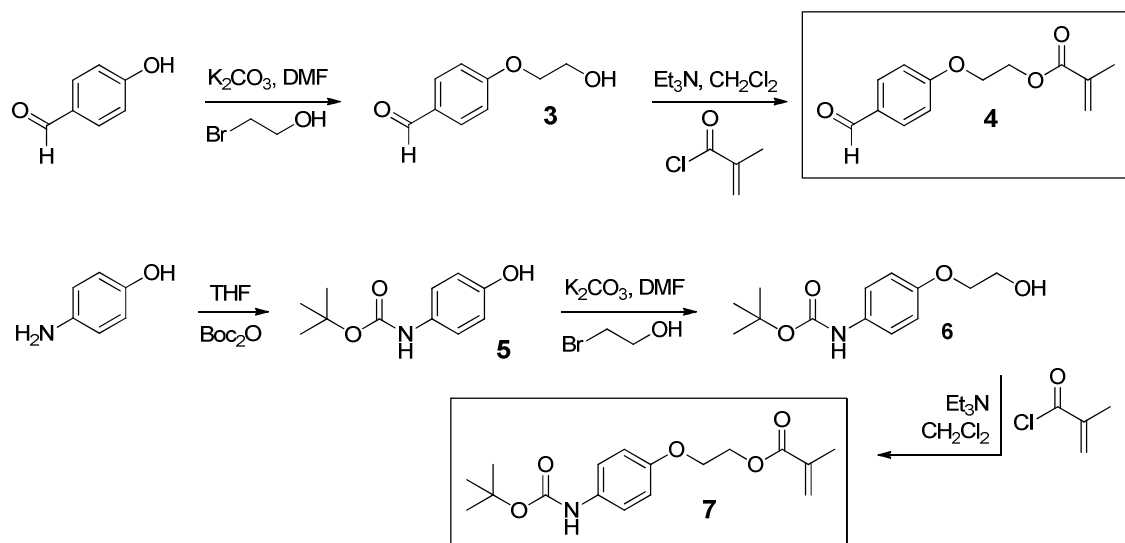
Scheme 3.3 Synthesis of aldehyde and amino-functionalized methyl methacrylate-based monomers **4** and **7**.

Attempts to utilize RAFT polymerizations to prepare analogues of copolymers **P1** and **P2b** possessing different functional group densities were unsuccessful, affording copolymers whose compositions differed from the feed ratio when this value deviated from 1: 1 of styrene: **1/2**. Although the reasons for this observation are uncertain, the differences in reactivities of the monomers are a possible source of the problem. We therefore chose to focus on methacrylate-based copolymers prepared by copolymerization of the monomers **4** or **7** (Scheme 3.4) with methyl methacrylate. The aldehyde or amine functional groups within these monomers are located sufficiently far

70

away from their vinyl groups to ensure these monomers possess similar reactivities to methyl methacrylate, thus ensuring that co-polymerizations can be better controlled and the ratios of the two monomers within the resulting copolymers accurately reflects the feed ratios. The monomer **4** was prepared (Scheme 3.3) by *O*-alkylation of 4-formylphenol to afford the alcohol **3** which was then acylated with methacryloyl chloride. Monomer **7** was prepared (Scheme 3.3) by Boc-protection of 4-aminophenol to afford **5**, which was then *O*-alkylated to furnish the alcohol **6**. Subsequent acylation with methacryloyl chloride afforded the monomer **7**. All synthetic steps to prepare these monomers proceeded with high yields and were experimentally straightforward, allowing significant quantities to be prepared quickly.
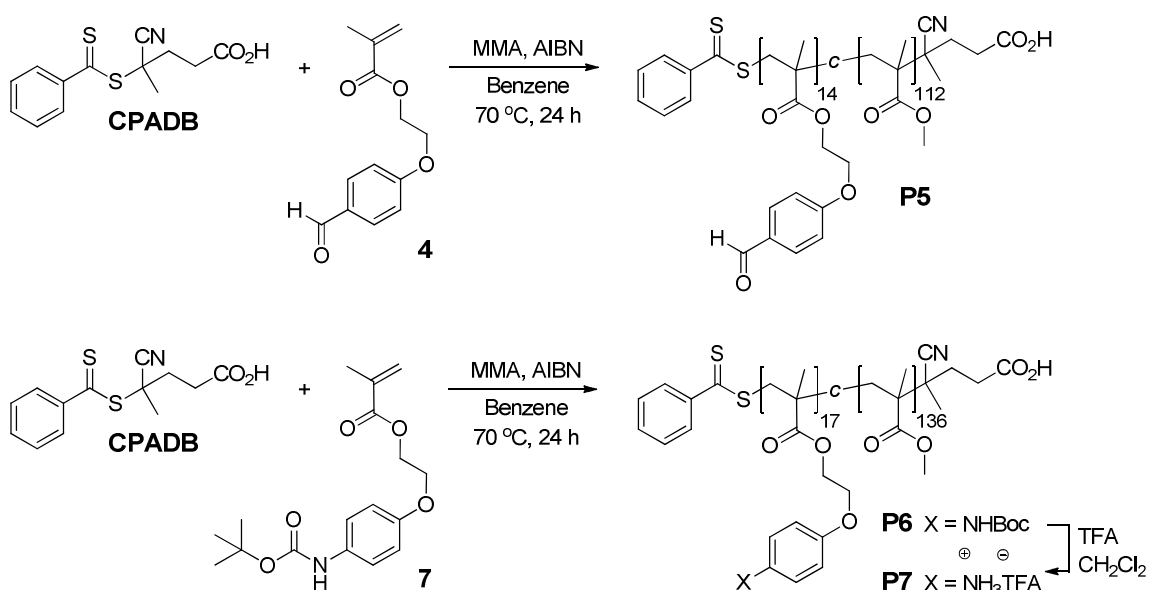
Scheme 3.4 Synthesis of aldehyde and amine functionalized copolymers **P5 – P7**.

polymer	$M_n{}^a$ (g mol^{-1})	$M_n{}^b$ (g mol^{-1})	$M_w{}^b$ (g mol^{-1})	PDI^b (M_w/M_n)	$R_h{}^c$ (nm)
P5	14,750	19,200	23,500	1.23	3.5
P6	19,350	34,600	46,200	1.34	5.4
P7	19,600	30,750	41,600	1.35	5.9

Table 3.3 Characterization of polymer **P5 – P7**. [a] As determined by ^{1}H NMR spectroscopy. [b] As determined by gel permeation chromatography in THF (1.0 mL/ min) calibrated against poly(methyl methacrylate) standards. [c] As determined by online dynamic light scattering measurements.

RAFT polymerization was used to prepare (Scheme 3.4) the functionalized copolymers **P5** – **P6**. The RAFT chain transfer agent 4-(4-cyanopentanoic acid)dithiobenzoate[27] (CPADB) was used to mediate the copolymerization of a 8: 1 mixture of methyl methacrylate: **4** in benzene at 70 ˚C to afford **P5**. Likewise, the copolymer **P6** was prepared via RAFT polymerization of a 8: 1 mixture of methyl methacrylate: **7** in benzene at 70 ˚C, which was then treated with TFA/CH$_2$Cl$_2$ to remove the protecting groups to yield **P7**. Polymers **P5** – **P7** were characterized (Table 3.3) by ^{1}H NMR spectroscopy and GPC. All copolymers prepared possessed compositions identical to the feed ratios of the monomers used, and GPC analysis (Figure 3.7a) confirmed mono-modal distributions and low PDIs, suggesting the polymerizations proceed with a good degree of control. These observations also suggest that the functional monomers **4** and **7** are of similar reactivity to methyl methacrylate and the distribution of the monomers along the copolymers are likely to be random. The number average molecular weight (M_n) of polymers **P5** – **P7** obtained by ^{1}H NMR spectroscopy are not consistent with the M_n values determined by GPC, although this discrepancy is probably on account of the relative structural differences between the functionalized copolymers **P5** – **P7** and the poly(methyl methacrylate) standards used for GPC calibration. The values of R_h as determined by online dynamic light scattering measurements are consistent with linear polymer chains and indicate that there is no aggregation between the polymer chains when dissolved in THF.
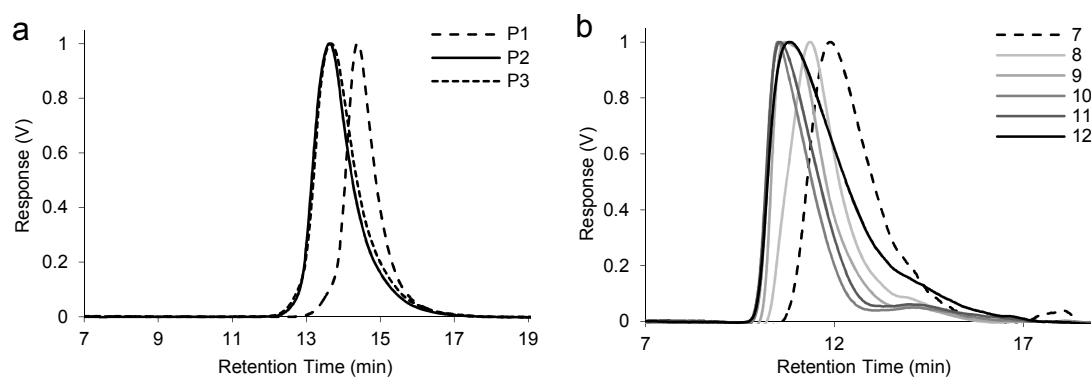
Figure 3.7 (a) Differential refractive index (dRI) GPC traces (in THF at 1.0 mL/ min) of functional copolymers **P5** – **P7**, (b) Differential refractive index (dRI) GPC traces (in THF at 1.0 mL/ min) for experiments **7** – **12**.

3.3.4 *Methyl Methacrylate-Based Cross-Linked Nanogels*

exp. no.	total diblock copolymer wt %	M_n[a] (g mol^{-1})	M_w[a] (g mol^{-1})	PDI[a] (M_w/M_n)	average no. of polymer chains per assembly[c]	R_g[a] (nm)	R_h[b] (nm)	structure sensitive ρ parameter (R_g/R_h)
7	0.1	777,600	797,400	1.03	24	8.8	12.8	0.69
8	0.25	2,299,000	2,385,000	1.04	73	11.9	15.5	0.77
9	0.5	4,870,000	5,515,000	1.13	169	18.7	21.0	0.89
10	1	10,550,000	12,280,000	1.16	377	24.6	25.7	0.96
11	1.5	17,540,000	20,600,000	1.17	633	30.9	29.9	1.03
12	2	23,335,000	27,620,000	1.18	849	39.0	34.4	1.13

Table 3.4 Characterization of methyl methacrylate nanogels. [a] As determined by online static light scattering in THF (1.0 mL/ min) using experimentally determined *dn/dc* value (0.095 mL/ g). [b] As determined by online dynamic light scattering in THF (1.0 mL/ min). [c] Calculated by dividing M_w for nanogels by the average M_w of **P5** and **P7**.

To investigate the formation of nanogels (Figure 3.1), equimolar solutions of **P5** and **P7** were mixed in THF and allowed to cross-link. A series of experiment (**7** – **12**, Table 3.4) were conducted over a range of concentrations (0.1 – 2 wt % of total copolymer building blocks). Solutions were left to equilibrate for 24 h before analysis by GPC-MALLS (Table 3.4) to obtain the measurement of M_n, M_w and R_g. Online dynamic light scattering measurements also furnished R_h. No macroscopic gelation was observed in any of these experiments, suggesting the formation of discrete nanogels. All GPC traces (Figure 3.7b) show a disappearance of peaks at ~ 13.5 – 14.5 min corresponding to diblock copolymers **P5** and **P7** and the appearance of a major peak at lower elution volume indicating the formation of high molecular weight species. As with the styrenic CCS polymers, these experiments indicate (Figure 3.8a) a concentration dependence, with the M_w of the nanogels formed dependent upon the initial concentration of the copolymer building blocks used during cross-linking. The M_w measurements as determined by GPC-MALLS were consistently larger than those determined by calibration against linear PMMA standards, an observation which suggests the nanogels formed are compact and their cross-linked nature reduces their volumes, subsequently decreasing their GPC elution volumes. Further evidence for the formation of nanogel architectures can again be obtained from the structure sensitive ρ parameter ($\rho = R_g/R_h$). Those nanogels formed at lower concentrations (experiments number **7** – **8**) possess ρ values < 0.8 which are consistent[23] with compact spherical shapes. The upward trend (Figure 8a) in ρ values for those nanogels formed at higher concentrations (experiments **9** – **12**) may indicate the presence of a degree of sphere-sphere couplings. These results

suggest that cross-linking is best performed at low concentrations to ensure the formation of nanogels possessing low polydispersity. More importantly, these results also indicate that 'inert' blocks are not required for the formation of discrete nanogels by imine formation when the density of the functional groups involved in cross-linking is sufficiently low.
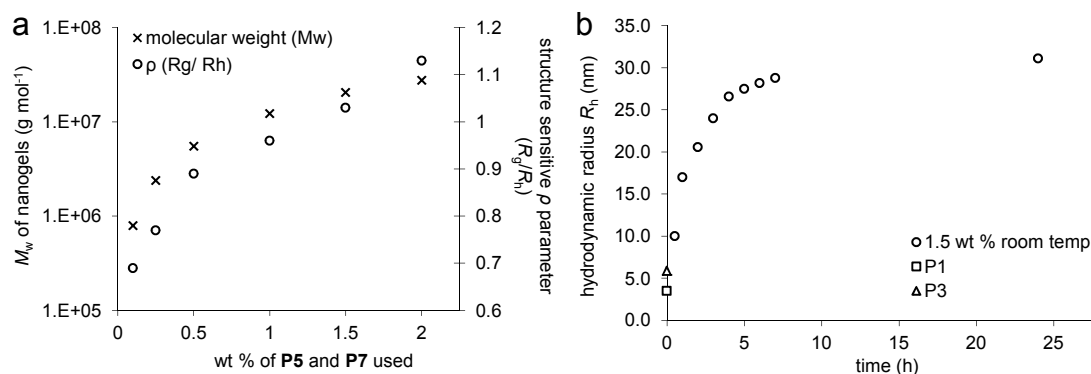
Figure 3.8 (a) The dependence of M_w and ρ of the nanogel obtained by cross linking on the wt % of polymer **P5** and **P7** used, (b) Nanogel formation over 24 h. The hydrodynamic radii of **P5** and **P7** are given for comparison.

To investigate whether the nanogels are susceptible to re-equilibration, solutions of nanogels containing sufficient TFA to ensure *trans*-imination could occur were stored for three days at concentrations lower and higher than the concentration at which they were prepared. Subsequent GPC analysis showed no change, suggesting that the nanogels are kinetically very stable and do not 'shrink' or 'grow' in response to concentration changes.

To gain insight into the kinetics of nanogel formation, experiment **5** (1.5 wt % of **P5** and **P7**) was repeated by following the progress of the cross-linking by GPC-MALLS as a function of time (Figure 3.8b). Unfortunately the molecular weight cut-off of our GPC columns was too low to allow us to follow the entire self-assembly process by GPC, but online R_h measurements gave useful insight. The hydrodynamic radius was found to increase over time, reaching a plateau of around 30 nm after 6 h at which point equilibrium is presumably attained. The GPC measurements indicated that the component polymers **P5** and **P7** are consumed almost immediately. We postulate that those species which are formed initially from the cross-linking of **P5** with **P7** possess a small excess of aldehyde or amine functions, and that as the cross-linking continues these species can further link together forming larger species until the system runs out of polymer building blocks and particles possessing a constant hydrodynamic radius are observed. It is also possible that the ability of the imine bonds to undergo *trans-*

imination processes also facilitates a certain amount of structural reorganization within the polymer assemblies.

As it was possible for our styrenic CCS polymers to undergo stimuli-triggered disassembly in organic solvents, we envisaged that these nanogel species should also be able to undergo the same process. To demonstrate this possibility, a large excess of ethanolamine was added to experiment **10** (1 wt % of **P5** and **P7**) and the solution left to equilibrate overnight before GPC analysis. The chromatogram obtained (Figure 3.9a) displayed a loss of the peak at ~ 11 min corresponding to nanogel species and the appearance of a peak at ~ 14 min which corresponds to regenerated **P7** and presumably ethanolamine capped-**P5**. This observation indicates that all the imine bonds present within the nanogels have undergone *trans*-imination with ethanolamine resulting in the disassembly of the nanogels into single polymer chains.

A series of cross-linking experiments were conducted at increased initial concentrations of **P5** and **P7** (3, 4 and 5 wt %). The solutions obtained at 3 and 4 wt % were very viscous and not suitable for GPC analysis on account of the presence of small precipitates. Cross-linking at 5 wt % resulted in the formation of a macroscopic cross-linked organogel, confirmed by the vial inversion test (Figure 3.9b). These results indicate that when cross-linking is performed at higher concentrations, the formation of macroscopic networks occurs instead of discrete nanogels.
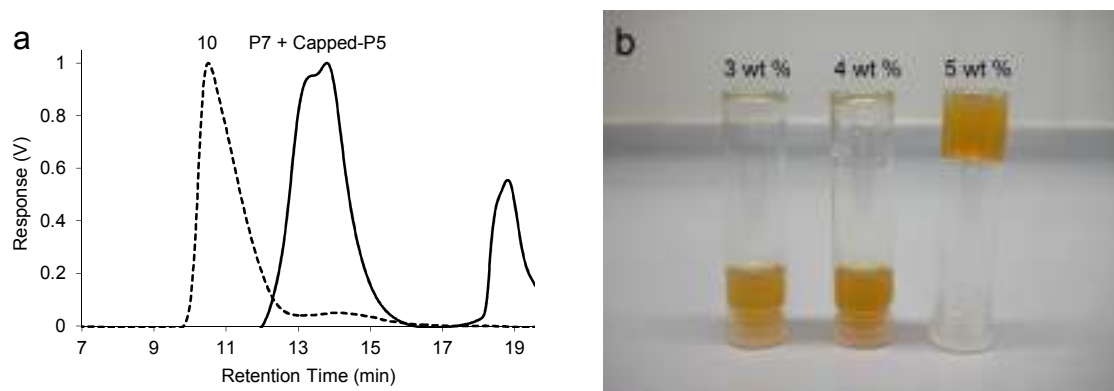
Figure 3.9 (a) Differential refractive index (dRI) GPC traces (in THF at 1.0 mL/ min) displaying the disassembly of nanogels obtained from experiment **10** (1 wt % of **P5** and **P7**), the peak at 19 mins corresponds to excess ethanolamine, (b) Photograph of vial inversion test after cross-linking between **P5** and **P7** at 3, 4 and 5 wt%.

3.4   Conclusions

RAFT polymerization has been utilized to prepare novel aldehyde and amine functional styrenic- and methyl methacrylate-based copolymers, and it has been demonstrated that these copolymers can cross-link through imine bond formation to prepare core cross-linked star polymers and cross-linked nanogels. These polymer-based assemblies have been characterized by GPC-MALLS, which proved to be a very powerful tool in the analysis of these species.   The potential for these assemblies to undergo stimuli-triggered disassembly has been shown through *trans*-imination with a small molecule amine, demonstrating the chemoresponsivness of these polymer systems. Functional copolymer building blocks have also been used to form macroscopic cross-linked organogel networks, where the presence of dynamic covalent imine linkages suggests that they may possess adaptive properties. A size dependence upon the initial concentration of copolymer building blocks was observed for both the formation of CCS and nanogel polymers, suggesting the self-assembly process is likely to be under kinetic control. We speculate that the reasons for this kinetic control are as a consequence of the relative stability of the imine bonds formed in organic solvents. Under the conditions of the self-assembly, imine bonds are reluctant to undergo hydrolysis back to their component amine and aldehyde reaction partners, presumably because of the low concentration of water in the reaction.   Although it is likely that *trans*-imination reactions can occur after the polymer assemblies have formed, permitting them a very limited potential for reconfiguration, the fact that the imine cross-links cannot readily break means that significant structural reconfigurations cannot occur. It would not be possible, for instance, for a single polymer chain to break all of its imine cross-links and leave its nanoparticle. This contrasts with the CCS polymer system of Otsuka and Takahara (Chapter 1), where the dynamic covalent linkages can be broken at elevated temperatures permitting a polymer chain to leave the cross-linked assembly, allowing far more scope for structural reconfiguration of the nanoparticle species after its initial formation. Thus the lack of reversibility of the imine bond in organic solvents limits its usefulness in preparing adaptive and responsive species. The ability of the imine bond to readily undergo component exchange does, however, permit a level of chemoresponsive behaviour, as shown by the abilities of our cross-linked species to convert to linear polymer chains in the presence of an excess of amine. The imine bond becomes a far more interesting dynamic covalent reaction in water, as it is possible to alter significantly the position of its equilibrium with pH.

3.5   Experimental

All chemicals were purchased from Sigma-Aldrich or Alfa Aesar and were used as received without further purification. ^1H and ^{13}C NMR spectra were recorded on a Bruker Avance 300 spectrometer at 300 and 75 MHz, respectively, with the residual solvent signal as an internal standard. FT-IR spectroscopy was performed on a Varian 800 FT-IR instrument (Varian Inc.). High-resolution mass spectrometry was performed on a Waters LCT premier mass spectrometer (Waters Inc.). Gel permeation chromatography (GPC) was conducted on a Varian ProStar instrument (Varian Inc.) equipped with a pair of PL gel 5 μm Mixed D 300 × 7.5 mm columns with guard column (Polymer Laboratories Inc.) in series, a Varian 325 UV-vis dual wavelength detector (254 nm), a Dawn Heleos II multi-angle laser light scattering detector (Wyatt Technology Corp.) and a Viscotek 3580 differential RI detector. Near monodisperse poly(methyl methacrylate) or poly(styrene) standards (Agilent Technologies) were used for calibration. Data collection was performed with Galaxie software (Varian Inc.) and chromatograms analyzed with the Cirrus software (Varian Inc.) and Astra software (Wyatt Technology Corp.). MALDI-TOF analysis was performed on a Bruker Microflex (Bruker Daltonics). Samples for analysis were prepared by mixing solutions of dithranol (20 mg/mL) and AgTFA (10 mg/mL) with solutions of the polymer sample (10 mg/ mL) in amounts of 100 μL: 40μL: 20μL respectively. 0.6 μL of solution was spotted onto the MALDI plate for analysis. Calibration was carried out against near monodisperse polystyrene standards. Data collection was performed with Flexcontrol and analysis of spectra was performed using Flexanalysis software.

4-Vinylbenzaldehyde (1)[19]

A solution of 4-vinylbenzyl chloride (20.0 g, 130.2 mmol) and sodium acetate (12.9 g, 157.1 mmol) in $(CH_3)_2SO$ (60 mL) was heated at 45 °C whilst stirring under N_2 for 24 h. The reaction mixture was transferred to a separating funnel and H_2O (100 mL) added. The product was extracted into EtOAc (3 × 100 mL). The organic extracts were combined and dried over $MgSO_4$, filtered and evaporated to dryness to afford crude 4-vinylbenzylacetate as a pale yellow oil (24.8 g, 99 %), which was dried under high vacuum. 20 % $NaOH_{(aq)}$ (50 mL) was then added to a stirred solution of crude 4-vinylbenzylacetate (24.8 g, 140.8 mmol) in EtOH (50 mL) and the reaction mixture was heated at reflux for 4 h, allowed to cool to room temperature and then transferred into a

separating funnel with EtOAc (100 mL). The aqueous layer was washed with EtOAc (2 × 100 mL), and the organic extracts were combined and dried over MgSO$_4$, filtered and evaporated to dryness to afford crude 4-vinylbenzyl alcohol as a brown oil (26.4 g, 100%) which was dried under high vacuum. A solution of (COCl)$_2$ (8.6 g, 67.4 mmol) in CH$_2$Cl$_2$ (50 mL) was cooled to -78 °C whilst stirring under N$_2$. A solution of (CH$_3$)$_2$SO (10.7 g, 134.8 mmol) in CH$_2$Cl$_2$ (50 mL) was added dropwise over 15 min, and a solution of crude 4-vinylbenzyl alcohol (8.2 g, 61.3 mmol) in CH$_2$Cl$_2$ (50 mL) was then added dropwise over 30 min. Et$_3$N (19.8 g, 196.0 mmol) was added to the reaction mixture and the solution was allowed to reach room temperature. The reaction mixture was left to stir under N$_2$ for 16 h, then transferred into a separating funnel with HCl$_{(aq)}$ (1 M, 100 mL) and H$_2$O (100 mL). The organic layer was collected and dried over MgSO$_4$, filtered and evaporated to dryness to afford crude brown oil (8.1 g, 100 %). The crude product was purified by vacuum distillation to afford 4-vinylbenzaldehyde as a colourless oil (4.2 g, 52 %). ^{1}H NMR (CDCl$_3$): δ 5.44 (d, 1H, J = 10.8 Hz), 5.92 (d, 1H, J = 17.4 Hz), 6.76 (dd, 1H, J = 10.8 Hz, J = 17.4 Hz), 7.55 (d, 2H, J = 8.4 Hz), 7.84 (d, 2H, J = 8.4 Hz), 9.99 (s, 1H).

N-Boc-4-aminostyrene (2)[20]

A solution of 4-aminostyrene (4.5 g, 37.6 mmol) and di-*tert*-butyl dicarbonate (9.9 g, 45.2 mmol) in THF (100 mL) was heated at reflux under N$_2$ for 16 h. After evaporation to dryness crude material was transferred to a separating funnel in H$_2$O (50 mL) and the product was extracted with CH$_2$Cl$_2$ (3 × 50 mL). The organic extracts were combined and dried over Na$_2$SO$_4$, filtered, and evaporated to dryness to obtain a crude solid which was purified by column chromatography [SiO$_2$, Hexane-EtOAc (9:1)] to afford *N*-Boc-4-aminostyrene as a white solid (6.7 g, 80 %). ^{1}H NMR (CDCl$_3$): δ 1.52 (s, 9H), 5.15 (d, 1H, J = 9.9 Hz), 5.65 (d, 1H, J = 16.5 Hz), 6.53 (s, 1H), 6.65 (dd, 1H, J = 9.9 Hz, J = 16.5 Hz), 7.33 (s, 4H).

p-(2-Hydroxyethoxy)benzaldehyde (3)

Potassium carbonate (17.0 g, 0.123 mol) was suspended in a solution of 4-hydroxybenzaldehyde (5.0 g, 0.041 mol), 2-bromoethanol (5.1 g, 0.041 mol) and DMF (100 mL) under reflux conditions for 24 h. After filtration and evaporation to dryness, crude material was transferred into a separating funnel in CH$_2$Cl$_2$ (100 mL). The organic

layer was washed with NaCl$_{(aq)}$ (2 × 100 mL), dried over MgSO$_4$, filtered and evaporated to dryness to obtain a crude solid which was purified by column chromatography [SiO$_2$, Hexane-EtOAc (1:1)] to afford *p*-(2-hydroxyethoxy)-benzaldehyde (**1**) as a colourless oil (4.2 g, 62 %). ^{1}H NMR (CDCl$_3$): δ 3.10 (br, s, 1H), 3.95 (t, 2H, J = 4.8 Hz), 4.11 (t, 2H, J = 4.8 Hz), 6.95 (d, 2H, J = 8.7 Hz), 7.75 (d, 2H, J = 8.7 Hz), 9.79 (s, 1H). ^{13}C NMR (CDCl$_3$): δ 61.4, 71.0, 115.2, 130.4, 132.4, 164.2, 191.5. FT-IR (wavenumber, cm^{-1}): 3403 (O–H), 2934 (C–H), 2747 (C–H), 1676 (C=O), 1509 (C=C), 1427 (C=C). HRMS$^+$ C$_9$H$_{11}$O$_3$: Theoretical: 167.0708. Actual: 167.0709.

p-(2-Methacryloxyethoxy)benzaldehyde (4)

A solution of *p*-(2-hydroxyethoxy)benzaldehyde (**3**) (3.8 g, 0.023 mol) and Et$_3$N (2.8 g, 0.027 mol) in CH$_2$Cl$_2$ (75 mL) was cooled to 0 ˚C. To this mixture a solution of methacryloyl chloride (2.7 g, 0.026 mol) in CH$_2$Cl$_2$ (25 mL) was added dropwise over 30 min whilst stirring under an atmosphere of N$_2$. The reaction mixture was then allowed to reach room temperature and was left to stir for 2 h before transferring to a separating funnel with H$_2$O (100 mL). The organic layer was washed with NaCl$_{(aq)}$ (2 × 100 mL), dried over MgSO$_4$, filtered and evaporated to dryness to obtain a crude oil which was purified by column chromatography [SiO$_2$, Hexane-EtOAc (4:1)] to afford *p*-(2-methacrylate-ethoxy)-benzaldehyde (**4**) as a white solid (2.8 g, 52 %). ^{1}H NMR (CDCl$_3$): δ 1.92 (s, 3H), 4.29 (t, 2H, J = 5. 1 Hz), 4.51 (t, 2H, J = 5.1 Hz), 5.57 (m, 1H), 6.12 (s, 1H), 7.00 (d, 2H, J = 8.7 Hz), 7.81 (d, 2H, J = 8.7 Hz), 9.86 (s, 1H). ^{13}C NMR (CDCl$_3$): δ 18.7, 63.0, 66.6, 115.3, 126.7, 130.7, 132.3, 136.2, 163.9, 167.5, 191.1. FT-IR (wavenumber, cm^{-1}): 2981 (C–H), 2735 (C–H), 1694 (C=O), 1509 (C=C), 1449 (C=C). HRMS$^+$ C$_{13}$H$_{15}$O$_4$: Theoretical: 235.0970. Actual: 235.0972.

N-Boc-4-aminophenol (5)

A solution of 4-aminophenol (12.6 g, 0.115 mol) and di-*tert*-butyl dicarbonate (30.3 g, 0.139 mol) in THF (100 mL) was stirred at 40 ˚C for 1.5 h. The reaction mixture was allowed to cool to room temperature and then filtered and evaporated to dryness to afford a pale yellow solid which was re-dissolved in EtOAc (150 mL) and transferred to a separating funnel with H$_2$O (150 mL). The organic layer was dried over Na$_2$SO$_4$, filtered and evaporated to dryness to obtain a crude solid which was purified by recrystallization (EtOAc/ CH$_2$Cl$_2$) to afford *N*-Boc-4-aminophenol (**4**) as a white solid

(18.2 g, 76 %). ^{1}H NMR (CD$_3$CN): δ 1.46 (s, 9H), 6.73 (d, 2H, J = 8.7 Hz), 6.79 (s, 1H), 7.20 (d, 2H, J = 8.7 Hz), 7.29 (s, 1H). ^{13}C NMR (CD$_3$CN): δ 27.3, 78.8, 114.9, 117.0, 120.5, 131.0, 152.3. FT-IR (wavenumber, cm^{-1}): 3400 (O–H), 3352 (N–H), 2981 (C–H), 1695 (C=O), 1505 (C=C), 1436 (C=C). HRMS$^+$ C$_{11}$H$_{15}$O$_3$NNa: Theoretical: 232.0950. Actual: 232.0949.

p-(2-Hydroxyethoxy)-N-boc-aminobenzene (6)

Potassium carbonate (11.2 g, 0.081 mol) was added to a solution of *N*-Boc-4-aminophenol (**5**) (5.7 g, 0.027 mol) and 2-bromoethanol (10.2 g, 0.082 mol) in DMF (100 mL) and the resulting suspension heated under reflux conditions for 24 h. After filtration and evaporation to dryness, the crude material was dissolved in EtOAc (100 mL) and transferred into a separating funnel. The organic layer was washed with NaCl$_{(aq)}$ (2 × 100 mL), dried over Na$_2$SO$_4$, filtered and evaporated to dryness to obtain a crude oil which was purified by column chromatography [SiO$_2$, Hexane-EtOAc (3:1)] to afford *p*-(2-hydroxyethoxy)-*N*-Boc-aminobenzene (**5**) as a white solid (4.2 g, 62 %). ^{1}H NMR (CDCl$_3$): δ 1.50 (s, 9H), 2.61 (s, 1H), 3.91 (t, 2H, J = 4.8 Hz), 4.01 (t, 2H, J = 4.8 Hz), 6.66 (s, 1H), 6.82 (d, 2H, J = 9 Hz), 7.25 (d, 2H, J = 9 Hz). ^{13}C NMR (CD$_3$CN): δ 28.7, 61.8, 64.8, 70.3, 80,6, 115.6, 121.2, 132.5, 153.6. FT-IR (wavenumber, cm^{-1}): 3400 (O–H), 3360 (N–H), 2982 (C–H), 2932 (C–H), 1695 (C=O), 1518 (C=C), 1459 (C=C). HRMS$^+$ C$_{13}$H$_{19}$O$_4$NNa: Theoretical: 276.1212. Actual: 276.1211.

p-(2-Methacryloxyethoxy)-N-boc-aminobenzene (7)

A solution of *p*-(2-hydroxyethoxy)-*N*-boc-aminobenzene (**6**) (2.9 g, 0.011 mol) and Et$_3$N (1.4 g, 0.014 mol) in CH$_2$Cl$_2$ (75 mL) was cooled to 0 ˚C. A solution of methacryloyl chloride (1.3 g, 0.012 mol) in CH$_2$Cl$_2$ (25 mL) was added dropwise over 30 min whilst stirring under N$_2$ and the reaction mixture was allowed to reach room temperature and then stirred for 2 h before transferring to a separating funnel with H$_2$O (100 mL). The organic layer was washed with NaCl$_{(aq)}$ (2 × 100 mL), dried over Na$_2$SO$_4$, filtered and evaporated to dryness to obtain a crude oil which was purified by column chromatography [SiO$_2$, Hexane-EtOAc (9:1)] to afford *p*-(2-methacryloxyethoxy)-*N*-boc-aminobenzene (**M2**) as a white solid (2.3 g, 65 %). ^{1}H NMR (CDCl$_3$): δ 1.51 (s, 9H), 1.95 (s, 3H), 4.18 (t, 2H, J = 5.1 Hz), 4.48 (t, 2H, J = 5.1

Hz), 5.59 (m, 1H), 6.15 (s, 1H), 6.56 (s, 1H), 6.85 (d, 2H, J = 9 Hz), 7.28 (d, 2H, 9 Hz). ^{13}C NMR (CDCl$_3$): 18.4, 27.8, 63.5, 67.1, 80.6, 115.8, 121.1, 126.0, 132.6, 136.6, 153.5, 155.2, 167.6. FT-IR (wavenumber, cm^{-1}): 3331 (N–H), 2981 (C–H), 1694 (C=O), 1525 (C=C), 1463 (C=C). HRMS$^+$ C$_{17}$H$_{23}$O$_5$NNa: Theoretical: 344.1474. Actual: 344.1488.

*Aldehyde-Functionalized Copolymer (**P1**)*

S-1-Dodecyl-*S'*-(α,α-dimethyl-α''-acetic acid)trithiocarbonate (DDMAT) (1 eq, 57.5 mg, 0.158 mmol) and AIBN (0.2 eq, 5.2 mg, 31.6 μmol) were added to a small schlenk tube. Styrene (65 eq, 1.07 g, 10.3 mmol) and 4-vinylbenzaldehyde (**1**) (65 eq, 1.37 g, 10.3 mmol) was then added followed by dioxane (2.5 mL). The reaction mixture was degassed five times, and then the vessel was backfilled with N$_2$, purged with N$_2$, and allowed to warm to room temperature. The reaction mixture was then placed in an oil bath at 70 °C, and the polymerization was quenched after 21 h and solvent was removed on the rotary evaporator. The resulting yellow oil was dissolved in a minimal amount of THF and added dropwise to a large excess of ice-cold hexane. The resulting polymer precipitate was then isolated by filtration and dried under high vacuum. Polymer **P1** was obtained as a pale yellow solid (1.77 g, 91 %). ^1H NMR (CDCl$_3$): δ 0.84 (br, SC$_{11}$H$_{22}$C*H$_3$*, of the chain terminus), 1.42 (br, CHC*H$_2$*, polymer backbone), 1.61 (br, C*H*CH$_2$, polymer backbone), 3.29 (br, SC*H$_2$*C$_{11}$H$_{23}$, of the chain terminus), 6.51 (br, Ar, polymer backbone), 7.03 (br, Ar, polymer backbone), 7.50 (br, Ar, polymer backbone), 9.89 (br, C*H*O, polymer backbone). The composition of **P1** can be determined simply by comparing the integration of the aldehyde protons with the total integration of the aromatic protons. The monomer composition was determined to be 1: 1 styrene: 4-vinylbenzaldehyde.

*N-Boc-Protected Amine-Functionalized Copolymer (**P2a**)*

S-1-Dodecyl-*S'*-(α,α-dimethyl-α''-acetic acid)trithiocarbonate (DDMAT) (1 eq, 52.1 mg, 0.143 mmol) and AIBN (0.2 eq, 4.7 mg, 28.6 μmol) were added to a small schlenk tube. Styrene (75 eq, 1.12 g, 10.7 mmol) and *N*-boc-4-aminostyrene (**2**) (75 eq, 2.35 g, 10.7 mmol) were then added followed by dioxane (3 mL). The reaction mixture was degassed five times and then the vessel was backfilled with N$_2$, purged with N$_2$, and allowed to warm to room temperature. The reaction mixture was then placed in an oil

bath at 70 ˚C, and the polymerization was quenched after 22 h and solvent was removed on the rotary evaporator. The resulting yellow oil was dissolved in a minimal amount of THF and added dropwise to a large excess of ice-cold hexane. The resulting polymer precipitate was then isolated by filtration and dried under high vacuum. Polymer **P2a** was obtained as a pale yellow solid (1.18 g, 62%). ^{1}H NMR (CDCl$_3$): δ 0.89 (br, SC$_{11}$H$_{22}$CH_3, of the chain terminus), 1.38 (br, CHCH_2, polymer backbone), 1.55 (br, C(CH_3)$_3$), 1.76 (br, CHCH$_2$, polymer backbone), 3.29 (br, SCH_2C$_{11}$H$_{23}$, of the chain terminus), 6.53 (br, Ar, polymer backbone), 7.05 (br, Ar, polymer backbone). The composition of **P2a** can be determined simply by comparing the integration of the *Boc* protons at δ = 1.55 ppm with the total integration of the aromatic protons. The monomer composition was determined to be 1:1 styrene:*N*-Boc-4-aminostyrene.

*Amine-Functionalized Copolymer (**P2b**)*

TFA (1 mL) was added to a stirred solution of **P2a** (0.1 g, 7.53 μM) in CH$_2$Cl$_2$ (1 mL) at room temperature. After 1 h the reaction mixture was evaporated to dryness to afford a crude yellow oil which was dissolved in minimal amount of THF and added dropwise to a large excess of ice-cold hexane. The resulting polymer precipitate was then isolated by filtration and dried under high vacuum. Polymer **P2b** was obtained as a pale yellow solid (0.09 g, 87%). ^{1}H NMR (THF-d^8): δ 0.85 (br, SC$_{11}$H$_{22}$CH_3, of the chain terminus), 1.45 (br, CHCH_2, polymer backbone), 1.79 (br, CHCH$_2$, polymer backbone), 3.29 (br, SCH_2C$_{11}$H$_{23}$, of the chain terminus), 6.56 (br, Ar, polymer backbone), 7.02 (br, Ar, polymer backbone), 7.44 (br, Ar, polymer backbone).

*Aldehyde-Functionalized Diblock Copolymer (**P3**)*

P1 (1 eq, 1.02 g, 85 μmol) and AIBN (0.2 eq, 2.8 mg, 17 μmol) were added to a small schlenk tube. Styrene (300 eq, 2.66 g, 25.5 mmol) was then added followed by dioxane (3 mL) and the reaction mixture was degassed five times. The vessel was backfilled with N$_2$, purged with N$_2$, and allowed to warm to room temperature. The reaction mixture was then placed in an oil bath at 70 ˚C, and the polymerization was quenched after 24 h and solvent was removed on the rotary evaporator. The resulting yellow oil was dissolved in a minimal amount of THF and added dropwise to a large excess of ice-cold methanol. The resulting polymer precipitate was then isolated by filtration and dried under high vacuum. Polymer **P3** was obtained as a pale yellow solid (3.03 g,

96%). ^{1}H NMR (CDCl$_3$): δ 0.89 (br, SC$_{11}$H$_{22}$C*H$_3$*, of the chain terminus), 1.43 (br, CHC*H$_2$*, polymer backbone), 1.86 (br, C*H*CH$_2$, polymer backbone), 6.57 (br, Ar, polymer backbone), 7.05 (br, Ar, polymer backbone), 7.52 (br, Ar, polymer backbone), 9.89 (br, C*H*O, polymer backbone).

Amine-Functionalized Diblock Copolymer (*P4*)

P2a (1 eq, 1.05 g, 79 μmol) and AIBN (0.2 eq, 2.6 mg, 15.8 μmol) were added to a small schlenk tube. Styrene (400 eq, 3.29 g, 31.6 mmol) was then added followed by dioxane (4 mL) and the reaction mixture was degassed five times. The vessel was backfilled with N$_2$, purged with N$_2$, and allowed to warm to room temperature. The reaction mixture was then placed in an oil bath at 70 ˚C, and the polymerization was quenched after 25.5 h and solvent was removed on the rotary evaporator. The resulting yellow oil was dissolved in a minimal amount of THF and added dropwise to a large excess of ice-cold methanol. The resulting polymer precipitate was then isolated by filtration and dried under high vacuum. The pale yellow solid obtained was dissolved in CH$_2$Cl$_2$ (3 mL) and TFA (3 mL) was added, solution was left to stir at room temperature. The reaction mixture was evaporated to dryness after 1 h, and the resulting crude yellow oil was dissolved in minimal amount of THF and added dropwise to a large excess of ice-cold hexane. The polymer precipitate was then isolated by filtration and dried under high vacuum. Polymer **P4** was obtained as a pale yellow solid (1.11 g, 47%). ^{1}H NMR (CDCl$_3$): δ 0.89 (br, SC$_{11}$H$_{22}$C*H$_3$*, of the chain terminus), 1.44 (br, CHC*H$_2$*, polymer backbone), 1.87 (br, C*H*CH$_2$, polymer backbone), 3.29 (br, SC*H$_2$*C$_{11}$H$_{23}$, of the chain terminus), 6.59 (br, Ar, polymer backbone), 7.05 (br, Ar, polymer backbone).

Aldehyde-Functionalized Copolymer (*P5*)

4-(4-Cyanopentanoic acid)dithiobenzoate (CPADB) (1 eq, 17.33 mg, 0.062 mmol) and AIBN (0.15 eq, 1.53 mg, 9.3 μmol) were added to a small schlenk tube. Methyl methacrylate (224 eq, 1.39 g, 13.89 mmol) and *p*-(2-Methacryloxyethoxy)benzaldehyde (**4**) (28 eq, 407 mg, 1.74 mmol) were then added followed by benzene (2.5 mL). The reaction mixture was degassed five times, and then the vessel was backfilled with N$_2$, purged with N$_2$, and allowed to warm to room temperature. The reaction mixture was then placed in an oil bath at 70 ˚C, and the polymerization was quenched after 24 h. The

reaction mixture was dissolved in a minimal amount of THF and added dropwise to a large excess of hexane. The resulting polymer precipitate was then isolated by filtration and the precipitation was repeated before drying under high vacuum. Polymer **P5** was obtained as a pale red solid (0.84 g). ^{1}H NMR (CDCl$_3$): 0.84 (br, C(CH_3), polymer backbone), 1.80 (br, CH_2, polymer backbone), 3.59 (br, OCH_3), 4.31 (br, CH_2CH_2), 7.05 (br, Ar), 7.86 (br, Ar), 9.91 (br, CHO). The composition of **P5** can be determined by comparing the integration of the aldehyde protons of **4** with the integration of the OCH_3 protons of methyl methacrylate (MMA). The monomer composition was determined to be 8:1 MMA: **4** (identical to the feed ratio).

*N-Boc-Protected Amine-Functionalized Copolymer (**P6**)*

4-(4-Cyanopentanoic acid)dithiobenzoate (CPADB) (1 eq, 19.7 mg, 0.071 mmol) and AIBN (0.15 eq, 1.73 mg, 10.5 μmol) were added to a small schlenk tube. Methyl methacrylate (224 eq, 1.58 g, 15.8 mmol) and *p*-(2-methacryloxyethoxy)-*N*-boc-aminobenzene (**7**) (28 eq, 0.634 mg, 1.97 mmol) were then added followed by benzene (2.5 mL). The reaction mixture was degassed five times, and then the reaction vessel was backfilled with N$_2$, purged with N$_2$, and allowed to warm to room temperature then placed in an oil bath at 70 ˚C. The polymerization was quenched after 24 h and the reaction mixture was dissolved in a minimal amount of THF and added dropwise to a large excess of hexane. The resulting polymer precipitate was then isolated by filtration and the precipitation was repeated before drying under high vacuum. Polymer **P6** was obtained as a pale red solid (1.36 g). ^{1}H NMR (CDCl$_3$): 0.85 (br, C(CH_3), polymer backbone), 1.50 (br, C(CH_3)$_3$), 1.80 (br, CH_2, polymer backbone), 3.59 (br, OCH_3), 4.20 (br, CH_2CH_2), 6.69 (br, NH), 6.85 (br, Ar), 7.30 (br, Ar). The composition of **P6** can be determined by comparing the integration of the aromatic protons of **7** with the integration of the OCH_3 protons of methyl methacrylate (MMA). The monomer composition was determined to be 8: 1 MMA: **7** (identical to the feed ratio).

*Amine-Functionalized Copolymer (**P7**)*

P6 (0.63 g) was dissolved in CH$_2$Cl$_2$ (5 mL) and TFA (3 mL) and the reaction mixture stirred for 2 h. The solvent and excess TFA were removed on the rotary evaporator and the oil obtained was dissolved in a minimal amount of THF and added dropwise to a large excess of hexane. The resulting polymer precipitate was then isolated by filtration

and dried under high vacuum. Polymer **P7** was obtained as a pale red solid (0.59 g). ^{1}H NMR (THF-d$_8$): 0.86 (br, C(CH_3), polymer backbone), 1.83 (br, CH_2, polymer backbone), 3.56 (br, OCH_3), 4.21 (br, CH_2CH_2), 6.90 (br, Ar), 7.05 (br, Ar).

*Procedure for Macroscopic Gelation between **P1** and **P2b***

Solutions of **P1** (0.5 and 5 wt %) in THF with TFA (10 eq) were prepared and allowed to stir at room temperature for 10 min to allow complete dissolution of the polymer sample. Solutions of **P2b** (0.5 and 5 wt %) were prepared in THF with TFA (10 eq) under identical conditions. Equal volumes of these corresponding solutions were mixed and gelation was observed in both cases after 15 min and 2h respectively.

*Procedure for the Preparation of CCS Polymers (**1** – **6**)*

Solutions of the aldehyde functional diblock copolymer component **P3** (0.5 – 5 wt %) were prepared in THF with TFA (10 eq). Solutions of the amine functional diblock copolymer component **P4** (0.5 – 5 wt %) were also prepared under identical conditions. Equal volumes of corresponding solutions of the same concentration were combined with rapid stirring and left to equilibrate at room temperature for 16 h before GPC–MALLS analysis. GPC Analysis of all crude reaction mixtures revealed no evidence for any unreacted reactive polymers, indicating that the cross-linking reaction proceeded with 100% conversion.

Procedure for the Disassembly of CCS Polymers

A sample of CCS polymers (2 mL, containing 2 wt % of polymer building blocks) was isolated. To this solution a large excess of propylamine (10 eq per aldehyde functional group) was added. TFA (0.1 eq with respect to propylamine) was then added and the reaction mixture was left to stir overnight at room temperature before GPC analysis.

*Procedure for Macroscopic Gelation between **P5** and **P7***

Equimolar solutions of **P5** and **P7** in THF with TFA (10 eq) were mixed to afford a range of solutions with a total polymer concentration of 3, 4 and 5 wt %. Solutions were left to equilibrate at room temperature for 24 h.

Procedure for the Preparation of Nanogels (7 – 12)

Equimolar solutions of **P5** and **P7** in THF with TFA (10 eq) were combined under rapid stirring to afford a range of solutions with a total polymer concentration of 0.1 – 2 wt %. Solutions were left to equilibrate at room temperature for 24 h before GPC–MALLS analysis. GPC Analysis of all crude reaction mixtures revealed no evidence for any unreacted reactive polymers, indicating that the cross-linking reaction proceeded with 100% conversion.

Procedure for the Disassembly of Nanogels

An excess of ethanolamine (10 eq per aldehyde functional group) was added to a solution of nanogels formed at 1 wt % of total copolymer building blocks. TFA (0.1 eq with respect to ethanolamine) was then added and the solution left to equilibrate at room temperature for 24 h before GPC analysis.

3.6   References

1.   C. T. Black, C. B. Murray, R. L. Sandstrom and S. H. Sun, *Science*, 2000, **290**, 1131-1134.
2.   J. W. Taylor and M. A. Winnik, *J. Coat. Technol. Res.*, 2004, **1**, 163-190.
3.   Z. L. Tyrrell, Y. Q. Shen and M. Radosz, *Prog. Polym. Sci.*, 2010, **35**, 1128-1143.
4.   Y. Amamoto, Y. Higaki, Y. Matsuda, H. Otsuka and A. Takahara, *J. Am. Chem. Soc.*, 2007, **129**, 13298-13304.
5.   Z. Ge, J. Hu, F. Huang and S. Liu, *Angew. Chem., Int. Ed.*, 2009, **48**, 1798-1802.
6.   J. M. J. Paulusse and R. P. Sijbesma, *J. Polym. Sci., Part A*, 2006, **44**, 5445-5453.
7.   T. F. Scott, A. D. Schneider, W. D. Cook and C. N. Bowman, *Science*, 2005, **308**, 1615-1617.
8.   D.-S. Guo, S. Chen, H. Qian, H.-Q. Zhang and Y. Liu, *Chem. Commun.*, 2010, **46**, 2620-2622.
9.   E. B. Murphy and F. Wudl, *Prog. Polym. Sci.*, 2010, **35**, 223-251.
10.   H. F. Gao and K. Matyjaszewski, *Prog. Polym. Sci.*, 2009, **34**, 317-350.
11.   A. Blencowe, J. F. Tan, T. K. Goh and G. G. Qiao, *Polymer*, 2009, **50**, 5-32.
12.   A. V. Kabanov and S. V. Vinogradov, *Angew. Chem., Int. Ed.*, 2009, **48**, 5418-5429.
13.   J. T. Wiltshire and G. G. Qiao, *Aust. J. Chem.*, 2007, **60**, 699-705.
14.   K. I. Fukukawa, R. Rossin, A. Hagooly, E. D. Pressly, J. N. Hunt, B. W. Messmore, K. L. Wooley, M. J. Welch and C. J. Hawker, *Biomacromolecules*, 2008, **9**, 1329-1339.
15.   T. Terashima, M. Kamigaito, K. Y. Baek, T. Ando and M. Sawamoto, *J. Am. Chem. Soc.*, 2003, **125**, 5288-5289.

16. B. Helms, S. J. Guillaudeu, Y. Xie, M. McMurdo, C. J. Hawker and J. M. J. Frechet, *Angew. Chem., Int. Ed.*, 2005, **44**, 6384-6387.

17. T. Terashima, M. Ouchi, T. Ando, M. Kamigaito and M. Sawamoto, *Macromolecules*, 2007, **40**, 3581-3588.

18. J. K. Oh, R. Drumright, D. J. Siegwart and K. Matyjaszewski, *Prog. Polym. Sci.*, 2008, **33**, 448-477.

19. R. Manzotti, T. S. Reger and K. D. Janda, *Tetrahedron Lett.*, 2000, **41**, 8417-8420.

20. J. Jiang and S. Thayumanavan, *Macromolecules*, 2005, **38**, 5886-5891.

21. J. T. Lai, D. Filla and R. Shea, *Macromolecules*, 2002, **35**, 6754-6756.

22. W. Burchard, M. Schmidt and W. H. Stockmayer, *Macromolecules*, 1980, **13**, 1265-1272.

23. P. Lang, W. Burchard, M. S. Wolfe, H. J. Spinelli and L. Page, *Macromolecules*, 1991, **24**, 1306-1314.

24. M. Spiniello, A. Blencowe and G. G. Qiao, *J. Polym. Sci., Part A*, 2008, **46**, 2422-2432.

25. C. J. Kloxin, T. F. Scott, B. J. Adzima and C. N. Bowman, *Macromolecules*, 2010, **43**, 2643-2653.

26. Y. Higaki, H. Otsuka and A. Takahara, *Macromolecules*, 2006, **39**, 2121-2125.

27. Y. Mitsukami, M. S. Donovan, A. B. Lowe and C. L. McCormick, *Macromolecules*, 2001, **34**, 2248-2256.

Chapter 4

Dual Stimuli-Responsive Core Cross-Linked Star Polymers

This chapter is based on the publication:

Table of Contents:

4.1 Abstract

Water soluble acrylamide-based diblock copolymers possessing an "inert" block composed of N,N'-dimethylacrylamide and a "reactive" block containing N-isopropylacrylamide and either aldehyde or amine functional monomer units have been prepared via reversible addition-fragmentation chain transfer (RAFT) polymerization. These linear copolymer building blocks have been shown to self-assemble at pH 11.0 through imine bond formation into core cross-linked star polymers, and disassemble back into linear copolymer chains at pH 5.0. The N-isopropylacrylamide monomer units impart thermoresponsive properties into the cross-linked cores of these star polymers, and changes in pH and temperature were used to trigger the release and uptake of a hydrophobic dye.

4.2 Introduction

In the drive to prepare polymeric nanoparticles which possess responsive and adaptive properties it was decided to develop a water-soluble analogous system to the chemoresponsive CCS polymers prepared in Chapter 3. Whilst chemoresponsivness can be a very useful feature,[1] the incorporation of imine cross-links between multiple polymer chains in an aqueous environment results in nanoparticles which can reconfigure their structural properties with changes in pH[2-4] and is an important stepping stone towards the eventual development of CCS polymers which may find application in biomedical sciences.

This Chapter describes the synthesis and characterization of dual stimuli-responsive water-soluble CCS polymers which are prepared *via* dynamic covalent imine bond formation (Figure 4.1). These CCS polymers are constructed, in a similar fashion to those described in Chapter 3, from linear polymer chains possessing an ''inert'' block which discourages macroscopic cross-linking, and a ''reactive'' block which contains aldehyde- or amine-functions which facilitate cross-linking of polymer chains through reversible imine bond formation. The reversible nature of this bond allows the position of the imine equilibrium to be modulated by changing the pH, as imine formation is favoured at high pH and disfavoured at low pH.[5] Consequently, the assembly and disassembly of aqueous CCS polymers can be triggered simply by changing the pH. It is demonstrated here that this reversible process can lead to the release and uptake of hydrophobic dye molecules complexed within the polymer cores. In addition to pH

responsiveness, these CCS polymers also possess thermoresponsive cores which endow them with the ability to reversibly switch from hydrophilic to hydrophobic, and we demonstrate here the temperature controlled uptake and release of the same hydrophobic dye (Figure 4.1).
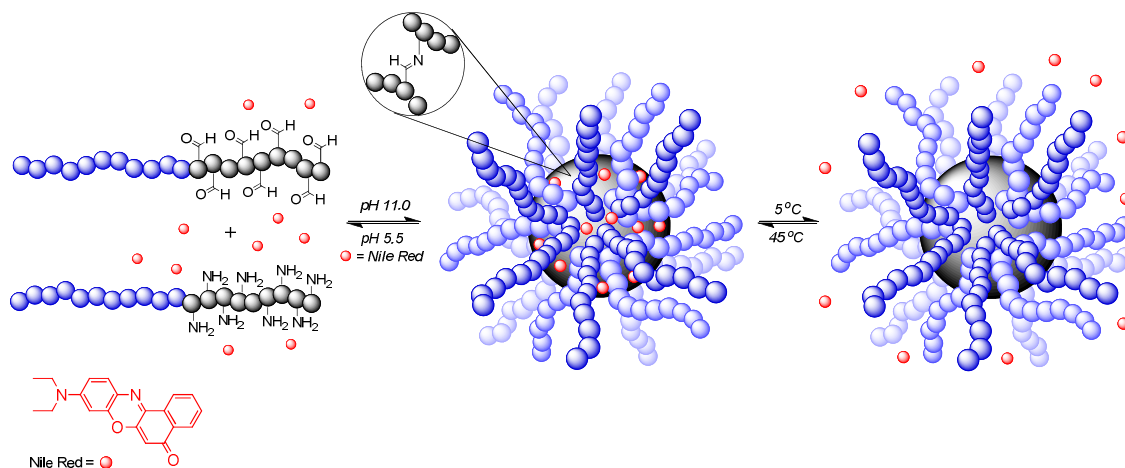
Figure 4.1 Polymers possessing aldehyde and amino groups cross-link at pH 11 to form CCS polymers. Nile Red can be encapsulated within the hydrophobic core of the CCS polymer at 45 °C. The release of Nile Red can be triggered by pH-induced disassembly of the CCS polymer system, or temperature-induced loss of the hydrophobicity of the cross-linked core.

The polymerization of certain water-soluble monomers such as N-isopropylacrylamide (NIPAm),[6] oligo(ethylene glycol) methyl ether methacrylates (OEGMA),[7] N-vinylcaprolactam (VCP)[8] and vinyl methyl ether (VME)[9] affords polymer chains which undergo a coil to globule phase transition with changes in temperature. Below a specific lower critical solution temperature (LCST) the polymer chains in solution are solvated and hydrophilic. Above their LCST the hydrogen bonding between water molecules and the polymer chain decreases, and the solubilising water molecules return to the bulk solution and the polymer chains become hydrophobic and precipitate from solution. In this work it was decided to introduce N-isopropylacrylamide monomer units into the "reactive" block of our diblock copolymer chains, which would then impart a thermoresponsive nature into the core of the resulting CCS polymers. It was demonstrated that upon heating the cores are able to switch from hydrophilic to hydrophobic, providing the driving force for the encapsulation and release of the hydrophobic fluorescent probe Nile Red. As the "inert" block is composed entirely of N,N'-dimethylacrylamide (DMA), a monomer whose polymers are known[10] not to possess an LCST when polymerized, the cores do not precipitate from solution when heated, and the coronal arms are able to shield and solubilise the hydrophobic core and its cargo above its LCST.

91

4.3 Results and Discussions

4.3.1 *Acrylamide-Based Aldehyde/ Amine Diblock Copolymers*
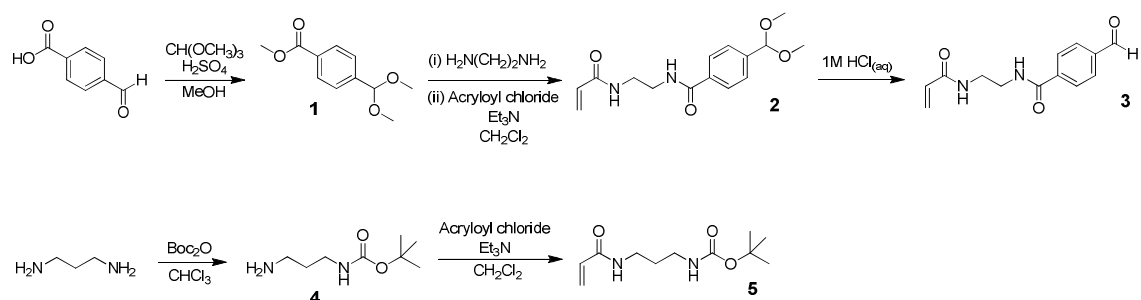
Scheme 4.1 Synthesis of aldehyde and amine-functional monomers **3** and **5**.

The first objective was to synthesize (Scheme 4.1) acrylamide-based monomers for the eventual preparation of linear copolymer building blocks displaying the required pendant functional groups. Monomer **3** was prepared starting from 4-carboxybenzaldehyde, which was refluxed in the presence of trimethylorthoformate to afford methyl 4-(dimethoxymethyl)benzoate (**1**).[11] This compound was then transformed into **2** using a two-step procedure involving reflux in ethylenediamine and then acylation of the resulting primary amine with acryloyl chloride. Hydrolysis of the dimethyl acetal function in 1M HCl afforded the monomer **3**. The *mono-N-boc-*protection of 1,3-diaminopropane afforded[12] compound **4** which was acylated with acryloyl chloride to furnish the monomer **5**. All steps to prepare the monomers were synthetically straightforward and relatively high yielding, allowing their preparation on a multi gram scale.

Scheme 4.2 Synthesis of aldehyde and amine-functional diblock copolymers **P2** and **P4b**.
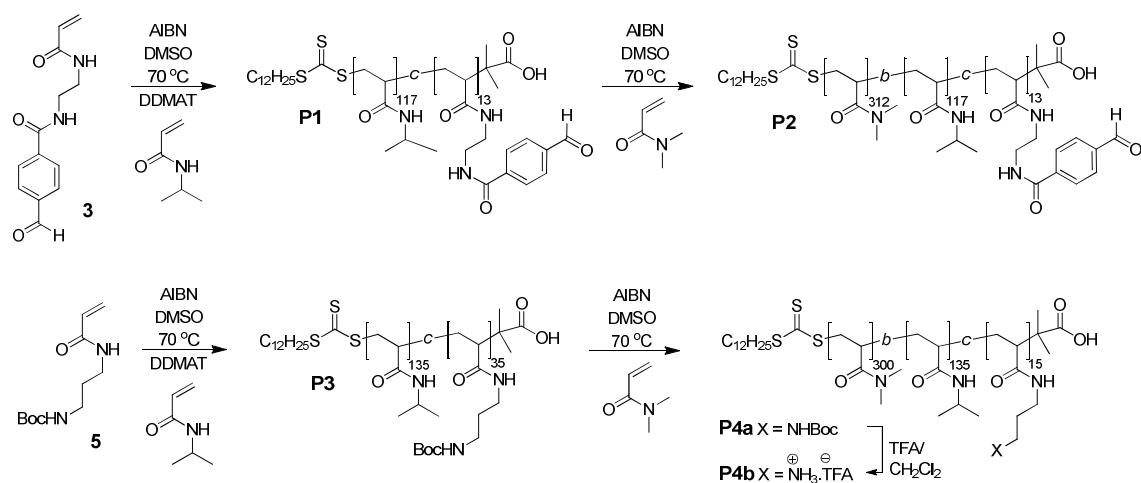
The diblock copolymer buildings blocks **P2** and **P4b** were prepared by RAFT polymerization. The RAFT chain transfer agent *S*-1-dodecyl-*S'*-(α,α-dimethyl-α''-acetic acid)trithiocarbonate[13] (DDMAT) was used (Scheme 4.2) to mediate the copolymerization of a 1:9 mixture of **3** and *N*-isopropylacrylamide at 70 ˚C in DMSO to afford **P1**. This copolymer acts as the "reactive" block, incorporating both the pendant aldehyde functionality and the thermoresponsive property. After purification by precipitation into diethyl ether **P1** was used as a macro-CTA and extended via RAFT polymerization with *N,N'*-dimethylacrylamide at 70 ˚C in DMSO to afford **P2**. This block acts as the "inert" block, possessing no reactive functionality or thermoresponsive character. Comparison of the GPC trace of the chain-extended polymer **P2** with the macro-CTA **P1** (Figure 4.2a) indicates complete and successful chain extension. The copolymer **P3** was prepared via RAFT polymerization of a 1:9 mixture of **5** and *N*-isopropylacrylamide at 70 ˚C in DMSO, which was then used as a macro-CTA and extended via RAFT polymerization with *N,N'*-dimethylacrylamide at 70 ˚C in DMSO to afford, after the removal of the protecting groups, **P4b**. Comparison of the GPC trace of the chain-extended polymer **P4a** with the macro-CTA **P2** (Figure 4.2b) indicates complete and successful chain extension. GPC of **P4b** was not possible on account of the cationic nature of the reactive block, and so the *boc*-deprotection was confirmed by ^{1}H NMR spectroscopy and the polymeric nature further inferred from the GPC trace of **P4a**. Copolymer **P4b** contains a "reactive" block comprised of the amine-functional monomer to facilitate cross-linking, and *N*-isopropylacrylamide to introduce thermoresponsive properties, in addition to an "inert" block of *N,N'*-dimethylacrylamide units. All polymers prepared were characterized (Table 4.1) by GPC and ^{1}H NMR spectroscopy.
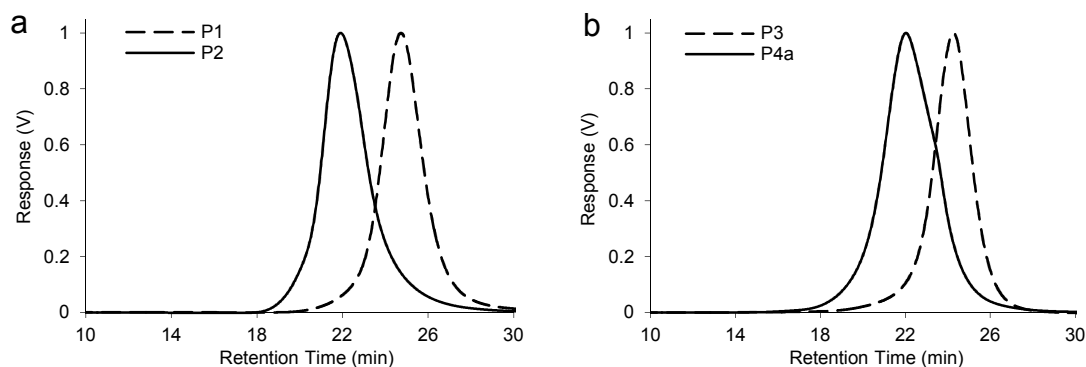
Figure 4.2 (a) Differential refractive index (dRI) GPC traces (DMF 0.6 mL/ min) of **P2** and resulting diblock copolymer **P4** after chain extension, (b) dRI GPC traces (DMF 0.6 mL/ min) of **P3** and resulting diblock copolymer **P4a** after chain extension.

polymer	M_n^a (g mol^{-1})	M_n^b (g mol^{-1})	M_w^b (g mol^{-1})	PDI^b (M_w/M_n)
P1	16,800	16,100	21,200	1.32
P2	47,700	47,400	65,600	1.38
P3	19,000	22,200	27,200	1.23
P4a	48,800	48,200	68,900	1.43

Table 4.1 Characterization of diblock copolymer building blocks. ^{a} As determined by ^{1}H NMR spectroscopy, ^{b} As determined by gel permeation chromatography in DMF (0.6 mL/ min) calibrated against near monodisperse methyl methacrylate standards.

Copolymers **P2** and **P4b** were readily soluble in water, and batch dynamic light scattering (DLS) studies (Figure 4.3) at 20 °C reveals hydrodynamic radii of 6.6 nm and 6.0 nm respectively, suggesting strongly that these polymers exist as unimolecular species in aqueous solutions and do not form micellar aggregates. This conclusion is further supported by ^{1}H NMR spectroscopy in D$_2$O of polymers **P2** (Figure 4.4) and **P4b** (Figure 4.5), which display well-defined signals corresponding to all monomer units present within the "reactive" block, signals which would be expected to diminish in intensity if the polymer chains were packed within the interior of micellar aggregates.
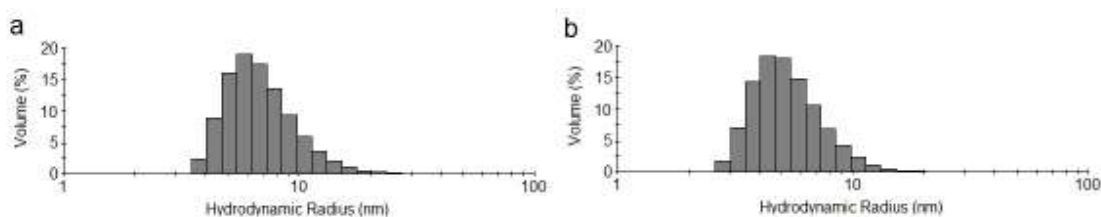
Figure 4.3 Histograms showing the particle size distributions in H$_2$O at 20 °C of (a) **P2** and (b) **P4b** as obtained by batch dynamic light scattering experiments.

As a consequence of their high content of *N*-isopropylacrylamide monomer units, both copolymers display (Figure 4.6) lower critical solution temperatures (LCSTs). The cloud point of **P2** was measured by turbidity to be 27 °C, whereas the cloud point of **P2b** was measured to be 55 °C. The differences in measured cloud points are simply on account of the relative hydrophobicity of the aromatic aldehyde functions of **P2**, lowering the cloud point, and the hydrophilic amino functions of **P4b**, which raise the cloud point. Above their cloud points, no evidence was found from DLS for the formation of micellar aggregates as the polymers precipitate from solution.
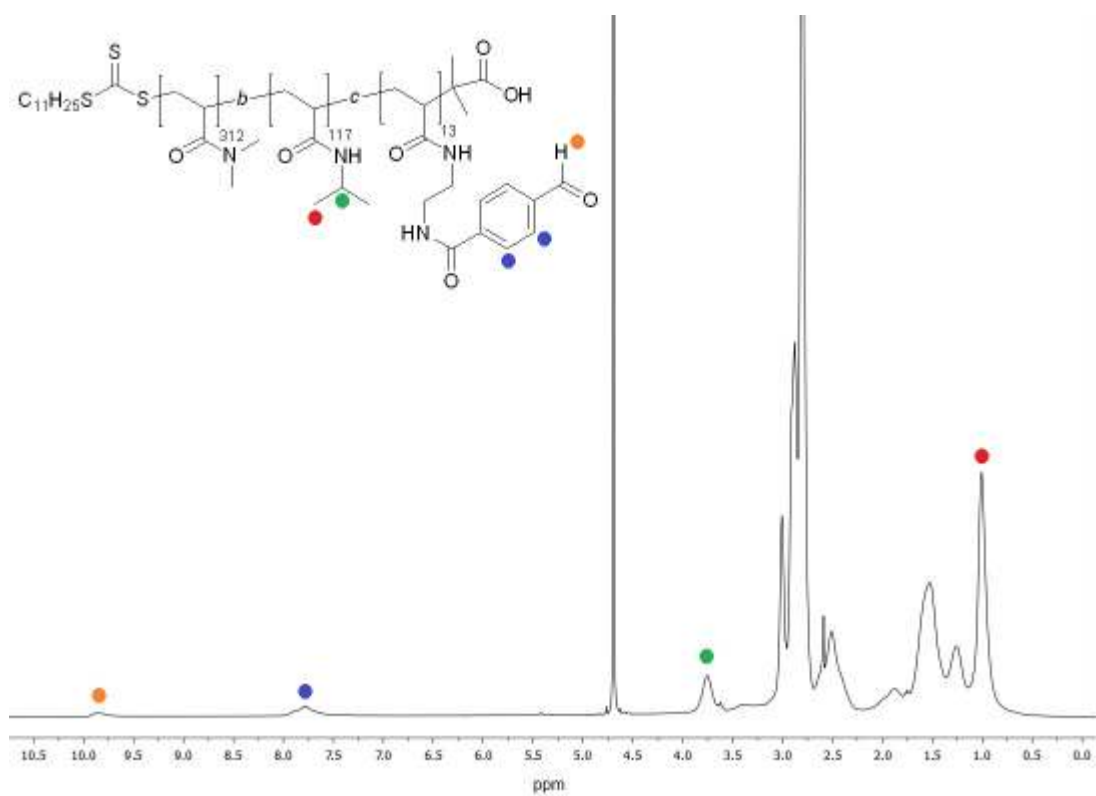
Figure 4.4 ^{1}H NMR spectrum (300 MHz) of **P2** in D$_2$O.
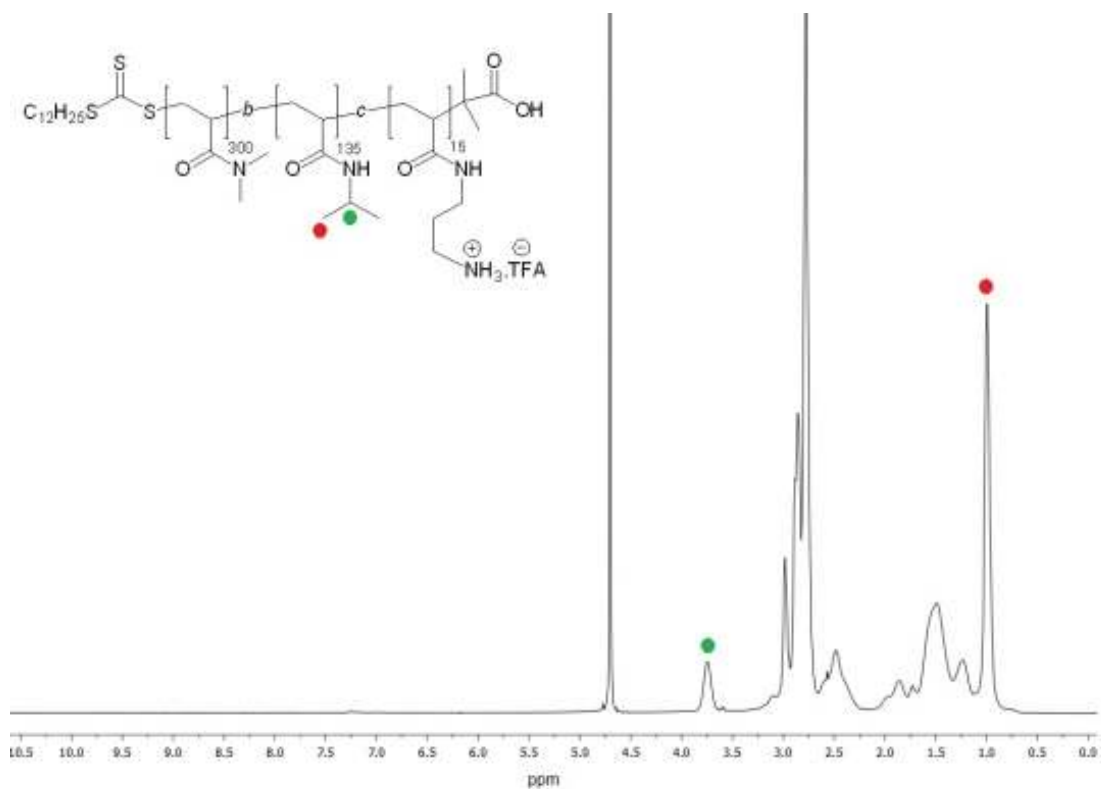
Figure 4.5 ^{1}H NMR spectrum (300 MHz) of **P4b** in D$_2$O.
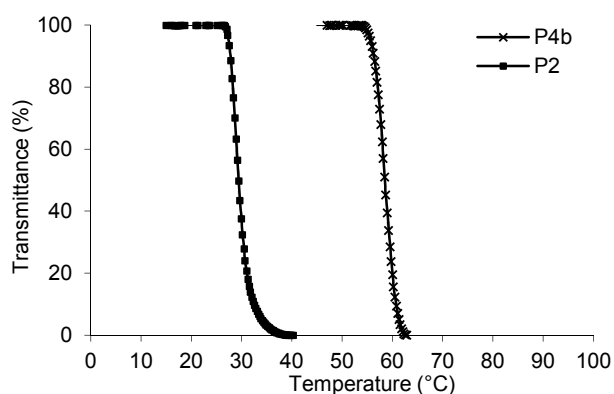
Figure 4.6 Temperature-turbidity curves for diblock copolymers **P2** and **P4b** at pH 11.0 (5 mg/ mL).

4.3.2 *Reversible Core Cross-Linked (CCS) Polymer Assembly*

CCS Polymers were prepared by mixing equimolar solutions of **P2** and **P4b** in water to afford a solution with a total polymer concentration of 1 wt %. The pH was adjusted to 11.0 with small aliquots (5 µL) of 1M $NaOH_{(aq)}$, and the reaction was left to equilibrate for 16 h at room temperature. No precipitation or macroscopic gelation was observed in the reaction mixture, an observation which suggests macroscopic cross-linking is inhibited by the 'inert' blocks within the polymer chains. GPC analysis (Figure 4.7a) displayed a significant reduction in the intensity of the peaks corresponding to the diblock copolymers **P2** and **P4a** at retention time ~ 22.5 min, and the appearance of a significant peak indicating the formation of high molecular weight aggregates at ~ 14 min. The minor peaks at ~ 20 min and ~ 23 min are probably as a consequence of small quantities of CCS polymers possessing very low numbers of arms. Evidence of a two-armed core cross-linked species as a minor by-product of CCS polymer formation by the approach used here was discussed in Chapter 3 and we speculate that these minor peaks are probably in part as a consequence of the formation of 2-armed species. Online multi-angle laser light scattering (MALLS) experiments (Figure 4.7b) were used to estimate the M_w of the CCS polymer assembly to be 2,332 kDa, suggesting that the CCS polymers possess on average about 49 arms, calculated by dividing M_w for CCS polymers by the average M_w of **P2** and **P4b.** These experiments also furnished the radius of gyration (R_g) = 24.3 nm and hydrodynamic radius (R_h) = 19.3 nm. The structure sensitive ρ parameter ($\rho = R_g/R_h$) defined by Burchard and co-workers,[14, 15] was found to be ~1.26, which is consistent with monodisperse regular star architectures.
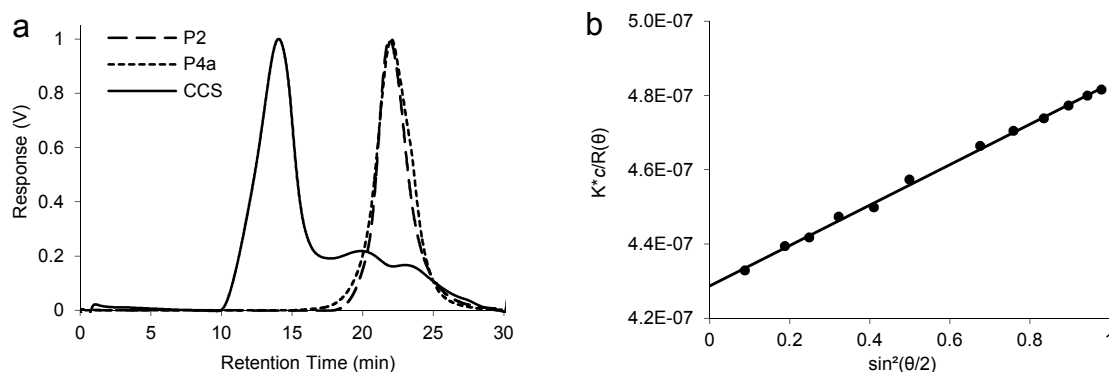
Figure 4.7 (a) Differential refractive index (dRI) GPC trace (in DMF 0.6 mL/ min) displaying the formation of CCS polymer, (b) Debye plot for CCS polymer at (2.5 mg/ mL). Multi-angle laser light scattering analysis performed in H_2O (1 mL/ min) over a range of concentrations (0.3 – 5 mg/ mL), using experimentally determined *dn/dc* value of 0.166 mL/ g. M_w was estimated to be 2,332 kDa (49 polymer chains per assembly). R_g = 24.3 nm, R_h = 19.3 nm and structure sensitive ρ parameter (ρ = R_g/ R_h) was found to be ~ 1.26.

The formation of CCS polymers was also supported by ^1H NMR spectroscopy. The aldehyde signals of **P2** at 9.9 ppm, which are evident at pH 5.5, disappear at pH 11.0 suggesting that imine bond formation is occurring. Significant reductions in the intensity of the *N*-isopropylacrylamide signals at 1.0 and 3.8 ppm relative to *N,N'*-dimethylacrylamide signals at 2.8 were observed after the pH increased to 11.0 (Figure 4.8), suggesting the *N*-isopropylacrylamide units are located within the interior of the CCS polymer assembly. The progress of this reaction was also followed by batch DLS at 20 ˚C, which shows the disappearance of unimolecular polymeric species of R_h = 6-7 nm and the formation of a larger monomodal distribution of aggregates possessing R_h = 18.9 nm at pH 11.0 (Figure 4.9a) and the re-appearance of unimolecular polymeric species at pH 5.5 (Figure 4.9b). All of these observations suggest strongly that the polymer chains cross-link through imine bond formation to form CCS polymers, and are consistent with those reported in Chapter 3 for the self-assembly of CCS polymers within an analogous organic-soluble system.
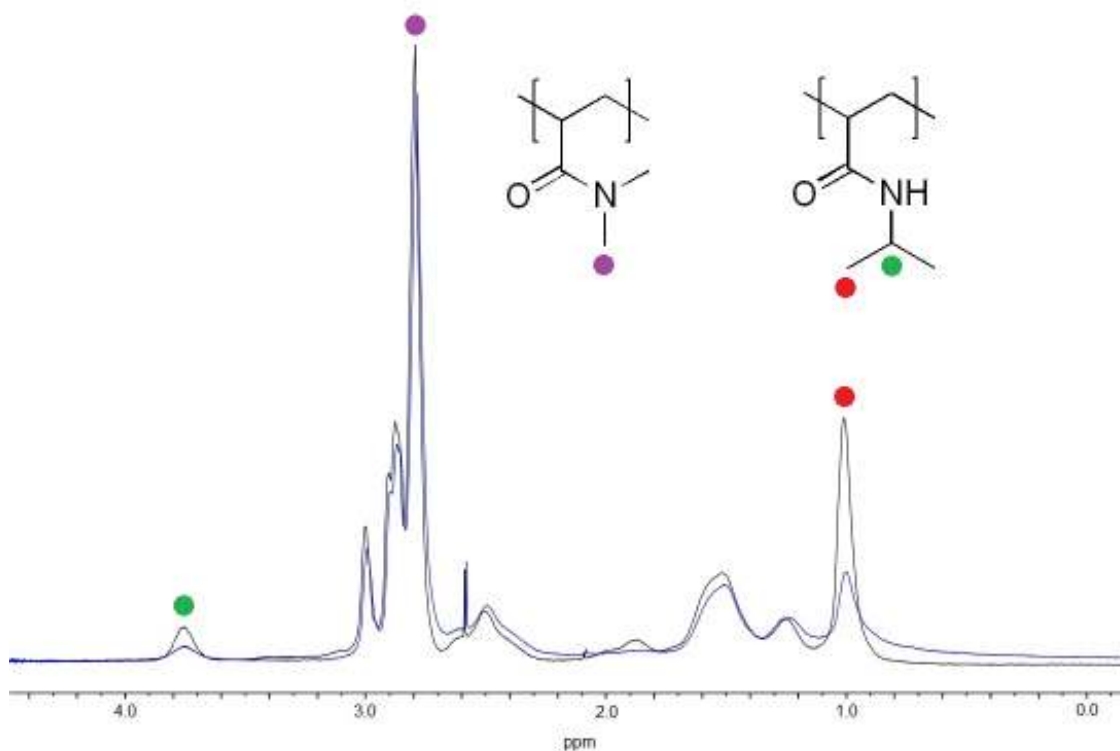
Figure 4.8 Partial ^{1}H NMR spectra before (black line) and after (blue line) CCS polymer formation. pH 5.5 (black line) and pH 11.0 (blue line). Decrease in relative intensity of *N*-isopropylacrylamide signals to *N,N'*-dimethylacrylamide suggest the "reactive" blocks are within the interior of the CCS polymer assembly.
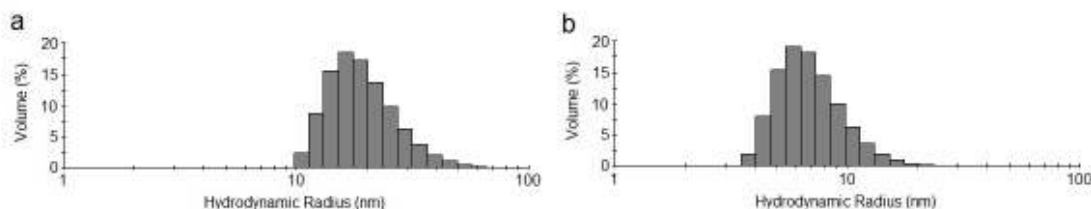
Figure 4.9 Histograms showing the particle size distributions of (a) CCS formation at pH 11.0 and (b) subsequent disassembly at pH 5.5. Data collected at 20 °C.

The disassembly of the CCS polymers back into their component unimolecular polymer chains was triggered by simply adjusting the pH of the solution to 5.5 with small aliquots (5 μL) of 1M HCl$_{(aq)}$. After leaving the solution to re-equilibrate for 4 h, batch DLS analysis (Figure 4.9b) at 20 ˚C showed the disappearance of the CCS polymers and the appearance of a monomodal distribution of species possessing hydrodynamic radii of 6-7 nm which corresponds to unimolecular polymer chains. This observation supports the idea that the CCS polymers have disassembled into their component polymer building blocks, a conclusion also supported by GPC analysis (Figure 4.10a) which shows the disappearance of the large molecular weight CCS species and the reappearance of the polymer chain building blocks. The disassembly process is entirely

reversible, and the ability of this polymeric system to reversibly cycle back and forth between the CCS polymer architecture and single polymer chains was demonstrated (Figure 4.10b) by repeatedly switching the pH between 11.0 and 5.5 and monitoring the particle size distribution of the polymer solution by batch DLS, observations which suggest the system can be switched without any loss in switching efficiency.
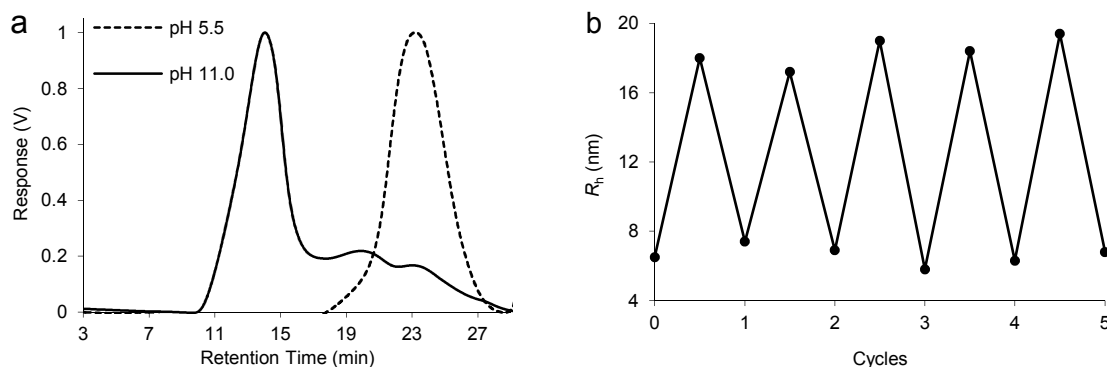
Figure 4.10 (a) Differential refractive index (dRI) GPC trace (in DMF 0.6 mL/ min) displaying pH-triggered disassembly of CCS polymers. To prevent diblock copolymer building blocks reacting together in column, acetone (1 drop) was added to GPC sample to cap amine functionalities, (b) pH-Triggered CCS polymer assembly and disassembly, going from pH 5.5 (cycles 0, 1, 2, 3, 4 and 5) to pH 11.0 (cycles 0.5, 1.5, 2.5, 3.5 and 4.5). Hydrodynamic radii obtained from batch dynamic light scattering analysis at 20 °C.

To demonstrate that the CCS polymers could be kinetically fixed, the imine bonds were reduced. Excess $NaCNBH_3$ (approx. 100 eq $NaCNBH_3$ per imine bond) was added to a 1 % wt solution of CCS polymers at pH 11.0 and the solution was left to stir at room temperature for 2 h. The pH was then adjusted to 5.5 with small aliquots (5 μL) of 1M $HCl_{(aq)}$ and the sample was left overnight. DLS analysis (Figure 4.11a) revealed a monomodal particle size distribution whose R_h = 19.4 nm, suggesting that the imine bonds have been successfully reduced to amines, thus preventing the disassembly of the CCS polymer back into its constituent polymer building blocks at low pH. The position of the imine equilibrium is known to be sensitive to temperature, a factor which might affect the stability of these CCS polymers. To investigate this possibility, a solution of CSS polymers at pH 11.0 were investigated at a range of temperatures (5 – 50 °C) by DLS analysis (Figure 4.11b), displaying near identical hydrodynamic radii across this temperature range. The hydrodynamic radius of the CCS polymer would be expected to 'shrink' as the core passes through its LCST. We speculate that no 'shrinking' of the CCS polymer assembly is observed on account of the relatively high cross-linking density of the core which makes the core rigid, and the relatively small size of the core, meaning any 'shrinkage' may not be within the limits of detection of dynamic light

scattering experiments. This observation confirms that any temperature-induced shift in the position of the imine equilibrium does not lead to the disassembly of CCS polymers. We speculate that because each polymer chain is incorporated into the assembly through multiple imine linkages, then even as the equilibrium shifts away from imine formation, there are still enough imine links present to ensure the integrity of the CCS polymer assembly.
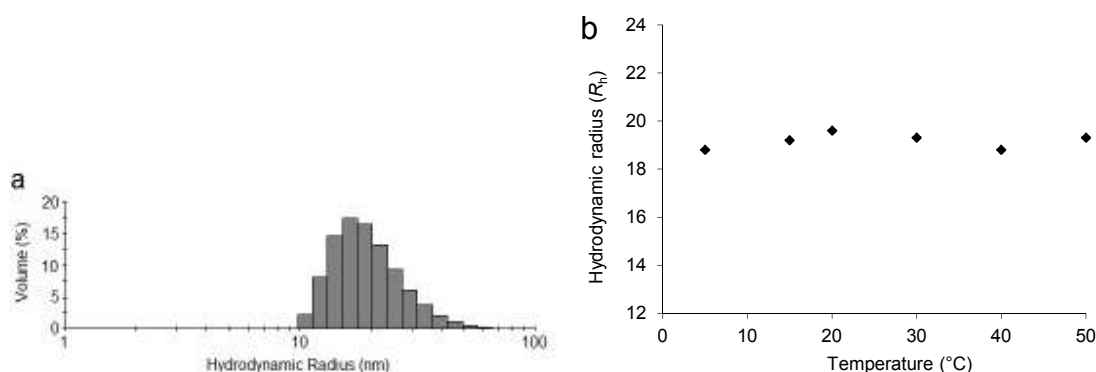
Figure 4.11 (a) Histogram showing the particle size distributions at 20 °C of reduced CCS polymer species at pH 5.5 after addition of NaCNBH$_3$, (b) Hydrodynamic radii of CCS polymers (pH 11.0, 1 wt %) as a function of temperature. Batch dynamic light scattering analysis for data point at 5 °C was carried out at 15 °C after sample was stored overnight at 5 °C.

4.3.3   pH-Triggered Encapsulation and Release

The pH-triggered disassembly was examined further using fluorescence emission spectroscopy and the dye Nile Red as a hydrophobic probe. The CCS polymers possess cores which are composed of copolymers based upon poly(N-isopropylacrylamide), a thermoresponsive polymer which can undergo a reversible phase transition from hydrophilic to hydrophobic at its LCST. The possibility therefore exists that above their LCSTs the CCS polymers can reversibly uptake hydrophobic molecules into their cores, and then release these hydrophobes upon the pH-triggered disassembly of the CCS polymers. Nile Red (1 mg per 10 mg of CCS polymer) was added to a 1 wt % solution of CCS polymer at pH 11.0 and the resulting suspension stirred overnight at 45 °C, a temperature above the estimated LCST of the CCS polymer core, followed by filtration to remove excess Nile Red. The obtained solution displayed a bright red/ purple colour (Figure 4.12b), which was analyzed by fluorescence emission spectroscopy to confirm the uptake of Nile Red (Figure 4.13a). The pH of the solution was then adjusted to 5.5 to trigger disassembly and the reaction was left overnight at room temperature to re-equilibrate. The solution became noticeably less intense in color (Figure 4.12c) and a

purple precipitate was observed. Fluorescence spectroscopy revealed a decrease in the emission intensity (Figure 4.13a), observations which suggest the release of Nile Red as the CCS polymer disassembles into its unimolecular polymer chains. The reversibility of this encapsulation process was investigated by fluorescence emission spectroscopy whilst cycling the pH (Figure 4.13b), suggesting the complexation and release of hydrophobic Nile Red dye within the core can triggered over several cycles.
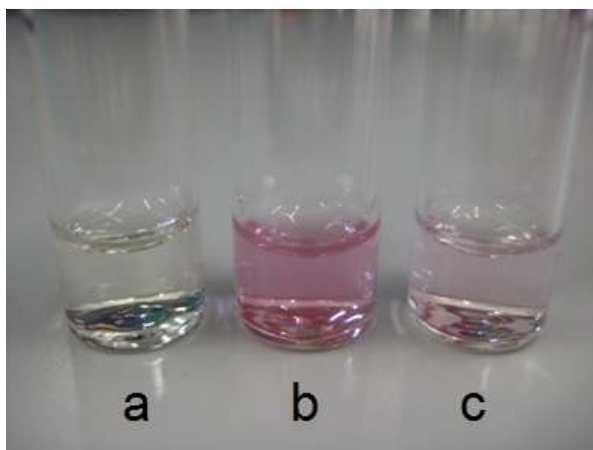
Figure 4.12 (a) Nile Red in H_2O, (b) CCS polymer + Nile Red at pH 11.0 and (c) CCS polymer + Nile Red at pH 5.5 after CCS polymer disassembly. All solutions have been filtered to remove excess or precipitated Nile Red.
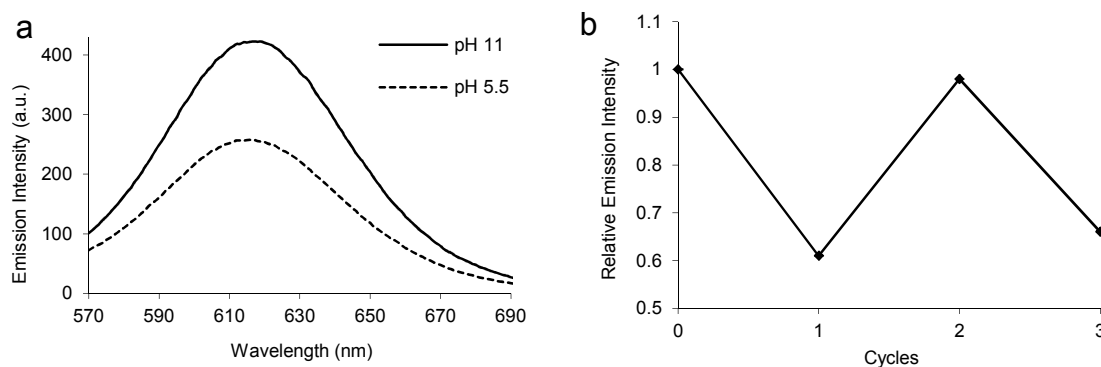
Figure 4.13 (a) Fluorescence spectra displaying the pH-triggered release of Nile Red from a solution of CCS polymers, (b) Reversible Nile Red encapsulation cycling from pH 11.0 (cycles 0 and 2) to pH 5.5 (cycles 1 and 3).

4.3.4 *Temperature Triggered Encapsulation and Release*

The ability to trigger, in response to temperature, the uptake and release of guest molecules from the thermoresponsive cores of the CCS polymers was investigated. A sample of CCS polymer containing complexed Nile Red (1 wt %, pH 11.0) was stored at 5 ˚C for 48 h. After this time a purple precipitate was observed and fluoresence spectroscopy (Figure 4.14a) displayed a relative decrease in the emission intensity,

suggesting that at low temperatures the core switches from hydrophobic to hydrophilic, releasing Nile Red from the core. The solution was then heated to 45 °C for 24 h and fluorescence spectroscopy (Figure 4.14b) confirmed the re-encapsulation of Nile Red. These observations suggest the the cross-linked cores can reversibly switch from hydrophilic to hydrophobic and thus possesses the ability to complex then release hydrophobic guest molecules in response to changes in temperature.
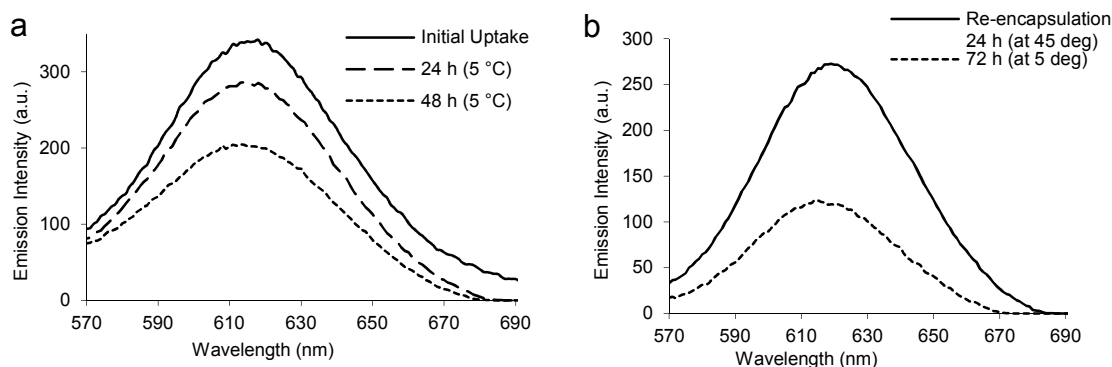
Figure 4.14 (a) Fluorescence spectra as a function of time following the temperature-triggered release of Nile Red from a solution of CCS polymers, (b) Temperature triggered re-encapsulation of Nile Red followed by fluorescence spectroscopy. After cooling to 5 °C for 72 h at pH 11.0 (dotted line), the solution was heated to 45 °C for 24 h at pH 11.0 (solid line). The increase in fluorescence intensity suggests the encapsulation of Nile Red with the CCS polymers.

4.4   Conclusions

We have developed novel water-soluble CCS polymer nanoparticles possessing pH- and thermoresponsiveness, and it is demonstrated that both of these stimuli can be used to trigger the release and uptake of a hydrophobic guest molecule. Changes in pH were shown to trigger the reversible assembly and disassembly of the CCS polymers through dynamic covalent imine bond re-equilibration. Changes in temperature were shown to result in a hydrophilic-hydrophobic switch of the CCS polymer cores, allowing for the reversible uptake and release of Nile Red whilst maintaining the structural integrity of the architecture. This water-soluble system has better capitalised upon the responsive and adaptive nature of imine cross-links compared to the CCS polymers described in Chapter 3, which display only a chemoresponsive characteristic upon the addition of a small molecule. The CCS polymers described in this chapter are truly dynamic, and can switch between assembled-disassembled or hydrophilic-hydrophobic without any evidence of polymer degradation. This work opens the way for the development of new

multi-stimuli responsive CCS polymers which may find applications in the controlled delivery of high value guest molecules.

4.5   Experimental

All chemicals were purchased from Sigma-Aldrich or Alfa Aesar and were used as received without further purification. *N,N'*-Dimethylacrylamide was purified by vacuum distillation at 60 ˚C. *N*-isopropylacrylamide was recrystallized from hexane prior to use. ^{1}H and ^{13}C NMR spectra were recorded on a Bruker Advance 300 spectrometer at 300 and 75 MHz, respectively, with the residual solvent signal as an internal standard. FT-IR spectroscopy was performed on a Varian 800 FT-IR instrument (Varian Inc.). High-resolution mass spectrometry was performed on a Waters LCT premier mass spectrometer (Waters Inc.). Fluorescence emission spectra were recorded on a Digilab F-2500 Fluorescence Spectrophotometer (Hitachi) (λ_{ex} = 550 nm). pH Measurements were recorded with a Hanna HI 98103 instrument that was calibrated daily with commercial buffer solutions (Sigma-Aldrich). The pH adjustments of cross-linking reactions were carried out using small aliquots (5 µL) of 1M NaOH$_{(aq)}$ and 1M HCl$_{(aq)}$ solutions. Gel permeation chromatography (GPC) was conducted on a Varian ProStar instrument (Varian Inc.) equipped with a Varian 325 UV-vis dual wavelength detector (254 nm), a Dawn Heleos II multi-angle laser light scattering detector (Wyatt Technology Corp.), a Viscotek 3580 differential RI detector, and a pair of PL gel 5 µm Mixed D 300 × 7.5 mm columns with guard column (Polymer Laboratories Inc.) in series. Near monodisperse poly(methyl methacrylate) standards (Agilent Technologies) were used for calibration. Data collection was performed with Galaxie software (Varian Inc.) and chromatograms analyzed with the Cirrus software (Varian Inc.) and Astra software (Wyatt Technology Corp.). Hydrodynamic radii (R_h) of polymers and core cross-linked star (CCS) polymers in aqueous solutions were determined by dynamic light scattering (DLS). The DLS instrumentation consisted of a MALVERN Instruments HPPS-ET 5002 operating at 20 ˚C with a 633-nm laser module. Measurements were made at a detection angle of 173˚ (back scattering), and Malvern DTS 4.20 software was utilized to analyze the data. All determinations were made in duplicate. The lower critical solution temperatures (LCST) of polymers **P2** and **P4b** (5 mg/ mL) were measured on a Cary 100 Bio UV-Vis spectrophotometer (Varian Inc.) fitted with a peltier block. Transmittance of polymer solutions was monitored at 550 nm as a function of temperature (cell path length 10 mm).

Methyl-4-(dimethoxymethyl)benzoate (1)[11]

A solution of 4-carboxybenzaldehyde (15.4 g, 102.6 mmol), trimethylorthoformate (32.7 g, 307.8 mmol) and conc. H_2SO_4 (8 drops) in MeOH (100 mL) was heated under reflux conditions for 48 h. The reaction mixture was transferred to a separating funnel with saturated $NaHCO_{3(aq)}$ (100 mL). The aqueous layer was extracted with CH_2Cl_2 (3 × 150 mL). The organic extracts were combined and dried over Na_2SO_4, filtered and evaporated to dryness to afford a crude liquid which was purified by vacuum distillation to afford the title product as a colourless liquid (19.8 g, 92 %). ^1H NMR ($CDCl_3$): δ 3.30 (s, 6H, CH(OCH_3)$_2$), 3.89 (s, 3H, OCH_3), 5.42 (s, 1H, CH(OCH$_3$)$_2$), 7.51 (d, 2H, Ar, J = 8.1 Hz), 8.02 (d, 2H, Ar, J = 8.1 Hz). ^{13}C NMR ($CDCl_3$): δ 52.2, 53.0, 103.0, 127.1, 129.8, 130.8, 143.8, 167.1. FT-IR (wavenumber, cm^{-1}): 2947 (C–H), 2905 (C–H), 2834 (C–H), 1724 (C=O), 1452 (C=C), 1436 (C=C), 1410 (C=C).

N-ethylacrylamide-2-(4-(dimethoxymethyl)benzamide) (2)

A solution of methyl-4-(dimethoxymethyl)benzoate (**1**, 6.0 g, 28.5 mmol) in 1,2-diaminoethane (100 mL) was heated under reflux for 24 h then evaporated to dryness. The viscous yellow oil obtained was dissolved in CH_2Cl_2 (100 mL) and Et$_3$N (5.7 g, 56.3 mmol) added. The solution was cooled to 0 ˚C in an ice bath. Acryloyl chloride (2.6 g, 28.5 mmol) in CH_2Cl_2 (50 mL) was added dropwise over 30 min. The reaction was stirred overnight at room temperature then transferred to a separating funnel with saturated $NaHCO_3$(aq) (150 mL). The aqueous layer was extracted with CH_2Cl_2 (2 × 150 mL), and the organic extracts were combined and dried over Na_2SO_4, filtered and evaporated to dryness to afford a crude solid which was purified by column chromatography [SiO$_2$, EtOAc-Et$_3$N (95:5)] to afford the title product as a white solid (3.3 g, 40 %). ^1H NMR ($CDCl_3$): δ 3.28 (s, 6H, CH(OCH_3)$_2$), 3.52 (m, 4H, (CH_2)$_2$), 5.37 (s, 1H, CH(OCH$_3$)$_2$), 5.58 (dd, 1H, J = 1.8 Hz, J = 9.9 Hz), 6.14 (dd, 1H, J = 9.9 Hz, J = 17.0 Hz), 6.23 (dd, 1H, J = 1.8 Hz, J = 17.0 Hz), 7.37 (s, 1H, NH), 7.45 (d, 2H, Ar, J = 8.1 Hz), 7.79 (d, 2H, Ar, J = 8.1 Hz), 7.84 (s, 1H, NH). ^{13}C NMR ($CDCl_3$): δ 41.3, 53.1, 103.1, 127.3, 128.2, 130.0, 131.3, 134.6, 142.1, 167.5, 168.6. FT-IR (wavenumber, cm^{-1}): 3290 (N–H), 3096 (C–H, alkene), 2947 (C–H, alkyl), 1634 (C=O), 1593 (C=O), 1448 (C=C, aromatic), 1413 (C=C, aromatic). HRMS$^+$ $C_{15}H_{21}N_2O_4$: Theoretical: 293.1501. Actual: 293.1503.

N-ethylacrylamide-2-(4-formylbenzamide) (3)

A solution of *N*-ethylacrylamide-2-(4-(dimethoxymethyl)benzamide) (**2**, 1.4 g, 4.8 mmol) in 1M $HCl_{(aq)}$ (20 mL) was stirred at room temperature for 2 h then neutralized with saturated $NaHCO_3$(aq) (100 mL). The aqueous layer was extracted with EtOAc (3 × 150 mL), and the organic extracts were combined and dried over $MgSO_4$, filtered and evaporated to dryness to afford the title product as a white solid (1.0 g, 84 %). ^{1}H NMR (DMSO-d_6): δ 3.72 (m, 4H, (CH_2)$_2$), 5.59 (dd, 1H, J = 2.5 Hz, J = 9.8 Hz), 6.09 (dd, 1H, J = 2.5 Hz, J = 17.1 Hz), 6.23 (dd, 1H, J = 9.8 Hz, J = 17.1 Hz), 7.99 (d, 2H, Ar, J = 8.4 Hz), 8.03 (d, 2H, Ar, J = 8.4 Hz), 8.23 (s, ^{1}H, NH), 8.79 (s, 1H, NH), 10.07 (s, 1H, CHO). ^{13}C NMR (DMSO-d_6): δ 38.7, 125.2, 128.3, 129.6, 132.3, 138.2, 140.1, 165.5, 166.1, 193.0. FT-IR (wavenumber, cm^{-1}): 3264 (N–H), 3091 (C–H, alkene), 2943 (C–H, alkyl), 1699 (C=O, aldehyde), 1627 (C=O, amide), 1549 (C=O, amide), 1447 (C=C, aromatic), 1414 (C=C, aromatic). HRMS$^+$ $C_{13}H_{15}N_2O_3$: Theoretical: 247.1083. Actual: 247.1085.

N-(tert-butoxycarbonyl)-l,3-diaminopropane (4)[12]

A solution of 1,3-diaminopropane (25.0 g, 337 mmol) in CHCl$_3$ (200 mL) was cooled to 0 ˚C in an ice bath. A solution of di-*tert*-butyl dicarbonate (10.5 g, 48 mmol) in CHCl$_3$ (100 mL) was added dropwise over 30 min and the reaction mixture was stirred overnight at room temperature, then filtered and the filtrate evaporated to dryness. Saturated $NaCl_{(aq)}$ (150 mL) was added to the clear oil obtained and the solution was filtered to remove the *bis*-protected product, transferred into a separating funnel with diethyl ether (150 mL). The aqueous layer was extracted with diethyl ether (2 × 150 mL). The organic extracts were combined and dried over Na_2SO_4, filtered and evaporated to dryness to afford the title product as a colourless liquid (6.1 g, 73 %). ^{1}H NMR (CDCl$_3$): δ 1.20 (s, 2H, NH_2), 1.38 (s, 9H, C(CH_3)$_3$), 1.54 (m, 2H, CH$_2$-CH_2-CH$_2$), 2.68 (m, 2H, CH_2N), 3.14 (m, 2H, CH_2N), 5.03 (s, 1H, NH). ^{13}C NMR (CDCl$_3$): δ 28.8, 31.5, 33.9, 40.0, 79.4, 156.5. FT-IR (wavenumber, cm^{-1}): 3358 (N–H), 3308 (N–H), 2975 (C–H), 2933 (C–H), 2869 (C–H), 1687 (C=O). HRMS$^+$ $C_8H_{19}N_2O_2$: Theoretical: 175.1447. Actual: 175.1449.

N-(tert-butoxycarbonyl)-propylaminoacrylamide (5)

A solution of *N*-(*tert*-butoxycarbonyl)-l,3-diaminopropane (**4**, 3.1 g, 17.8 mmol) and Et$_3$N (2.2 g, 21.4 mmol) in CH$_2$Cl$_2$ (75 mL) was cooled to 0 ˚C in an ice bath. Acryloyl chloride (1.6 g, 17.8 mmol) in CH$_2$Cl$_2$ (50 mL) was added dropwise over 30 min, and the reaction was stirred overnight at room temperature, then transferred to a separating funnel with saturated NaHCO$_{3(aq)}$ (150 mL). The aqueous layer was extracted with CH$_2$Cl$_2$ (2 × 150 mL) and the organic extracts were combined and dried over Na$_2$SO$_4$, filtered and evaporated to dryness to afford a crude solid which was purified by column chromatography [SiO$_2$, Hexane-EtOAc (1:1)] to afford the title product as a white solid (3.2 g, 79 %). ^{1}H NMR (CDCl$_3$): δ 1.37 (s, 9H, C(C*H$_3$*)$_3$), 1.59 (m, 2H, CH$_2$-C*H$_2$*-CH$_2$), 3.10 (m, 2H, C*H$_2$*N), 3.30 (m, 2H, C*H$_2$*N), 5.27 (s, 1H, N*H*), 5.56 (dd, 1H, J = 1.9 Hz, J = 9.8 Hz), 6.10 (dd, 1H, J = 9.8 Hz, J = 17.0 Hz), 6.20 (dd, 1H, J = 1.9 Hz, J = 17.0 Hz), 7.02 (s, 1H, N*H*). ^{13}C NMR (CDCl$_3$): δ 27.8, 30.5, 36.6, 37.9, 79.6, 125.9, 131.7, 157.0, 166.4. FT-IR (wavenumber, cm^{-1}): 3230 (N–H), 3066 (C–H, alkene), 2941 (C–H, alkyl), 1686 (C=O), 1652 (C=O). HRMS$^+$ C$_{11}$H$_{20}$N$_2$O$_3$Na: Theoretical: 251.1372. Actual: 251.1374.

Aldehyde-Functionalized Copolymer (P1)

S-1-Dodecyl-*S'*-(α,α-dimethyl-α''-acetic acid)trithiocarbonate (DDMAT) (1 eq, 21.5 mg, 0.059 mmol) and AIBN (0.2 eq, 1.93 mg, 12 μmol) were added to a small schlenk tube. *N*-Isopropylacrylamide (180 eq, 1.20 g, 10.62 mmol) and *N*-ethylacrylamide-2-(4-formylbenzamide) (**3**, 20 eq, 0.29 g, 1.18 mmol) were then added followed by DMSO (2.5 mL). The reaction mixture was degassed five times, and then the vessel was backfilled with N$_2$, purged with N$_2$, and allowed to warm to room temperature. The reaction mixture was then placed in an oil bath at 70 ˚C, and the polymerization was quenched after 1 h. The reaction mixture was dissolved in a minimal amount of THF and added dropwise to a large excess of ice-cold diethyl ether. The polymer precipitate was then isolated by filtration and the precipitation was repeated before drying under high vacuum. Polymer **P1** was obtained as a pale yellow solid (0.93 g). ^{1}H NMR (CDCl$_3$): 1.09 (br, CH(C*H$_3$*)$_2$), 1.61 (br, CHC*H$_2$*, polymer backbone), 2.12 (br, C*H*CH$_2$, polymer backbone), 3.49 (br, (C*H$_2$*)$_2$), 3.96 (br, C*H*(CH$_3$)$_2$), 6.50 (br, N*H*), 7.89 (br, Ar), 8.04 (br, Ar), 8.45 (br, N*H*), 10.04 (br, C*H*O). The composition of **P1** can be determined by comparing the integration of the aldehyde protons of **3** with the integration of the

C*H*(CH₃)₂ protons of NIPAm. The monomer composition was determined to be 9: 1 NIPAm: **3** (identical to the feed ratio).

*Aldehyde-Functionalized Diblock Copolymer (**P2**)*

P1 (1 eq, 0.74 g, 43.8 µmol) and AIBN (0.2 eq, 1.44 mg, 8.8 µmol) were added to a small schlenk tube. *N,N'*-Dimethylacrylamide (400 eq, 1.74 g, 17.5 mmol) was then added followed by DMSO (4 mL) and the reaction mixture was degassed five times. The vessel was backfilled with N_2, purged with N_2, and allowed to warm to room temperature. The reaction mixture was then placed in an oil bath at 70 ˚C, and the polymerization was quenched after 1 h. The reaction mixture was dissolved in a minimal amount of THF and added dropwise to a large excess of ice-cold diethyl ether. The polymer precipitate was then isolated by filtration and the precipitation was repeated before drying under high vacuum. Polymer **P2** was obtained as a pale yellow solid (2.09 g). ¹H NMR (D_2O): δ 1.10 (br, CH(C*H₃*)₂), 1.36 (br, CHC*H₂*, polymer backbone), 1.62 (br, C*H*CH₂, polymer backbone), 2.90 (br m, N(C*H₃*)₂), 3.86 (br, C*H*(CH₃)₂), 7.89 (br, Ar), 9.97 (br, C*H*O).

*Boc-Amine-Functionalized Copolymer (**P3**)*

S-1-Dodecyl-*S'*-(α,α-dimethyl-α''-acetic acid)trithiocarbonate (DDMAT) (1 eq, 26.1 mg, 0.072 mmol) and AIBN (0.2 eq, 2.35 mg, 14 µmol) were added to a small schlenk tube. *N*-Isopropylacrylamide (180 eq, 1.46 g, 12.9 mmol), *N*-(*tert*-butoxycarbonyl)-propylaminoacrylamide (**5**, 20 eq, 0.33 g, 1.43 mmol) were then added followed by DMSO (2.5 mL). The reaction mixture was degassed five times, and then the vessel was backfilled with N_2, purged with N_2, and allowed to warm to room temperature. The reaction mixture was then placed in an oil bath at 70 ˚C, and the polymerization was quenched after 1 h. The reaction mixture was dissolved in a minimal amount of THF and added dropwise to a large excess of ice-cold diethyl ether. The polymer precipitate was then isolated by filtration and the precipitation was repeated before drying under high vacuum. Polymer **P3** was obtained as a pale yellow solid (1.33 g). ¹H NMR (CDCl₃): 1.11 (br, CH(C*H₃*)₃), 1.39 (br, C(C*H₃*)₃), 1.62 (br, CHC*H₂*, polymer backbone), 2.11 (br, C*H*CH₂, polymer backbone), 3.09 (br, NHCH₂C*H₂*), 3.58 (br, NHC*H₂*CH₂), 3.97 (br, C*H*(CH₃)₂), 5.50 (br, N*H*), 6.50 (br, N*H*). The composition of **P3** can be determined by comparing the integration of the *Boc* protons of **5** with the

integration of the $CH(CH_3)_2$ protons of NIPAm. The monomer composition was determined to be 9: 1 NIPAm: **5** (identical to the feed ratio).

*Boc-Amine-Functionalized Diblock Copolymer (**P4a**)*

P3 (1 eq, 1.04 g, 54.8 μmol) and AIBN (0.2 eq, 1.8 mg, 10.9 μmol) were added to a small schlenk tube. *N,N'*-Dimethylacrylamide (400 eq, 2.17 g, 21.9 mmol) was then added followed by DMSO (4 mL) and the reaction mixture was degassed five times. The vessel was backfilled with N_2, purged with N_2, and allowed to warm to room temperature. The reaction mixture was then placed in an oil bath at 70 ˚C, and the polymerization was quenched after 1 h. The reaction mixture was dissolved in a minimal amount of THF and added dropwise to a large excess of ice-cold diethyl ether. The polymer precipitate was then isolated by filtration and the precipitation was repeated before drying under high vacuum. Polymer **P4a** was obtained as a pale yellow solid (2.37 g). ^{1}H NMR (CDCl$_3$): 1.09 (br, CH(CH_3)$_2$), 1.38 (br, C(CH_3)$_3$), 1.58 (br, CHCH_2, polymer backbone), 2.07 (br, CHCH$_2$, polymer backbone), 2.86 (br, N(CH_3)$_2$), 3.95 (br, CH(CH$_3$)$_2$), 5.50 (br, NH), 6.50 (br, NH).

*Amine-Functionalized Diblock Copolymer (**P4b**)*

P4a (2.08 g) was dissolved in CH$_2$Cl$_2$ (5 mL) and TFA (3 mL) was added, the reaction mixture was left to stir for 2 h. After this time the solvent and excess TFA were removed on the rotary evaporator and the oil obtained was dissolved in a minimal amount of THF and added dropwise to a large excess of diethyl ether. The polymer precipitate was then isolated by filtration and dried under high vacuum. Polymer **P4b** was obtained as a pale yellow solid (1.82 g). ^{1}H NMR (D$_2$O): δ 1.09 (br, CH(CH_3)$_2$), 1.34 (br, CHCH_2, polymer backbone), 1.59 (br, CHCH$_2$, polymer backbone), 2.87 (br, N(CH_3)$_2$), 3.84 (br, CH(CH$_3$)$_2$).

Formation of CCS Polymers and Encapsulation of Nile Red

P2 (47.4 mg, 1 μmol, 1 eq) was dissolved in H$_2$O (4.73 mL) and **P4b** (48.2 mg, 1 μmol, 1 eq) was dissolved in H$_2$O (4.73 mL), these solution were then combined under rapid stirring resulting in a solution with a total diblock copolymer concentration of 0.211 mM (1 wt %). The pH was adjusted to 11.0 with small aliquots (5 μL) of 1M NaOH$_{(aq)}$

and left to equilibrate overnight at room temperature to allow for the formation of CCS polymers. After this time Nile Red (9.56 mg, 30 μmol, 30 eq per polymer chain) was added resulting in a solution with a Nile Red concentration of 3.17 mM. This solution was stirred at 45 ˚C for 16 h. After this time the excess Nile Red was removed by filtration. The encapsulation was then confirmed by fluorescence spectroscopy (λ_{ex} = 550 nm).

Disassembly of CCS Polymers and Release of Nile Red

To trigger the disassembly of CCS polymers and the subsequent release of Nile Red the pH was adjusted to 5.5 with small aliquots (5 μL) of 1M HCl$_{(aq)}$ and left to equilibrate overnight at room temperature. Fluorescence spectroscopy (λ_{ex} = 550 nm) confirmed the release of Nile Red.

4.6   References

1. A. P. Bapat, D. Roy, J. G. Ray, D. A. Savin and B. S. Sumerlin, *J. Am. Chem. Soc.*, 2011, **133**, 19832-19838.
2. J. Gu, W.-P. Cheng, J. Liu, S.-Y. Lo, D. Smith, X. Qu and Z. Yang, *Biomacromolecules*, 2007, **9**, 255-262.
3. C. X. Ding, J. X. Gu, X. Z. Qu and Z. Z. Yang, *Bioconjugate Chem.*, 2009, **20**, 1163-1170.
4. X. W. Xu, J. D. Flores and C. L. McCormick, *Macromolecules*, 2011, **44**, 1327-1334.
5. C. Godoy-Alcantar, A. K. Yatsimirsky and J. M. Lehn, *J. Phys. Org. Chem.*, 2005, **18**, 979-985.
6. S. Fujishige, K. Kubota and I. Ando, *J. Phys. Chem.*, 1989, **93**, 3311-3313.
7. J.-F. Lutz, Ö. Akdemir and A. Hoth, *J. Am. Chem. Soc.*, 2006, **128**, 13046-13047.
8. A. Laukkanen, L. Valtola, F. M. Winnik and H. Tenhu, *Macromolecules*, 2004, **37**, 2268-2274.
9. J. Persson, H. O. Johansson, I. Galaev, B. Mattiasson and F. Tjerneld, *Bioseparation*, 2000, **9**, 105-116.
10. H. Y. Liu and X. X. Zhu, *Polymer*, 1999, **40**, 6985-6990.
11. I. T. Crosby, G. A. Pietersz and J. A. Ripper, *Aust. J. Chem.*, 2008, **61**, 138-143.
12. D. Boturyn, A. Boudali, J. F. Constant, E. Defrancq and J. Lhomme, *Tetrahedron*, 1997, **53**, 5485-5492.
13. J. T. Lai, D. Filla and R. Shea, *Macromolecules*, 2002, **35**, 6754-6756.
14. W. Burchard, M. Schmidt and W. H. Stockmayer, *Macromolecules*, 1980, **13**, 1265-1272.
15. P. Lang, W. Burchard, M. S. Wolfe, H. J. Spinelli and L. Page, *Macromolecules*, 1991, **24**, 1306-1314.

Chapter 5

Triggering Polymeric Nanoparticle Disassembly through the Simultaneous Application of Two Different Stimuli

Table of Contents:

5.1 Abstract

Reversible addition-fragmentation chain transfer (RAFT) polymerization was utilized to prepare acrylamide-based linear copolymers displaying pyridyl disulfide appendages and either aldehyde or amine functional groups. These copolymer chains were intermolecularly cross-linked through imine bond formation at pH 8.0 and then through disulfide bond formation to afford polymeric nanoparticles possessing hydrodynamic radii of 76 nm and consisting of multiple polymer chains cross-linked through both imine and disulfide bonds. By performing the cross-linking reactions in the presence of the hydrophobic dye Nile Red it was demonstrated that these polymeric nanoparticles could encapsulate a cargo of small molecules. The disassembly of the polymeric nanoparticles into their component polymer chains was triggered by lowing the pH to 5.5 in the presence of the disulfide reducing agent tris(2-carboxyethyl) phosphine (TCEP), causing hydrolysis of the imine cross-links and cleavage of the disulfide cross-links and demonstrating that the simultaneous application of both low pH and a reducing environment are required to trigger the disassembly process. It was shown that application of either a low pH or the application of the reducing agent TCEP does not trigger the disassembly of the polymeric nanoparticle as there is sufficient density of the remaining imine or disulfide cross-links which are able to maintain the structural integrity of the polymeric nanoparticle. A 5 kDa polyethylene glycol was grafted onto the polymeric nanoparticle, demonstrating the potential of these polymeric nanoparticles to undergo post-assembly functionalization.

5.2 Introduction

The possibility of developing polymeric nanoparticles which require the simultaneous application of two distinct stimuli to trigger a desired response is intriguing. The ability to obtain a response by using a combination of stimuli applied simultaneously could lead to greater specificity regarding where and when events are triggered, a feature which would be highly advantageous in fields such as drug delivery. In this regard, the group of Thayumanavan has developed[1] triply-stimuli sensitive amphiphilic block copolymers which self-assemble into micelles possessing the abilities to encapsulate hydrophobic molecules. They have demonstrated that the kinetics of release of the encapsulated molecules from these micelles varied depending on whether single stimuli or multiple stimuli are applied, demonstrating the feasibility of combining different

orthogonal triggers. Although this elegant work represents a significant advance, it is worthwhile noting that the stimuli-triggered events, namely the disassembly of the micelles and the release of their encapsulated cargo, still occur upon the application of only a single stimulus, and that the simultaneous application of multiple stimuli only changes the rate at which events occur.

The approach described in this Chapter was to employ two orthogonal reversible covalent reactions to link pre-formed linear polymer chains into polymeric nanoparticle structures, namely the condensation of amine and aldehydes to form imines, and the oxidation of thiols to form disulfides. Imine formation in aqueous solution is pH sensitive,[2] with imine formation favored at high pH and disfavored at low pH (Chapter 1). Consequently, it is possible to modulate the position of the imine equilibrium by changing the pH, and depending on the reaction partners, it is possible to shift the equilibrium from a near 100% yield of imine in solution to complete hydrolysis within a narrow range of approximately three pH units. The stability of the imine bond in water and the pH at which it undergoes hydrolysis can be tuned by altering the stereoelectronic characteristics of the reaction partners, in particular the carbonyl-derived part. The formation of disulfides from thiols on the other hand is a redox sensitive process, with disulfides readily reducing to thiols within a reducing environment (Chapter 1). It was envisioned that these two orthogonal reversible reactions could be used to develop a dual stimuli-responsive polymeric nanoparticle prepared from the cross-linking of multiple polymer chains through both imine and disulfide bonds, and which would require the simultaneous application of *both* low pH and a reducing environment to trigger its complete disassembly into its component polymer chains. A further advantage of employing reversible covalent bonds to facilitate cross-linking is that the strength of the covalent bond ensures the product assemblies possess chemical robustness, an important issue to contemplate when considering possible applications. The feasibility of using reversible reactions to impart stimuli-responsive properties into polymeric nanoparticles has already been demonstrated (Chapter 1). The group of Thayumanavan has demonstrated[3, 4] that polymer chains can be intermolecularly cross-linked through disulfide bond formation, and used a redox trigger in the form of the peptide glutathione to cause their disassembly. In other work, the group of Davis and Boyer have shown[5, 6] that either acetal or disulfide linkages can be incorporated into star polymers possessing pH and redox responsiveness. While these systems demonstrate pH and redox responsiveness, only a single trigger is required for complete nanoparticle disassembly.

The work presented here shows that polymer chains can be intermolecularly cross-linked using both imine and disulfide bonds, and that the resulting polymeric nanoparticles can complex a cargo of hydrophobic molecules. It was then show that the disassembly of these nanoparticles can be triggered using the simultaneous application of both low pH and a reducing agent, causing the release of encapsulated guest molecules. Control experiments demonstrate that the application of either low pH or a reducing environment does not trigger disassembly of the polymeric nanoparticles. We also demonstrate the possibility that these polymeric nanoparticles to be functionalized with a 5 kDa PEG, suggesting that the surfaces of these particles can be decorated as required for their possible eventual applications.
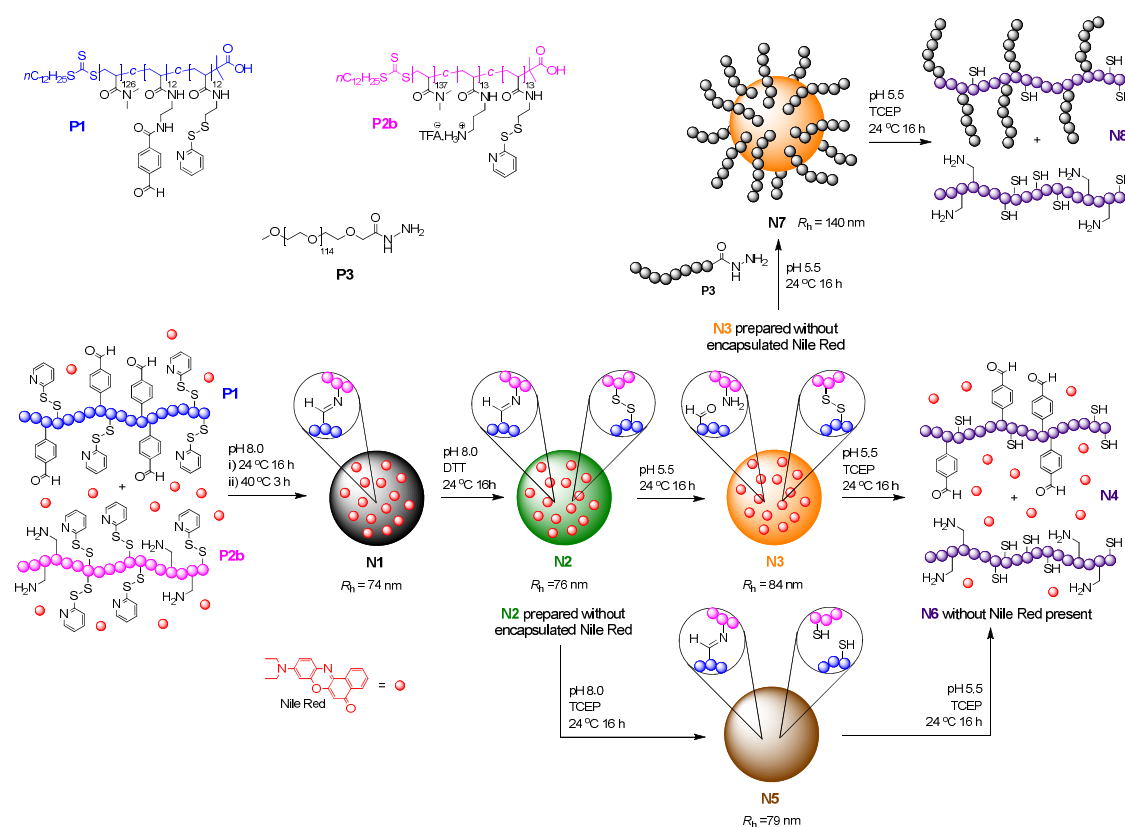
Figure 5.1 Polymer chains **P1** and **P2b** are cross-linked through imine bond formation in the presence of the dye Nile Red to form the polymeric nanoparticle **N1**. Further cross-linking through disulfide bond formation results in the formation of polymeric nanoparticle **N2**. Complete dissasembly of this particle is triggered through imine hydrolysis (**N3**) and then disulfide reduction to afford the component polymer chains (**N4**). Alternatively, disassembly is triggered through disulfide reduction to polymeric nanoparticle **N5** followed by hydrolysis of the imine cross links to afford the polymeric component polymer chains **N6** (identical to **N4** except disassembly was performed in the absence of Nile Red). Functionalization of **N3** with PEG-hydrazide (**P3**) was performed to afford the PEG-decorated polymeric nanoparticle **N7**, whose disassembly into component polymers **N8** was triggered through the addition of TCEP at pH 5.5.

5.3   Results and Discussions

5.3.1   *Aldehyde/ Amine and Pyridyl Disulfide Copolymers*
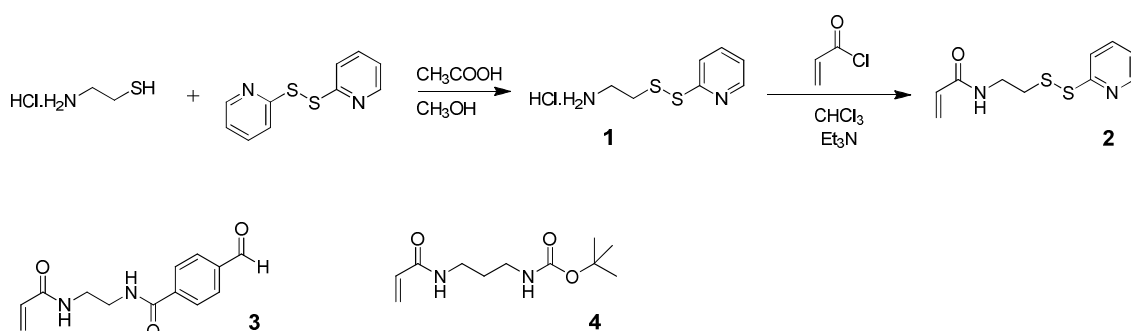
Scheme 5.1 Synthesis of pyridyl disulfide functional acrylamide-based monomer **2**, the structures of aldehyde and amine functional monomers **3** and **4** are shown. The synthesis of **3** and **4** is described in Chapter 4.

The first objective was to synthesize (Scheme 5.1) acrylamide-based monomers for the eventual preparation of linear copolymer building blocks displaying the required pendant functional groups. Monomer **2** was prepared starting from cysteamine hydrochloride, which was treated with aldrithiol to introduce the pyridyl disulfide functionality within compound **1**,[7] and then acylated by reaction with acryloyl chloride to yield the final monomer **2**. The synthesis of **3** and **4** is described in detail in Chapter 4. All steps to prepare the monomers were synthetically straightforward and relatively high yielding, allowing their preparation on the gram scale. It has previously been demonstrated that pyridyl-containing monomers[8, 9] can be subjected to controlled living radical polymerizations, and the utility of the pyridyl disulfide functionality to prepare disulfide linkages is well known.[10, 11]

   The RAFT chain transfer agent *S*-1-dodecyl-*S*'-(α,α-dimethyl-α''-acetic acid)-trithiocarbonate[12] (DDMAT) was used (Scheme 5.2a) to mediate the copolymerization of a 1: 1: 8 mixture of **2**: **3**: DMA (*N*,*N*'-dimethylacrylamide) at 70 °C in DMF to afford the copolymer **P1**. ^{1}H NMR spectroscopy revealed the polymer possessed a co-monomer composition of 1: 1: 10.5 (**2**: **3**: DMA) and confirmed the presence of the pendant aromatic aldehyde and pyridyl disulfide functional groups. The copolymer **P2a** was also prepared (Scheme 5.2b) via RAFT polymerization of **2**, **4** and DMA in a ratio of 1: 1: 8, respectively, in DMF at 70 °C. ^{1}H NMR spectroscopy revealed the polymer possessed a co-monomer composition of 1: 1: 10.5 (**2**: **4**: DMA) and confirmed the presence of the *boc*-protected alkylamine and pyridyl disulfide functional groups. It was

observed that the monomer feed ratios for the preparation of **P1** and **P2a** did not match the ratios obtained, this is presumably on account of the difference in reactivities between the *N*-monosubstituted acrylamide monomers (**2**, **3** and **4**) and the *N,N'*-disubstituted acrylamide monomer (*N,N'*-dimethylacrylamide). Polymer **P2a** was treated with TFA/ CH$_2$Cl$_2$ to afford polymer **P2b**, with ^{1}H NMR spectroscopy confirming complete removal of the *N-boc*-protecting groups. Polymer **P3** was prepared (Scheme 5.2c) from poly(ethylene glycol) monomethyl ether (5 kDa) by treatment with excess ethyl bromoacetate to afford the ethyl ester intermediate, which after hydrazinolysis afforded the hydrazide end-functionalized poly(ethylene glycol) **P3**. Polymers **P1** and **P2a** were also characterized by GPC (Table 5.1, Figure 5.2), which confirmed mono-modal distributions and acceptable PDIs. No meaningful GPC trace could be obtained from **P2b**, presumably on account of its polycationic nature, and thus its molecular weights and PDI were inferred from the analysis of its immediate precursor **P2a**.
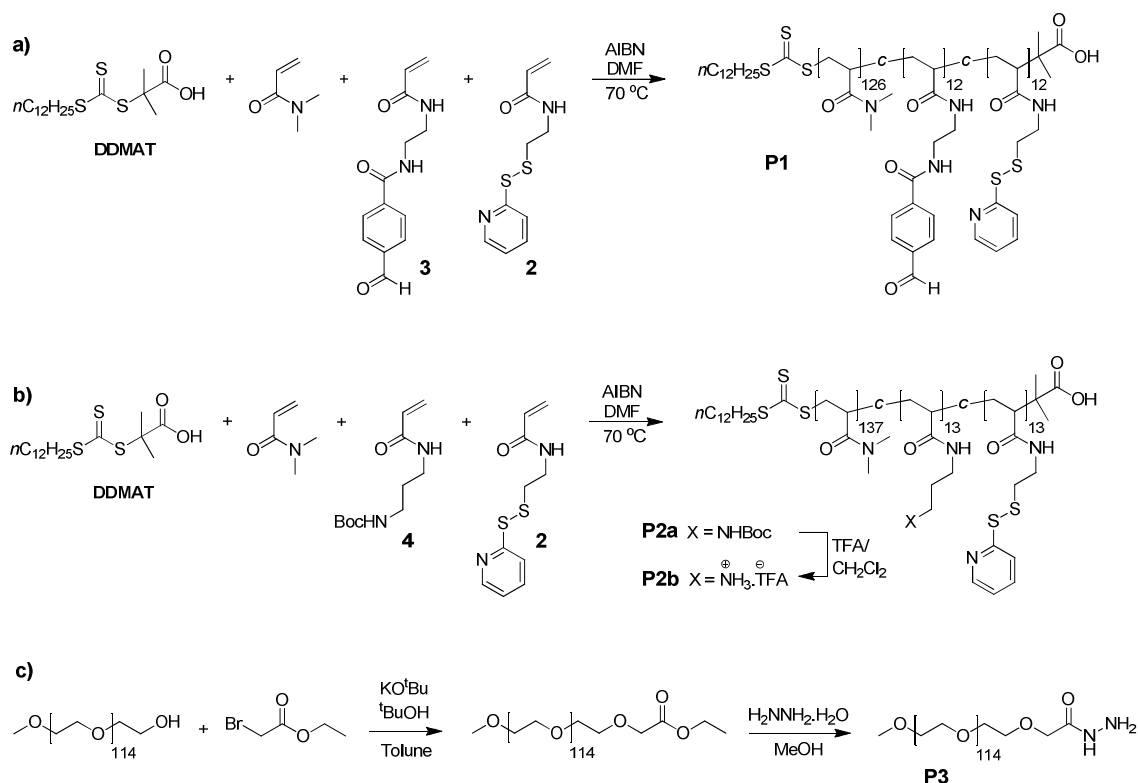
Scheme 5.2 Synthesis of linear copolymer building blocks (a) **P1** and (b) **P2**, and (c) hydrazide end-functionalized poly(ethylene glycol) (**P3**).

polymer	$M_n{}^a$ (g mol^{-1})	$M_n{}^b$ (g mol^{-1})	$M_w{}^b$ (g mol^{-1})	PDI^b (M_w/M_n)	$R_h{}^c$ (nm)
P1	18,700	14,500	20,200	1.39	4.2
P2a	20,000	16,200	24,200	1.49	4.5

Table 5.1 Characterization of polymers **P1** and **P2a**. ^{a} As determined by ^{1}H NMR spectroscopy (CDCl$_3$, 300 Hz). ^{b} As determined by gel permeation chromatography in DMF (0.6 mL/ min) containing LiBr (1 g/ L) calibrated against poly(methyl methacrylate) standards. ^{c} As determined by online dynamic light scattering measurements.
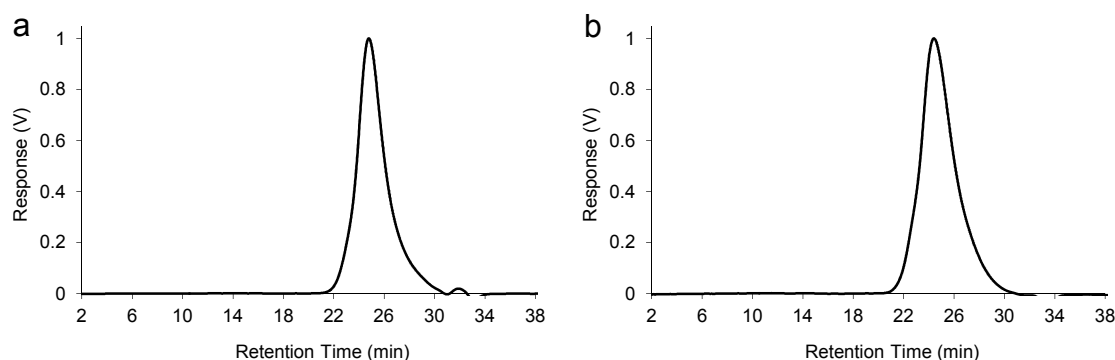
Figure 5.2 Differential refractive index (dRI) gel permeation chromatography (GPC) traces for (a) **P1** and (b) **P2a** in DMF (0.6 mL/ min, containing LiBr 1g/ L).

5.3.2 *Imine and Disulfide Nanoparticle Assembly and Disassembly*

Cross-linked nanoparticles were prepared by a two-step approach, where polymer chains were cross-linked through imine bond formation to form nanoparticle-like assemblies of polymer chains, which were then further cross-linked through the formation of disulfide bonds. Thus, copolymer **P1** and the hydrophobic dye Nile Red were dissolved in H$_2$O containing a minimal amount of THF to aid solubility. Copolymer **P2b** was dissolved in H$_2$O, and the two solutions were mixed to afford a solution with a 1 wt % concentration with respect to total copolymer building blocks and a 1: 1 molar ratio of the two copolymers **P1** and **P2b**, with Nile Red present as a fine suspension (1 mg per 10 mg of copolymer). The pH of the solution was then adjusted to 8.0 with aliquots (5 µL) of 0.1 M NaOH$_{(aq)}$ and the solution left to stir at room temperature for 16 h whilst open to the atmosphere to allow the THF to evaporate. After this time the reaction was sealed and heated to 40 °C for 3 h to optimize the encapsulation of Nile Red.
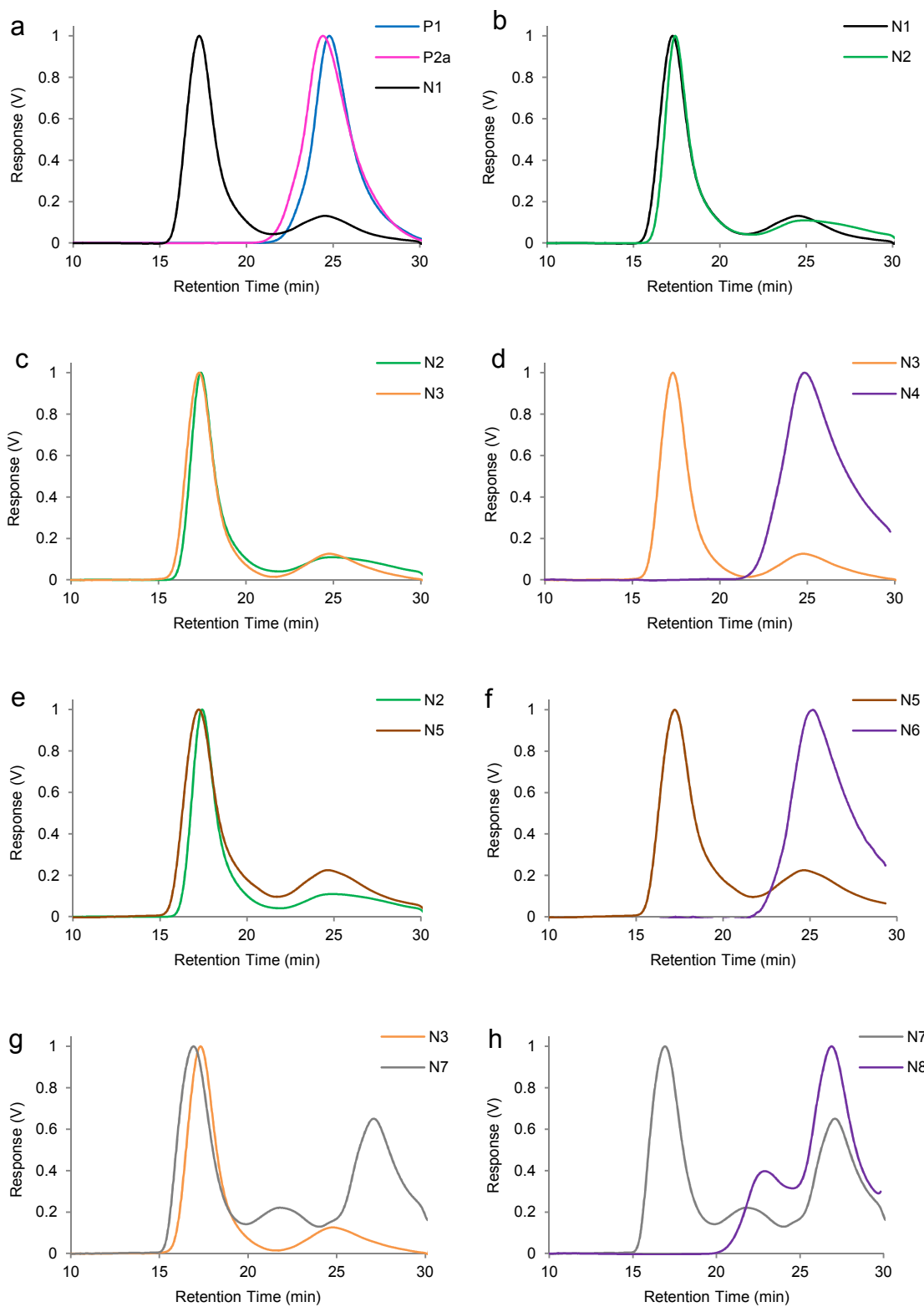
Figure 5.3 Differential refractive index (dRI) gel permeation chromatography (GPC) traces in DMF (0.6 mL/ min, containing LiBr 1 g/L) for formation of nanoparticles (a) **N1**, (b), **N2**, (c) **N3**, (d) nanoparticle disassembly **N4**, (e) nanoparticle **N5**, (f) nanoparticle disassembly **N6**, (g) nanoparticle functionalization with PEG-hydrazide **N7** and (h) disassembly of PEG functionalized nanoparticle **N8**.

Gel permeation chromatography (GPC) (Figure 5.3a) confirmed the disappearance of the linear copolymer building blocks of retention time ~ 25 min and the appearance of a peak at shorter retention time ~ 17 min, confirming the presence of a high molecular weight polymeric nanoparticle (**N1**) whose constituent polymer chains are cross-linked through the formation of imine bonds and which possesses a hydrodynamic radius of 74 nm and a PDI[13] of 0.137 as indicated by batch dynamic light scattering (Figure 5.5a). The presence of a minor peak in the GPC chromatogram at retention time ~ 25 min suggests all polymer chains are not incorporated into **N1**. We hypothesize that this minor species corresponds to a dimeric species formed from the cross-linking of one chain of **P1** with one chain of **P2b**, which is consistent with observations previously made.[14, 15]

The polymer chains within the assembly **N1** were then further cross-linked through the formation of disulfide bonds using dithiothreitol (Scheme 5.3), which was added to the reaction and left to stir at room temperature for 16 h. Under these reaction conditions dithiothreitol reduces rapidly the pendant pyridyl disulfide functional groups to the corresponding alkylthiols. Importantly, as the amount of DTT added (DTT, 0.5 eq per pyridyl disulfide functionality) can reduce no more than half of the available pyridyl disulfide functions, those alkylthiol functions formed can then intramolecularly cross-link with remaining pyridyl disulfide functional groups through disulfide exchange. This process is driven by the formation of 2-pyridinethione, a stable and inert reaction by-product, and the formation of highly stable 6-membered ring of the oxidized form of DTT.[4]
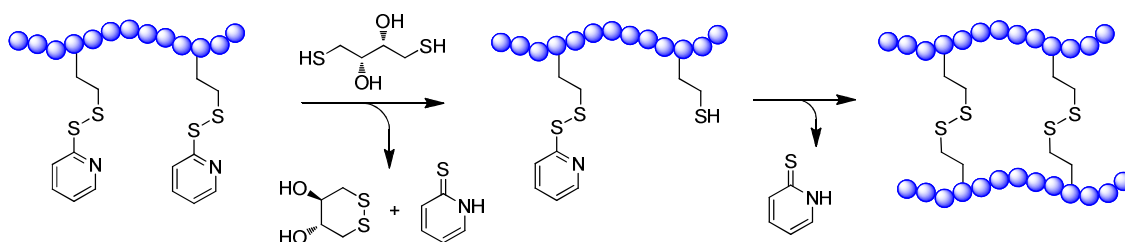
Scheme 5.3 Intermolecular cross-linking between multiple polymer chains through disulfide bond formation facilitated by the addition of dithiothreitol.

The progress of this cross-linking reaction can be monitored by performing the reaction in D_2O in the absence of Nile Red whilst using ^1H NMR spectroscopy (Figure 5.4) to observe the formation of the of 2-pyridinethione by-product. It was noted during this experiment that none of the resonances associated with the aromatic moieties of copolymer **P1** can be observed, which suggests strongly that the cross-linking units are

present within the interior of large polymer assemblies. GPC analysis (Figure 5.3b) displayed a near identical peak at retention time ~ 17 min corresponding to **N2**, which was revealed by batch dynamic light scattering (Figure 5.5b) to possess a hydrodynamic radius of 76 nm and a PDI of 0.140. The solution obtained displayed a bright red/ purple colour (Figure 5.6, inset), and fluorescence emission spectroscopy (Figure 5.6a) confirmed the presence of Nile Red as a result of its encapsulation within the polymeric nanoparticles.
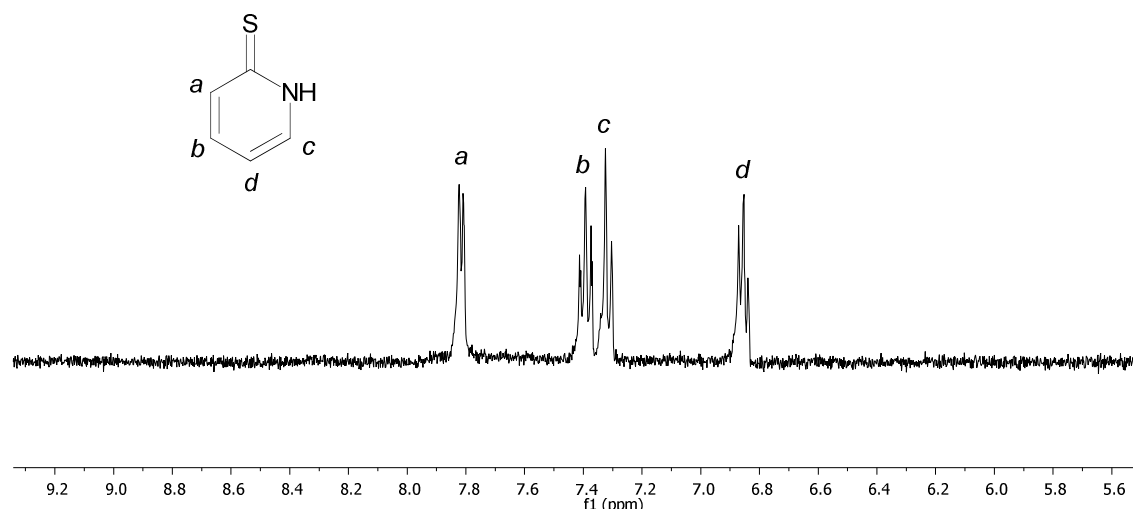
Figure 5.4 Partial ^{1}H NMR spectra (D$_2$O) of **N2** displaying release of 2-pyridinethione from nanoparticle assemblies.

We then performed experiments which demonstrate that the simultaneous application of both low pH and a reductive environment are required to cause triggered disassembly of the polymeric nanoparticles, and that application of either low pH or a reducing agent do not trigger nanoparticle disassembly. The pH of a solution of polymeric nanoparticles possessing imine and disulfide cross-links (**N2**) was adjusted to 5.5 with 0.1 M HCl$_{(aq)}$ aliquots (5 µL), reaction conditions which cause hydrolysis of the imine cross-links but do not affect the disulfide cross-links, which are presumably present in sufficient density to maintain the structural integrity of the nanoparticle. After stirring for 16 h at room temperature, GPC analysis (Figure 5.3c) displayed a peak ~ 17 min corresponding to polymeric nanoparticle **N3**, which was shown by batch dynamic light scattering (Figure 5.5c) to possess a hydrodynamic radius of 84 nm and a PDI of 0.148. This observation confirms that the polymeric nanoparticle is kept intact through the disulfide cross-links even after imine hydrolysis occurs. After filtration, fluorescence emission spectroscopy (Figure 5.6a) displayed a slight reduction in intensity, an observation which suggests the release of a small amount (approx. 5 %) of Nile Red

from the polymeric nanoparticle, presumably because the hydrolysis of the imine cross-links makes the nanoparticle more porous and thus reducing its ability to complex its cargo. To trigger the complete disassembly of the polymer nanoparticles we then applied a reductive stimuli. The reducing agent *tris*(2-carboxyethyl) phosphine (TCEP) (5 eq per disulfide bond) was added to a solution of **N3** encapsulating a cargo of Nile Red and the reaction left to stir for 16 h at room temperature. TCEP is known to readily reduce disulfide bonds at both low and high pH.[16, 17] GPC analysis (Figure 5.3d) shows the disappearance of the peak at retention time ~ 17 min corresponding to the polymeric nanoparticle **N3**, and the appearance of a peak possessing a retention time of ~ 25 min which corresponds to the formation of linear copolymers (**N4**). Fluorescence emission spectra were also recorded (Figure 5.6a) periodically, showing that the disassembly process was accompanied by a reduction in the intensity of the fluorescence associated with Nile Red which precipitated out of solution as the nanoparticle disassembled, further evidence suggesting complete disassembly. This fluorescence experiment also gave an indication of the kinetics of the disassembly process (Figure 5.6b), with most of the dye being released during the first hour of the disassembly.
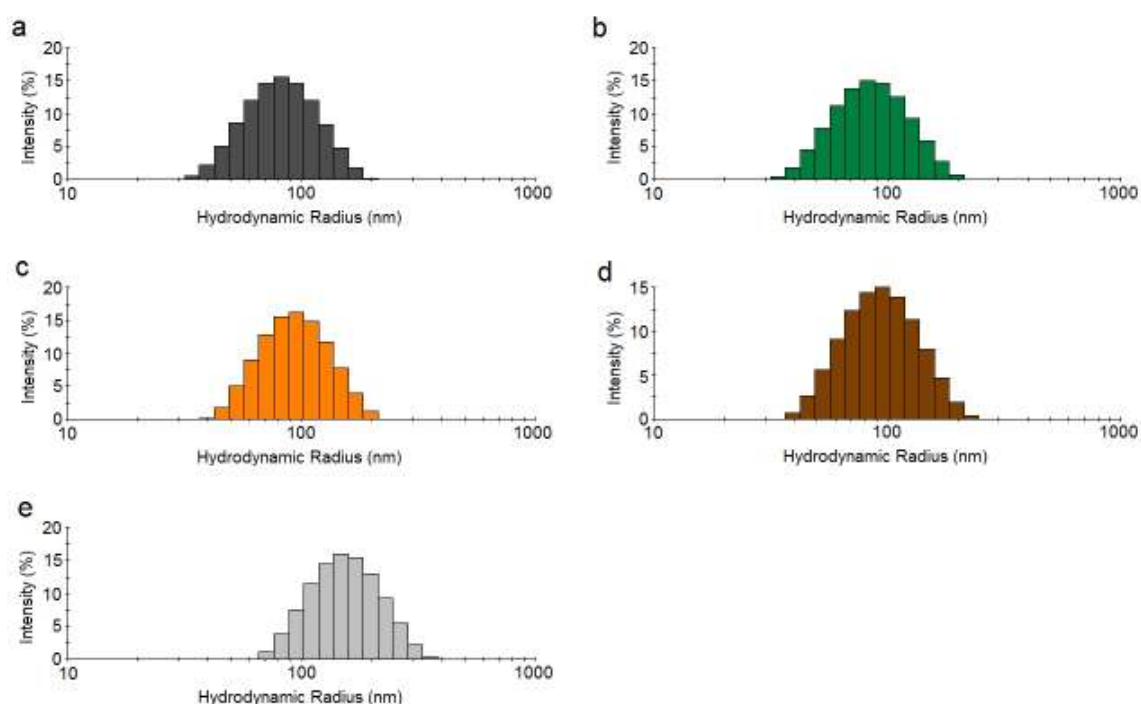
Figure 5.5 Histograms showing the particle size distributions of cross-linked polymeric nanoparticles (a) **N1**, (b) **N2**, (c) **N3**, (d) **N5** and (e) **N7**, obtained from batch dynamic light scattering analysis.

We then demonstrated that a reductive stimuli applied at high pH would not trigger the disassembly of the polymeric nanoparticles until low pH was also applied. Thus, to a solution of nanoparticles **N2** (prepared under identical condition but without Nile Red present) containing both imine and disulfide cross-links was treated with TCEP at pH 8.0, reaction conditions which cause reduction of disulfide cross-links but do not affect the imine cross-links. After stirring for 16 h at room temperature, GPC analysis (Figure 5.3e) displayed a near identical peak at retention time ~ 17 min corresponding to polymeric nanoparticle **N5**, and a minor peak at ~ 25 min which is likely a dimeric polymeric species. Batch dynamic light scattering analysis of **N5** (Figure 5.5d) displayed a hydrodynamic radius of 79 nm and a PDI of 0.142 nm. These observations confirm that the polymeric nanoparticles are kept intact through their imine cross-links after reduction of their disulfide cross-links occurs. Subsequent adjustment of the pH to 5.5 resulted in the complete disassembly of these polymeric nanoparticles through imine hydrolysis as confirmed by GPC analysis (Figure 5.3f), which displayed a peak (**N6**) at retention time ~ 25 min corresponding to the presence of the component linear copolymer chains. Taken together, these experiments demonstrate that polymeric nanoparticles containing imine and disulfide cross-links require simultaneous application of both acidic pH and a reducing environment to trigger their complete disassembly.
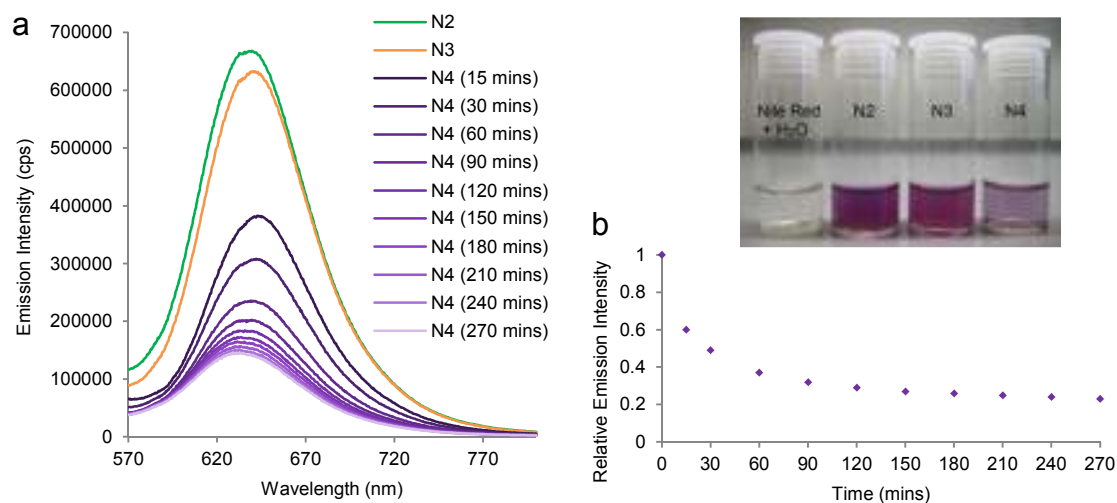
Figure 5.6 (a) Fluorescence emission spectra at λ_{ex} = 550 nm displaying uptake of Nile Red within **N2** (green peak) and **N3** (orange peak) and subsequent release after disassembly to **N4** (purple peaks). (b) The decrease in relative intensity plotted against time gives an insight into the kinetics of release. Photographs of solutions are also given (inset).

5.3.3 *Post-Formation Nanoparticle Functionalization*

Functional groups on or near the periphery of these polymeric nanoparticles present suitable handles to allow their further functionalization by decorating their surfaces with other potentially useful molecules, thus increasing their prospective utility. To demonstrate this possibility, we chose to adorn **N3** with a 5 kDa poly(ethylene glycol) due to its relatively straightforward synthesis (Scheme 5.2) and biocompatibility. Thus, **N3** (prepared without Nile Red present) containing disulfide cross-links and aldehyde and amine pendant functions was prepared, and the hydrazide end-functionalized poly(ethylene glycol) (**P3**) (1 eq per aldehyde) added at pH 5.5, a suitable pH to promote the formation of acylhydrazone bonds. GPC analysis (Figure 5.3g) displayed a major peak with a decreased retention time of ~ 16.5 min, an observation suggesting the polymeric nanoparticle undergoes an increase in its size as a consequence of the 5 kDa PEG conjugating onto the aldehyde functions to form a new particle **N7**. This GPC chromatogram also displays excess PEG-hydrazide (~ 27 min) and a minor product at ~ 22 min, which is likely as a consequence of the conjugation of PEG onto a dimeric polymer species. Dynamic light scattering analysis (Figure 5.5e) of **N7** revealed a hydrodynamic radius of 140 nm and a PDI of 0.136, and we hypothesize that this large increase in hydrodynamic radius is on account of chains of **P3** incorporating both onto the periphery of the particle and into its pores, causing significant swelling. The complete disassembly of the functionalized particle **N7** was triggered by addition of TCEP (5 eq per potential disulfide) as shown by GPC analysis (Figure 5.3h), which displayed (**N8**) two peaks corresponding to the excess PEG-hydrazide (~ 27 min) and **P1**-grafted with PEG-hydrazide (~ 23 min). We envisage that it should be possible to conjugate a range of polymers or modified biomolecules onto these polymeric nanoparticles through the formation of hydrolytically stable carbon-nitrogen double bonds such as hydrazones or oximes. This process provides these nanoparticles with the ability to protect encapsulated cargo or target specific biological environments.

5.4   Conclusions

Polymeric nanoparticles have been prepared by cross-linking component polymer chains through the formation of both imine and disulfide bonds. We have exploited the orthogonal nature of these dynamic covalent reactions to show that the disassembly of the polymeric nanoparticles requires the simultaneous application of *both* a low pH and reducing environment. This unique dual stimuli-responsiveness makes these polymeric nanoparticles the forerunners of a new generation of 'smart' delivery vehicles which may find application in *e.g.* the controlled intracellular delivery of high value cargos, such as pharmaceuticals possessing poor pharmakinetic properties. It is well known that nanoparticles can enter cells though the process of endocytosis, becoming encapsulated within endosomes which then undergo a pH drop from 7.4 to 5.5.[18, 19] Upon escape from the endosome, the particles enter the cell cytosol, which is known to be a highly reducing environment relative to the blood stream[20, 21] on account of high concentrations of biological reductants such as glutathione.[22, 23]   The polymeric nanoparticles described here are well-placed to take advantage of the pH and redox differences between the intra and extra-cellular environments, utilizing the orthogonal nature of their cross-links to ensure that their cargo is delivered in its desired locations with high levels of specificity. We hypothesize that such polymer-based drug delivery vehicles incorporating more than one dynamic covalent linkage could be manipulated to increase their abilities to target specific biological environments.

5.5   Experimental

All chemicals were purchased from Sigma-Aldrich or Alfa Aesar and were used as received without further purification. *N,N'*-Dimethylacrylamide was purified by vacuum distillation at 60 ˚C prior to use. ^{1}H and ^{13}C NMR spectra were recorded on a Bruker Advance 300 spectrometer at 300 and 75 MHz, respectively, with the residual solvent signal as an internal standard. FT-IR spectroscopy was performed on a Varian 800 FT-IR instrument (Varian Inc.). High-resolution mass spectrometry was performed on a Waters LCT premier mass spectrometer (Waters Inc.). Gel permeation chromatography (GPC) was conducted on a Varian ProStar instrument (Varian Inc.) equipped with a pair of PL gel 5 μm Mixed D 300 × 7.5 mm columns with guard column (Polymer Laboratories Inc.) in series, a Varian 325 UV-vis dual wavelength detector (254 nm), a Dawn Heleos II multi-angle laser light scattering detector (Wyatt Technology Corp.)

and a Viscotek 3580 differential RI detector. DMF (containing LiBr (1 g/ L)) was used as the eluent at 0.6 mL/ min. Near monodisperse poly(methyl methacrylate) standards (Agilent Technologies) were used for calibration. Data collection was performed with Galaxie software (Varian Inc.) and chromatograms analyzed with the Cirrus software (Varian Inc.) and Astra software (Wyatt Technology Corp.). Fluorescence emission spectra were recorded on a FluoroMax Fluorescence Spectrophotometer (SPEX) (λ = 550 nm). pH Measurements were recorded with a Hanna HI 98103 instrument that was calibrated daily with commercial buffer solutions (Sigma-Aldrich). Hydrodynamic radii (R_h) of cross-linked polymer nanoparticles in aqueous solutions were determined by dynamic light scattering (DLS). The DLS instrumentation consisted of a MALVERN Instruments HPPS-ET 5002 operating at 20 °C with a 633-nm laser module. Measurements were made at a detection angle of 173° (back scattering), and Malvern DTS 4.20 software was utilized to analyze the data. All determinations were made in duplicate.

2-(Pyridyldithio)-ethylamine Hydrochloride (1)[7]

Cysteamine hydrochloride (2.3 g, 20.2 mmol) in MeOH (20 mL) was added dropwise over 30 min to a solution of aldrithiol (8.8 g, 39.9 mmol) and acetic acid (1.6 mL) in MeOH (40 mL). The reaction was stirred overnight at room temperature then evaporated to dryness to afford a yellow oil, which was dissolved in MeOH (15 mL) and precipitated into diethyl ether (300 mL). The precipitate was isolated by filtration and precipitation was repeated five times to afford the title product as a white solid (3.1 g, 69 %). ^{1}H NMR (D$_2$O): δ 3.05 (t, 2H, J = 6.3 Hz), 3.29 (t, 2H, J = 6.3 Hz), 7.23 (m, 1H), 7.63 (m, 1H), 7.74 (m, 1H), 8.36 (m, 1H). ^{13}C NMR (D$_2$O): δ 34.8, 37.4, 121.7, 122.2, 138.5, 149.2, 157.2. FT-IR (wavenumber, cm^{-1}): 3131 (N–H), 2950 (C–H, alkyl), 2913 (C–H, alkyl) 1448 (C=C, aromatic), 1417 (C=C, aromatic). HRMS$^+$ C$_7$H$_{11}$N$_2$S$_2$: Theoretical: 187.0364. Actual: 187.0369.

2-Pyridyl-disulfide-ethylacrylamide (2)

A solution of 2-(pyridyldithio)-ethylamine hydrochloride (**1**, 1.9 g, 8.5 mmol) and Et$_3$N (1.8 g, 17.8 mmol) in CHCl$_3$ (50 mL) was cooled to 0 ˚C in an ice bath. To this solution acryloyl chloride (0.77 g, 8.5 mmol) in CHCl$_3$ (50 mL) was added dropwise over 30 min. The reaction mixture was stirred overnight at room temperature then transferred to

a separating funnel with H_2O (150 mL). The aqueous layer was extracted with $CHCl_3$ (2 × 100 mL) and the combined organic extracts dried over Na_2SO_4, filtered and evaporated to dryness to afford a crude oil which was purified by column chromatography [SiO_2, EtOAc-Hexane (1:1)] to afford the title product as a white solid (1.1 g, 54 %). ^{1}H NMR ($CDCl_3$): δ 2.95 (t, 2H, CH_2S, J = 5.7 Hz), 3.63, (m, 2H, CH_2N), 5.65 (dd, 1H, J = 1.7 Hz, J = 10.0 Hz), 6.15 (dd, 1H, J = 10.0 Hz, J = 17.0 Hz), 6.30 (dd, 1H, J = 1.7 Hz, J = 17.1 Hz), 7.14 (m, 1H), 7.49 (m, 1H), 7.61 (m, 1H), 8.49 (m, 1H). ^{13}C NMR ($CDCl_3$): δ 37.9, 39.4, 121.6, 126.1, 131.7, 137.2, 150.1, 159.8, 165.9. FT-IR (wavenumber, cm^{-1}): 3273 (N–H), 3048 (C–H, alkene), 2925 (C–H, alkyl), 1656 (C=O), 1446 (C=C), 1417 (C=C). HRMS$^+$ $C_{10}H_{13}N_2OS_2$: Theoretical: 241.0469. Actual: 241.0473.

*Aldehyde/ Disulfide-Functionalized Copolymer (**P1**)*

S-1-Dodecyl-*S'*-(α,α-dimethyl-α''-acetic acid)trithiocarbonate (DDMAT) (1 eq, 20.7 mg, 57 μmol) and AIBN (0.2 eq, 1.87 mg, 11.4 μmol) were added to a small schlenk tube. *N,N'*-Dimethylacrylamide (160 eq, 0.90 g, 9.12 mmol), *N*-ethylacrylamide-2-(4-formylbenzamide) (**3**, 20 eq, 0.28 g, 1.14 mmol) and 2-pyridyl-disulfide-ethylacrylamide (**2**, 20 eq, 0.27 g, 1.14 mmol) were then added followed by DMF (4 mL). The reaction mixture was degassed five times, and then the vessel was backfilled with N_2, and allowed to warm to room temperature. The reaction mixture was then placed in an oil bath at 70 ˚C, and the polymerization was quenched after 21 h. The reaction mixture was dissolved in a minimal amount of THF and added dropwise to a large excess of ice-cold diethyl ether. The polymer precipitate was then isolated by filtration and the precipitation was repeated before drying under high vacuum. Polymer **P1** was obtained as a pale yellow solid (1.06 g). ^{1}H NMR ($CDCl_3$): δ 0.84 (br, CH_2CH_3, of the chain terminus), 1.64 (br, CHCH_2), 2.41 (br, CHCH$_2$), 2.87 (br, N(CH_3)$_2$), 3.46 (br, (CH_2)$_2$), 7.09 (br, Ar), 7.61 (br, Ar), 7.89 (br, Ar), 8.08 (br, Ar), 8.44 (br, Ar), 10.04 (br, CHO). The composition of **P1** can be determined by comparing the integration of the aldehyde protons of **3** and the aromatic protons of **2** with the integration of the N(CH_3)$_2$ protons of DMA. The monomer composition was determined to be 10.5: 1: 1 (DMA: **3**: **2**) which differs to the feed ratio, presumably due to the difference in reactivity between DMA and the mono-substituted *N*-alkylacrylamide monomer **3** and **2**.

Boc-amine/ Disulfide-Functionalized Copolymer (P2a)

S-1-Dodecyl-*S'*-(α, α -dimethyl- α''-acetic acid)trithiocarbonate (DDMAT) (1 eq, 24.0 mg, 66 μmol) and AIBN (0.2 eq, 2.16 mg, 13.2 μmol) were added to a small schlenk tube. *N,N'*-Dimethylacrylamide (160 eq, 1.05 g, 10.56 mmol), *N*-(*tert*-butoxycarbonyl)-propylaminoacrylamide (**4**, 20 eq, 0.30 g, 1.32 mmol) and 2-pyridyl-disulfide-ethylacrylamide (**2**, 20 eq, 0.32 g, 1.32 mmol) were then added followed by DMF (4 mL). The reaction mixture was degassed five times, and then the vessel was backfilled with N_2, and allowed to warm to room temperature. The reaction mixture was then placed in an oil bath at 70 °C, and the polymerization was quenched after 21 h. The reaction mixture was dissolved in a minimal amount of THF and added dropwise to a large excess of ice-cold diethyl ether. The polymer precipitate was then isolated by filtration and the precipitation was repeated before drying under high vacuum. Polymer **P2a** was obtained as a pale yellow solid (1.28 g). ^{1}H NMR (CDCl$_3$): δ 0.83 (br, CH$_2$C*H$_3$*, of the chain terminus), 1.38 (br, C(C*H$_3$*)$_3$), 1.61 (br, CHC*H$_2$*), 2.42 (br, C*H*CH$_2$), 2.87 (br, N(C*H$_3$*)$_2$), 3.45 (br, (C*H$_2$*)$_3$), 7.10 (br, Ar), 7.61 (br, Ar), 8.45 (br, Ar). The composition of **P2a** can be determined by comparing the integration of the *boc* protons of **4** and the aromatic protons of **2** with the integration of the N(C*H$_3$*)$_2$ protons of DMA. The monomer composition was determined to be 10.5: 1: 1 (DMA: **4**: **2**) which differs to the feed ratio, presumably due to the difference in reactivity between DMA and the mono-substituted *N*-alkylacrylamide monomer **4** and **2**.

Amine/ Disulfide Functionalized Copolymer (P2b)

P2a (1.07 g) was dissolved in CHCl$_3$ (5 mL) and TFA (5 mL) was added, the reaction mixture was left to stir for 4 h. After this time the solvent and excess TFA were removed on the rotary evaporator and the oil obtained was dissolved in a minimal amount of CHCl$_3$ and added dropwise to a large excess of diethyl ether. The polymer precipitate was then isolated by filtration and dried under high vacuum. The polymer precipitate was then isolated by filtration and the precipitation was repeated before drying under high vacuum. Polymer **P2b** was obtained as a pale yellow solid (0.92 g). ^{1}H NMR (CDCl$_3$): δ 0.86 (br, CH$_2$C*H$_3$*, of the chain terminus), 1.71 (br, CHC*H$_2$*), 2.44 (br, C*H*CH$_2$), 2.87 (br, N(C*H$_3$*)$_2$), 3.42 (br, (C*H$_2$*)$_3$), 7.11 (br, Ar), 7.63 (br, Ar), 8.44 (br, Ar).

Hydrazide End-Functionalized Poly(ethylene glycol) (P3)

Potassium *tert*-butoxide (15 eq, 2.44 g, 21.75 mmol) in *tert*-butanol (17 mL) was added to poly(ethylene glycol) (5 kDa, 1 eq, 7.25 g, 1.45 mmol) in toluene (90 mL). Solution was purged with N_2 for 30 mins before the dropwise addition of ethyl bromoacetate (27.5 eq, 6.66 g, 39.88 mmol) over 30 mins. Reaction was left to stir overnight at room temperature before filtration and evaporation to dryness. The oil obtained was dissolved in THF (30 mL) and added dropwise to a large excess of diethyl ether. The precipitation was repeated three times before the precipitate obtained was dried under high vacuum. The ethyl ester end-functionalized polymer (1eq, 4.45 g, 0.89 mmol) was then dissolved in methanol (70 mL) and hydrazine monohydrate (100eq, 4.45 g, 0.089 mol) in methanol (30 mL) was added. Reaction was left to stir overnight at room temperature. The reaction mixture was evaporated to dryness, dissolved in CH_2Cl_2 (100 mL) and transferred into a separating funnel. Organic layer was washed with H_2O (3×100 mL), dried with $MgSO_4$, filtered and evaporated to dryness. The oil obtained was dissolved in THF (20 mL) and added dropwise to a large excess of diethyl ether. The precipitation was repeated three times before the precipitate obtained was dried under high vacuum. **P3** was obtained as a white solid (3.10 g). ^{1}H NMR ($CDCl_3$): δ 3.36 (br, OC*H$_3$*, of the chain terminus), 3.62 (br, (C*H$_2$*)$_2$), 4.06 (br, OC*H$_2$*CO, of the chain terminus), 8.39 (br, CON*H*NH$_2$, of the chain terminus).

Preparation of Imine Cross-Linked Nanoparticles (N1)

Polymer **P1** (1 eq, 43.8 mg, 2.34 μmol) and Nile Red (9.1 mg) were dissolved in THF (400 μL) to which was added H_2O (4.49 mL). Polymer **P2a** (1 eq, 46.8 mg, 2.34 μmol) was dissolved in H_2O (4.48 mL). These two solutions were combined with rapid stirring to afford a solution with a 1 wt % concentration with respect to total copolymer building blocks. The pH was adjusted to 8.0 with small aliquots (5 μL) of 0.1 M NaOH$_{(aq)}$. The pH was adjusted to 8.0 and the reaction was left to stir for 16 h open to the atmosphere to allow the organic solvent to evaporate. After this time the reaction mixture was sealed and heated to 40 °C for 3 h. The sample was analyzed by gel permeation chromatography (GPC) and dynamic light scattering.

Preparation of Imine/ Disulfide Cross-Linked Nanoparticles (N2)

To a sample of imine cross-linked nanoparticles (**N1**, 1 wt %, pH 8.0, 7.5 mL) dithiothreitol (0.5 eq per disulfide bond, 3.6 mg) was added, and the reaction was left to stir at room temperature for 16 h. After this time the reaction mixture was filtered to remove excess Nile Red, and the reaction mixture was analyzed by GPC, fluorescence emission spectroscopy ($\lambda = 550$ nm) and dynamic light scattering.

Preparation of Disulfide Cross-Linked Nanoparticles (N3)

The pH of a sample of imine/ disulfide cross-linked nanoparticles (**N2**, 1 wt %, pH 8.0, 6 mL) was adjusted to 5.5 with small aliquots (5 µL) of 0.1 M $HCl_{(aq)}$. The reaction was left to re-equilibrate at room temperature for 16 h before analysis by GPC, fluorescence emission spectroscopy ($\lambda = 550$ nm) and dynamic light scattering.

Disassembly of Disulfide Cross-Linked Nanoparticles (N4)

To a sample of disulfide cross-linked nanoparticles (**N3**, 1 wt %, pH 5.5, 2 mL) TCEP (*tris*(2-carboxyethyl)phosphine) (5 eq per disulfide bond, 9.0 mg) was added. The reaction was left to stir at room for 16 h. and during this time the reaction was periodically analyzed by fluorescence emission spectroscopy ($\lambda = 550$ nm). After 16 h the reaction mixture was filtered to remove Nile Red precipitate, before analysis by GPC.

Preparation of Poly(ethylene glycol) Functionalization Nanoparticles (N5)

To a sample of disulfide cross-linked nanoparticles (**N3**, 1 wt %, pH 5.5, 2 mL, prepared without Nile Red present) hydrazide end-functionalized poly(ethylene glycol) (**P3**, 1 eq per aldehyde function, 31.3 mg) was added. The reaction was left to stir at room for 16 h before analysis by GPC and dynamic light scattering.

Disassembly Poly(ethylene glycol) Functionalized Nanoparticles (N6)

To a sample of poly(ethylene glycol) functionalization disulfide cross-linked nanoparticles (**N5**, pH 5.5, 1 ml) TCEP (*tris*(2-carboxyethyl)phosphine) (5 eq per

disulfide bond, 4.5 mg) was added. The reaction was left to stir at room for 16 h before analysis by GPC.

Preparation of Imine Cross-Linked Nanoparticles (N7)

TCEP (5 eq per disulfide bond, 9.0 mg) was dissolved in H_2O (0.5 ml) and the pH adjusted to 8.0 with small aliquots (5 µL) of 0.1 M $NaOH_{(aq)}$. This was added to a sample of imine/ disulfide cross-linked nanoparticles (**N2**, 1 wt %, pH 8.0, 2 mL, prepared with Nile Red present). The reaction was left to stir at room temperature for 16 h before analysis by GPC and dynamic light scattering.

Disassembly of Imine Cross-Linked Nanoparticles (N8)

The pH of a sample of imine cross-linked nanoparticles (**N7**, 1 wt %, pH 8.0, 6 mL) was adjusted to 5.5 with small aliquots (5 µL) of 0.1 M $HCl_{(aq)}$. The reaction was left to re-equilibrate at room temperature for 16 h before analysis by GPC and dynamic light scattering.

5.6   References

1.   A. Klaikherd, C. Nagamani and S. Thayumanavan, *J. Am. Chem. Soc.*, 2009, **131**, 4830-4838.
2.   C. Godoy-Alcantar, A. K. Yatsimirsky and J. M. Lehn, *J. Phys. Org. Chem.*, 2005, **18**, 979-985.
3.   J. H. Ryu, R. T. Chacko, S. Jiwpanich, S. Bickerton, R. P. Babu and S. Thayumanavan, *J. Am. Chem. Soc.*, 2010, **132**, 17227-17235.
4.   J. H. Ryu, S. Jiwpanich, R. Chacko, S. Bickerton and S. Thayumanavan, *J. Am. Chem Soc.*, 2010, **132**, 8246-8247.
5.   J. A. Syrett, D. M. Haddleton, M. R. Whittaker, T. P. Davis and C. Boyer, *Chem. Commun.*, 2011, **47**, 1449-1451.
6.   H. T. T. Duong, C. P. Marquis, M. Whittaker, T. P. Davis and C. Boyer, *Macromolecules*, 2011, **44**, 8008-8019.
7.   G. T. Zugates, D. G. Anderson, S. R. Little, I. E. B. Lawhorn and R. Langer, *J. Am. Chem. Soc.*, 2006, **128**, 12726-12734.
8.   L. J. Wong, C. Boyer, Z. F. Jia, H. M. Zareie, T. P. Davis and V. Bulmus, *Biomacromolecules*, 2008, **9**, 1934-1944.
9.   C. Boyer, J. Liu, L. Wong, M. Tippett, V. Bulmus and T. P. Davis, *J. Polym. Sci., Part A*, 2008, **46**, 7207-7224.
10.   Z. F. Jia, J. Q. Liu, C. Boyer, T. P. Davis and V. Bulmus, *Biomacromolecules*, 2009, **10**, 3253-3258.
11.   C. Boyer, J. Q. Liu, V. Bulmus and T. P. Davis, *Aust. J. Chem.*, 2009, **62**, 830-847.

12. J. T. Lai, D. Filla and R. Shea, *Macromolecules*, 2002, **35**, 6754-6756.

13. The polydispersity measurement in dynamic light scattering is used to describe the width of the particle size distribution, and is calculated by cumulants analysis of the autocorrelation function within the software of the instrument used to perform the measurements.

14. A. W. Jackson and D. A. Fulton, *Chem. Commun.*, 2010, **46**, 6051-6053.

15. A. W. Jackson and D. A. Fulton, *Chem. Commun.*, 2011, **47**, 6807-6809.

16. J. A. Burns, J. C. Butler, J. Moran and G. M. Whitesides, *J. Org. Chem.*, 1991, **56**, 2648-2650.

17. J. C. Han and G. Y. Han, *Anal. Biochemistry*, 1994, **220**, 5-10.

18. D. Schmaljohann, *Adv. Drug Delivery Rev.*, 2006, **58**, 1655-1670.

19. Y. Bae, S. Fukushima, A. Harada and K. Kataoka, *Angew. Chem., Int. Ed.*, 2003, **42**, 4640-4643.

20. G. Saito, J. A. Swanson and K. D. Lee, *Adv. Drug Delivery Rev.*, 2003, **55**, 199-215.

21. S. Sivakumar, V. Bansal, C. Cortez, S. F. Chong, A. N. Zelikin and F. Caruso, *Adv. Mater.*, 2009, **21**, 1820-1824.

22. M. J. Heffernan and N. Murthy, *Ann. Biomed. Eng.*, 2009, **37**, 1993-2002.

23. A. Bernkop-Schnurch, *Adv. Drug Delivery Rev.*, 2005, **57**, 1569-1582.

The end